Title

Development and testing of a sensor package for sea surface mapping in the nearshore environment by human powered watercraft

Author

Davis, Benjamin D

Publication Date

2021

Peer reviewed|Thesis/dissertation

UNIVERSITY OF CALIFORNIA SAN DIEGO

Development and testing of a sensor package for sea surface mapping in the nearshore environment by human powered watercraft

A thesis submitted in partial satisfaction of the
requirements for the degree Master of Science

in

Oceanography

by

Benjamin D. Davis

Committee in charge:

Professor Todd Martz, Chair
Professor Andrew Dickson
Professor John Hildebrand

2021

The thesis of Benjamin D. Davis is approved, and it is acceptable in quality and form for publication on microfilm and electronically.

University of California San Diego

2021

TABLE OF CONTENTS

LIST OF ABBREVIATIONS

SWRO	Seawater reverse osmosis
CDP	Carlsbad desalination plant
GPS	Global positioning system
AHL	Agua Hedionda lagoon
OEM	Original equipment manufacturer
AADI	Aanderaa Data Instruments
CTD	Conductivity, Temperature and Depth sensor
SBE	SeaBird Electronics
4319	Aanderaa 4319 conductivity probe
EIR	Environmental impact report
GSW	Gibb’s Seawater
DIW	Deionized water
DM45	Mettler Toledo Density Meter 45
ODV	Ocean Data View
IDW	Inverse distance weighting
OK	Ordinary kriging
O_2	Oxygen
O_2 % Sat	Percent saturation of oxygen
CO_2	Carbon dioxide
GUI	Graphical user interface
OLC	Oceanside Littoral Cell

LIST OF FIGURES

ACKNOWLEDGEMENTS

I would first like to acknowledge Professor Todd Martz for his support as my advisor and the chair of my committee. From encouraging the pursuit of this project when I first visited campus as a prospective student to reading and revising multiple drafts, his mentorship has proven invaluable.

I also would like to recognize the guidance of Dr. Phil Bresnahan, who has taught me countless interdisciplinary skills that have undoubtedly played a vital role in my development over the past two years and carved a path that I aspire to follow.

Additionally, I am forever grateful for the leadership and compassion of the other members of the Martz Lab, especially Taylor Wirth and Wiley Wolfe, through their patience fielding countless questions and commitment to my success.

All of this would not be possible without my family and friends who have constantly supported me and my interests while providing a tremendously loving community that I will always cherish.

ABSTRACT OF THE THESIS

Development and testing of a sensor package for sea surface mapping in the nearshore environment by human powered watercraft

by

Benjamin D. Davis

Master of Science in Oceanography

University of California San Diego, 2021

Professor Todd Martz, Chair

The nearshore environment is an extremely dynamic seascape that is difficult to characterize with high spatial and temporal resolution. Here, I utilize a novel sensor package, the WavepHOx, to spatially depict the signature of the seawater reverse osmosis (SRWO) byproduct plume emanating from the outfall of the Carlsbad Desalination plant (CDP) over the course of 60 days and 10 different surveys with a human powered watercraft equipped with a global positioning system (GPS). Subsurface and surface measurements detected areas of seawater at the mouth of the desalination plant's outlet into the ocean with properties 1.5% higher salinity (RMS = ±0.17%) and 7.7% (±0.2%) higher temperature than nearby ambient values (~33.4 on the Practical Salinity scale and ~14 ºC respectively) and similar surface values as far as 600 m from the outfall. This brine-induced gravity current tended to propagate latitudinally southward parallel to shore, consistent with the encompassing Oceanside Littoral Cell. Possible explanations for vertical distributions of the plume are also discussed. These observations provide a pathway for a new method to map the nearshore environment's physical and biogeochemical processes.

INTRODUCTION

1.1 Sampling in the nearshore environment

The nearshore environment is generally defined as the indefinite zone extending from the shoreline to beyond the break, where the primary cause of the current system is a result of wave action (EPA, 1998). This environment serves as one of the most biologically diverse ecosystems in the world, but it is also as dynamic as it is abundant. For this reason, sampling in the nearshore proves to be difficult and not as rigid or consistent for processes with high spatiotemporal variability, and studies to quantify physical oceanographic processes in this domain have reached their limits (Liévana MacTavish et al., 2016; Shanafield et al., 2018; Sinnett et al., 2020).

Discrete bottle sampling is the most common form of data collection in this environment, with the ability to measure parameters with extremely precise instrumentation in laboratory settings. This suits the characterization of physical processes that progress at low frequencies (e.g. seasonal, annual and longer) but leaves room for low spatial and temporal resolution for ephemeral biogeochemical processes (Goodridge, 2018; Kekuewa, 2020). Recent satellite imagery analysis and high quality moored autonomous sensors have also been employed to describe the temporal variability of ocean biogeochemistry but are unable to continuously spatially detail the nearshore environments either due to array size or pixel resolution (Cao & Tzortziou, 2021; Hofmann et al., 2015; Janfelt et al., 2007; Le et al., 2019; T. Martz et al., 2014; Short et al., 2006; Volpe & Esser, 2002). And although GPS-tracked *in situ* sampling of carbon chemistry has been carried out in coastal areas on motorized vehicles, this limits data collection to non-fragile ecosystems and deeper waters (Omand et al., 2011). Therefore, this presents an incentive to surpass this technological barrier for collecting data in the nearshore environment.

The WavepHOx is a sensor package that was specifically designed for sea surface mapping of pH and oxygen for mobile platforms with minimal environmental disturbance (Bresnahan et al., 2016). Field deployment tests indicated that many carbon chemistry parameters were calculable from its measurements with a high spatiotemporal resolution in La Jolla and nearby waters, bridging the gap for accurate, continuous sampling of certain biogeochemical processes in the nearshore environment. However, with the addition of an OEM oceanographic conductivity probe, the WavepHOx expanded its capabilities to other interim physical processes and eliminated the external salinity verification for its sensor outputs. Innovative oceanographic tools like this one are enabling scientists to better understand rapid biogeochemical processes the impacts of coastal anthropogenic infrastructure.

1.2 The Carlsbad desalination plant

The Carlsbad desalination plant (CDP), the largest in North America, of north San Diego county generates over 50 million gallons of drinking water per day (at peak operation) to potentially supply over 750,000 people in the nearby region (City of Carlsbad, 2005). Brine resulting from the SWRO process is discharged into the adjacent ocean. Tracking the extent of the brine plume is important for a number of reasons. For example, brine has been shown to negatively impact coral and algal growth and induce osmotic shock in select fish species (Belkin et al., 2017; Roberts et al., 2010). In addition, the plume may contain various coagulants and antiscalants with unknown environmental impact. Before discharge, the CDP plume is diluted by 90% using water from the intake feed, located in the Agua Hedionda Lagoon (AHL). The biological and chemical implications of the CDP plume have been studied by state authorities and are not the subject of this work. We chose the CDP plume as a case study in order to evaluate the performance of an instrument that I developed as the primary component of this thesis.

There were several factors that indicated a salinity plume is measurable from sea surface observations. A recent study found that, under the right conditions, a down sloping gravity current (i.e., a brine plume seeping from shore) can vertically separate when interacting with an oncoming wave without evenly mixing throughout the water column. Part of the gravity current will “decapitate” and travel near the surface while the other portion of the higher density fluid continues to propagate along the bottom (Ouillon et al., 2019). Additionally, previous work at this site has shown that there was an increase of 2 salinity units above ambient values accompanied by warmer than normal temperatures along the seabed as far as 600m away from the outfall, violating the 2019 California Coastal Plan’s maximum distance of 200m for the effluent to extend (Petersen et al., 2018; Water Resources Control Board, 2019). These values were measured with discrete bottle samples and laboratory salinometry. My study builds off these surveys with the intention to map the plume with higher spatial resolution with less required personnel and a modified sensor package with a novel observational strategy for sea surface mapping.

MATERIALS AND METHODS

2.1 Sensor Package Modification and Validation

For this study, I utilized a novel sensor package, the WavepHOx, and modified it to incorporate a conductivity probe for high precision and accurate salinity measurements in place of the original ISE reference electrode, an addition to the already equipped Honeywell Durafet pH sensor and Aanderaa optode oxygen sensor (Figure 1). Three different conductivity sensors were implemented and tested extensively in laboratory settings and field deployments before arriving at my desired design.

The first, the SeaBird Electronics 37 CTD (SBE 37), was taken into the field alongside the original WavepHOx but this proved too impractical, due to the size of the SBE-37. Atlas Scientific K1.0 and K10 conductivity sensors were tested. The Atlas probes are OEM devices designed primarily for laboratory use. The K10 was found to be too fragile and not pursued after initial benchtop testing (not discussed here). After controlled tests in a 7000 L circulating seawater test tank, I concluded that the Atlas K1.0 did not meet my benchmark for accuracy or precision (Appendix D). Following the Atlas probe tests, I evaluated the Aanderaa 4319 conductivity probe which has been designed for seawater and extensively tested and calibrated for the marine environment and salinity range (Kononets et al., 2012). The primary reason for testing the Atlas probe first was cost, as it is valued at one tenth the price of the 4319 sensor.

To make the 4319 probe compatible with the sensor package, I modified the WavepHOx firmware to integrate a new serial sensor. This entailed updating the communication protocol on the main board for the 4319 port and the resulting dialog on the user interface. Hardware modifications were also made that included changing and rerouting the power supply, along with designing a new end cap to the WavepHOx housing in Solidworks that was manufactured for my specific assembly.

Adjustments to the factory calibration were applied to both the Aanderaa oxygen optode and 4319 conductivity probes per AADI recommendations. For the optode, a two-point calibration was performed with 100% oxygen saturated water and a zero-oxygen solution to compensate for individual sensor and foil variations as benchmarks for saturation state intercepts (AADI, 2021). A single point (gain only) calibration is recommended for the Aanderaa 4319 probe (Equation 1) to procure a corrected value for the cell constant, $CellCoef_c$.

$$CellCoef_c = CellCoef \cdot \frac{C_{ref}}{C_{meas}} \tag{1}$$

In this scenario, the ratio of conductivity between a reading from a referenced instrument, C_{ref}, and a reading from the 4319 sensor, C_{meas}, was multiplied by the uncorrected internal cell constant, $CellCoef$, which defines the relationship between the electrical signals in the seawater based on spatial configuration and external field effects (n=10). The corrected cell constant, $CellCoef_c$, is then multiplied by the raw conductivity to generate the sensor output salinity values, S_{meas}. The sensor is post-processed in salinity-space, as is customary for parameters of interest, on the PSS-78 scale and all salinity values reported here are on this scale. The modified sensor package was submerged into the test tank for three ~5-hour tests to track its stability, response rate, and accuracy. Parameters for discrete bottle samples was determined from density measured on a Mettler Toledo DM45 density meter and converted to salinity and/or conductivity using the Matlab Gibb's Seawater (GSW) Toolbox (Appendix A**: Density Meter Best Practices**). The density meter was calibrated with deionized water (DIW) and measurements of IAPSO salt standards provided by Scripps' Ocean Data Facility (Reference Batch: P160) corroborated its accuracy and precision. Due to COVID, it was not feasible to gain access to a salinometer for further validation. However, because of the repeatability of the instruments available, it would not significantly enhance the content of my work. The DM45 has a tolerance of 0.00001 $\frac{g}{cm^3}$ which, through the multiplication rule of error propagation, corresponds to a practical salinity value of $e_{DM} = \pm 0.023$ (Bendat & Piersol, 2012; Mettler Toledo, 2010).

Discrete bottle samples were also taken both at the beginning and end of deployments to calculate the pH offset in the Durafet using the Agilent pH spectrophotometric system in the data analysis process. Temperature corrections for oxygen and pH were determined from the optode thermistor because data displayed quicker equilibration time from the bias of the controller temperature (error $= \pm 0.03^{o}C$). This is likely due to the location of the thermistor at the foot of the optode; while the Durafet and 4319 contain internal temperature sensors where they can be subject to self-heating effects from irregular current draw. Furthermore, I employed the newly implemented conductivity probe to calculate the salinity-corrected oxygen and pH values (Garcia & Gordon, 1992; T. R. Martz et al., 2010).

To ensure the highest quality data, I set up a temperature-controlled water bath that had water with the temperature of the study site continuously flowing around the WavepHOx housing from the day prior up until time of deployment. After entering the sampling mode, I let the WavepHOx sit in the temperature-controlled water for an hour before taking a bottle sample. This allowed the sensor package's internal temperature to cool down and stabilize after initializing the sampling mode that would otherwise skew the sensors' outputs.

Figure 1 Preparing the WavepHOx for deployment on the stand-up paddle board (top). The fully assembled WavepHOx (left) and the sensor assembly under the end cap (right). From left to right, Aanderaa 3835 optode, Honeywell Durafet, and Aanderaa 4319 conductivity probe.

2.2 Study Site and Field Deployments

According to the 2005 Bud Lewis Carlsbad Desalination Project Environmental Impact Report (EIR), the brine generated from the CDP facility contains twice the coastal salt concentration before being diluted into the recycled power station's cooling system's water from the AHL with a ratio of 1:10, brine to lagoon water. In theory, this mixture can be detected not only from its relatively high salinity (max = 37) but also because the lagoon water that passes through the power station has a higher temperature signal from sensible heating. The processed water is released from an outfall about 50m from shore where it is intended to diffuse into the water column upon turbulent interaction with the surf. However, Lykkebo Petersen et al. 2017 discovered with discrete bottle samples that high salinity and warmer temperatures were found as far as 600m from the outfall, much beyond the predicted diffusion zone, before returning to ambient salinities and temperatures beyond that distance. Both the EIR and Petersen study provide evidence suggesting the plume tends to travel south along the coast, although there was little latitudinal variability in the previous sampling to verify this (Jenkins & Wasyl, 2005).

We anticipated that deployments during or shortly after a slack low tide will provide the highest likelihood of a plume signature, but still obtained data from four distinct tidal stages. Additionally, a predefined transect determined by the Garmin Quatix Marine watch also supplied temporal and spatial data for interpolation over a total of ten separate surveys. The number of deployments were limited to days with good to moderate conditions for the WavepHOx to be attached to a stand-up paddle board to safely and accurately follow the transect and the respective waypoints (Figure 2).

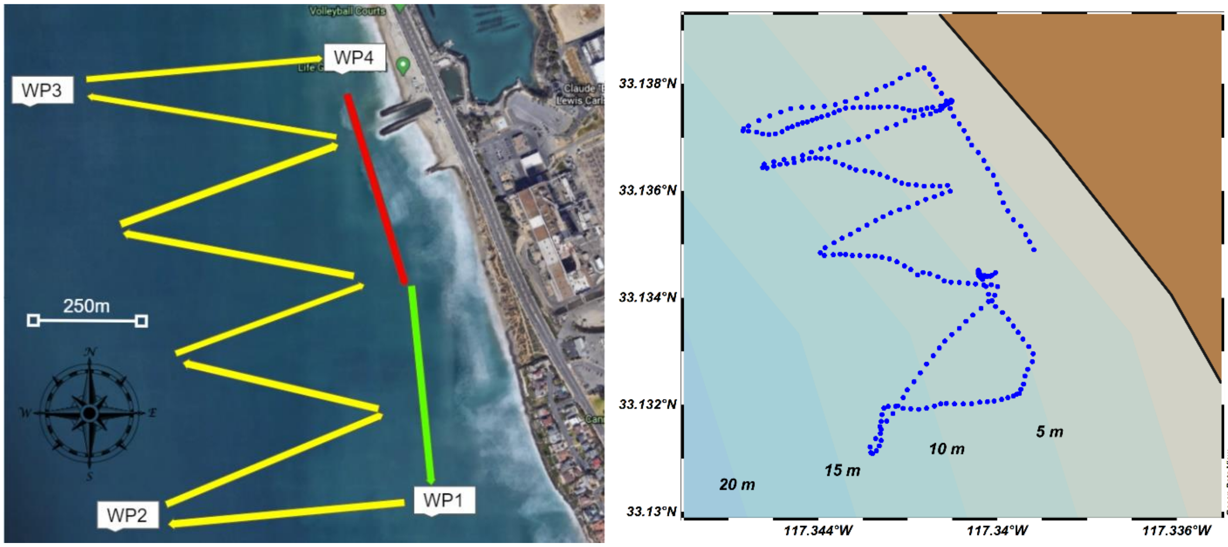

Figure 2 The idealized transect (left) with the respective waypoints in the area just south of the outfall of the Carlsbad desalination plant, next to WP4, and an actual transect performed on March 18th. Satellite imagery provided by Google Earth.

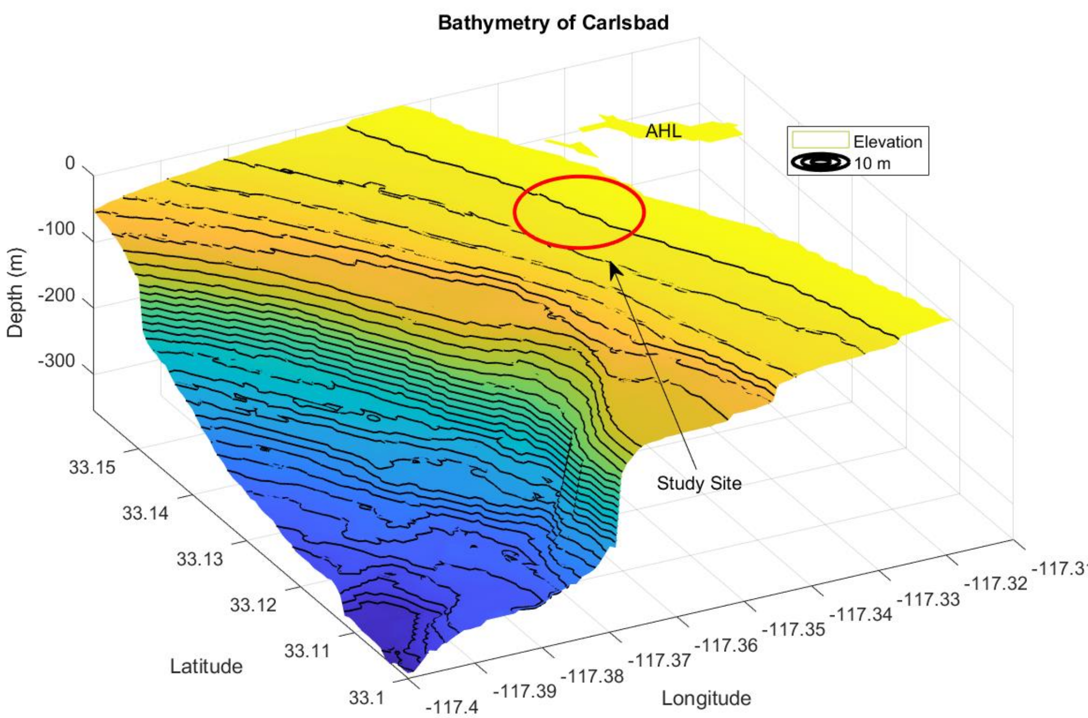

Figure 3 Bathymetry of the nearshore environment in Carlsbad with study site highlighted. The Agua Hediona Lagoon (AHL) is also pictured northeast of the study site. Each black contour line represents 10 meters of depth.

2.3 Handheld CTD Profiles

During the last four surveys, a handheld profiling CTD (CastAway, Xylem Instruments) was integrated into the deployment procedure to investigate the possibility of a subsurface plume when there is not a measurable signature at the surface, and potentially verify a decapitation event if there is a measurable plume at the surface. Casts were performed at the beginning of each deployment in the surf zone and as close to the outfall as possible, with the final deployment consisting of an array of casts throughout the transect.

RESULTS

3.1 Data Quality Control

To assess its response rate and stability, the tank tests of the Aanderaa 4319 conductivity probe integrated into the WavepHOx were conducted alongside a SBE 37 with an embedded conductivity sensor. According to the manufacturers, the Aanderaa and SBE 37 sensors have conductivity resolutions of 0.002 $\frac{mS}{cm}$ and 0.0001 $\frac{mS}{cm}$, respectively (AADI, 2013; Sea-Bird Scientific, 2018). Using standard propagation of uncertainty techniques with variables that go into the calculation of salinity from TEOS-10 to the first order, the resolution of the Aanderaa 4319 probe corresponds to a practical salinity value of $e_s = \pm 0.023$. Yet, because one salinity unit is roughly proportional to 1 $\frac{mS}{cm}$ to the first order with all other parameters held constant, these resolutions are definitively sensitive enough to detect a change in salinity in the range that I would expect at the study site ($\pm$ 1) (IOC et al., 2010; McDougall & Barker, 2015). To model a similar change in salinity in a controlled environment, a dilution test was performed by pouring three 5-gallon buckets of fresh water into a 7000 L circulating seawater tank at 15-minute intervals, and the results are displayed in the top panel of Figure 4, which confirms the Aanderaa probe's rapid response with sufficient flow through the conductivity cell.

Despite the precision and stability of the SBE 37, the post-processing of the Aanderaa 4319 data was ultimately done via validation of discrete bottle samples due to the possibility of long-term drift in the SBE 37. Holding the bottle sample values constant over the testing period, ratio plots of the measured (S_{meas}) to discrete values (S_{disc}) in the bottom half of the three panels in Figure 4 display the consistent relationship across a salinity range of 0.4 units when the controller temperature is stabilized, and thus the salinity, to generate an applicable gain factor, C_g, for future field deployments defined in Equation 2.

$$C_g = \frac{\sum_{i=1}^{n} \frac{S_{meas_i}}{S_{disc_i}}}{n} \tag{2}$$

The Bland-Altman plot of the raw values (Aanderaa 4319 salinity - bottle sample salinity) was created to identify an offset correction value, C_o, as comparison. The ensuing residual plots for both correction procedures denote a slightly lower root mean squared (RMS) value for the offset method ($\pm$0.037 in contrast to $\pm$0.039 for the gain corrected method), yet the resulting differences between the two correction procedures for field deployment measurements are marginal (Figure 5). Previous work to post-process salinity from inductive sensors has also employed a gain correction (Roquet et al., 2011). As stated previously, because inductive conductivity cells are dependent on the fluid velocity through the sensor's magnetic coils and other ambient electrical signals, any variation to the original spatial configuration that alters the flow cell and its properties (end cap of the WavepHOx housing and the neighboring sensors) requires a manual recalculation of the linear value that describes the relationship between conductance (mS) and the conductivity (mS/cm) (AADI, 2013; Kang Hui et al., 2020). For these reasons, the simple gain factor was chosen to rectify the Aanderaa 4319 raw salinity output to obtain a corrected value for salinity, S_{corr}, as described in Equation 3.

$$S_{corr} = \frac{S_{meas}}{C_g} \tag{3}$$

Where S_{meas} is the salinity output measured by the Aanderaa 4319 probe and C_g is the gain correction factor of 1.006. The accompanying RMS value for the residual plot for the gain correction ($\pm$0.039) functions as the error for the sensor. This demonstrates that at the salinity values I would typically encounter in the nearshore environment outside of the desalination plant (35 - 33), the Aanderaa 4319 probe fares well and just a simple gain correction could be applied to the sensor output to match the discrete bottle samples taken from the field site with high repeatability.

To ultimately describe the spatiotemporal sampling error between bottle and sensor measurements, we examined the propagated uncertainties for the Aanderaa 4319 sensor resolution (e_s) and the Mettler Toledo density meter (e_{DM}) via the addition rule to reach a value of $\pm$0.033 and subtracted that from the RMS of the residual plot for the gain correction ($\pm$0.039) to arrive at an error of $\pm$0.006. This confirms the notion that there lies an extra amount of uncertainty when post-processing the data solely based on discrete bottle measurements as the propagated uncertainty carries through the data collection method from the bias of the density meter values. One possible reason for this spatiotemporal sampling error to be relatively small is the ambling nature of salinity transmission in the ocean as it is not a highly dynamic process and not largely affected by biogeochemical factors.

For the subsurface measurements performed with the CastAway, an offset was implemented to all salinity profile values. This offset was found by subtracting the surface CTD measurements from the nearest ten corrected salinity values from the WavepHOx.

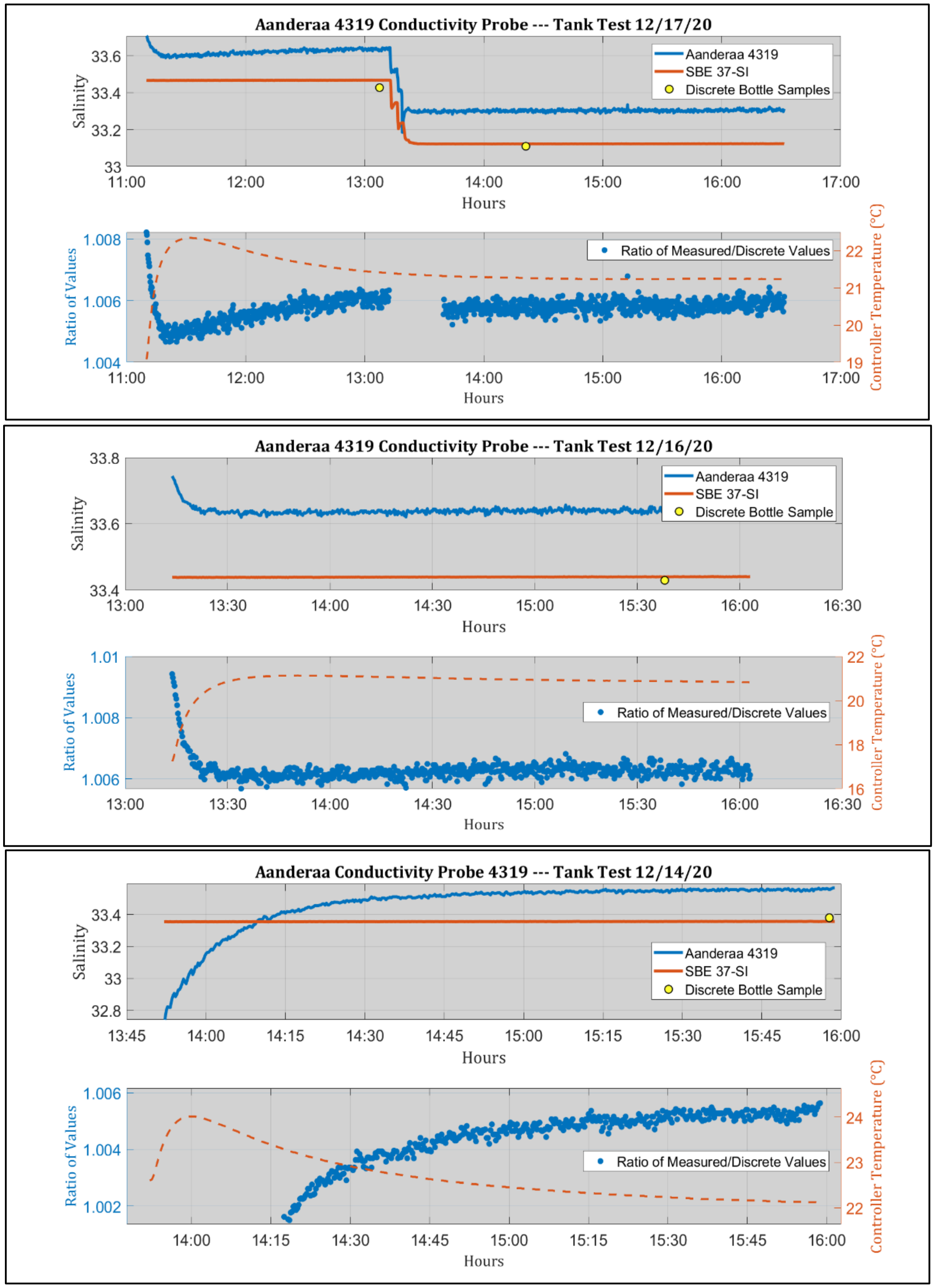

Figure 4 Three representative seawater tank tests of the Aanderaa 4319 conductivity sensor alongside the SBE 37 conductivity sensor, including a discrete bottle sample during each test. The bottom half of each panel shows the ratio of the 4319 measurement to the discrete bottle sample from which C_g was derived (Equation 2), and the controller temperature that strongly influences the sensor output before stabilization. The dilution test (top panel) was performed on December 17th, 2020.

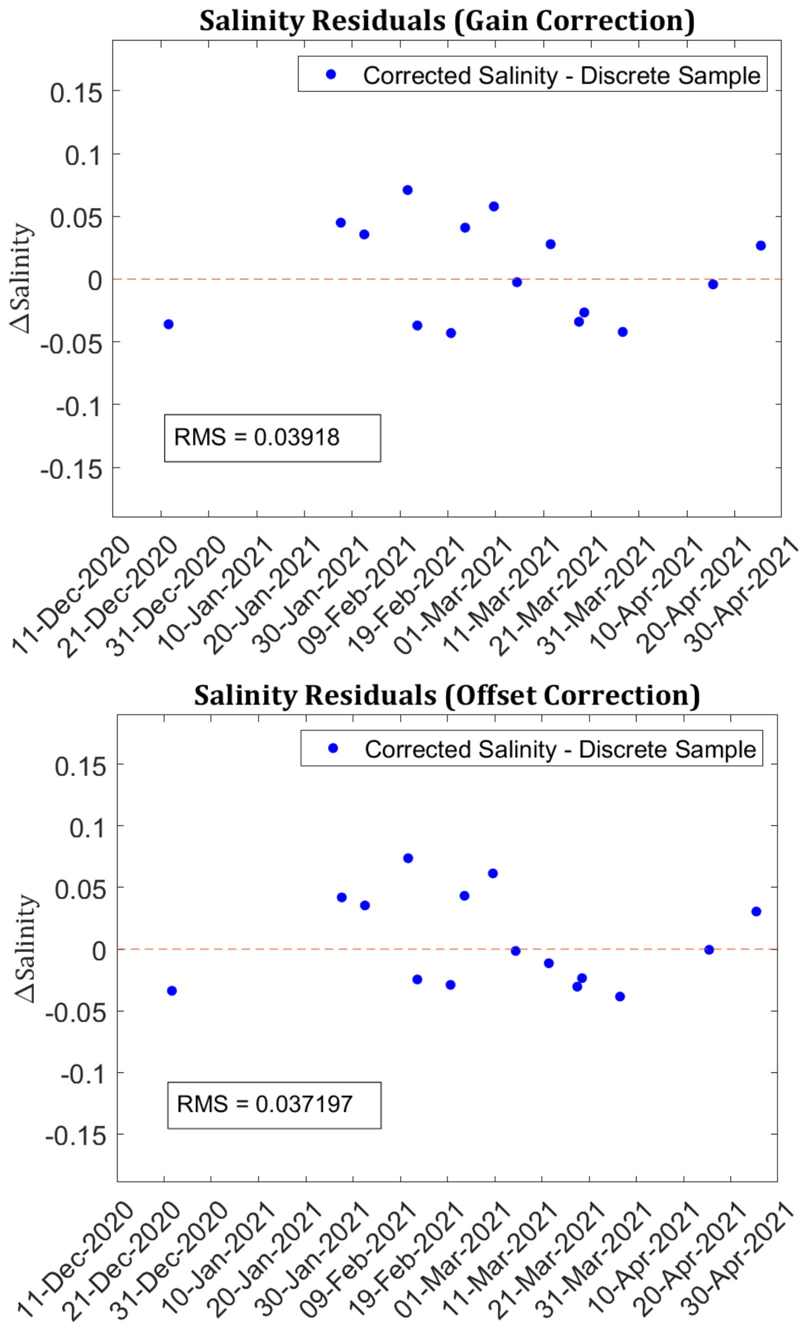

Figure 5 The residual plots of the two correction procedures. The gain correction procedure (top) utilizes C_g which was calculated by dividing the stable salinity measurements in a controlled tank by the discrete bottle samples of the same solution and averaging the quotients over three tests. This resulted in an RMS value of $\pm$0.039. The offset correction procedure (bottom) utilizes C_o which was calculated from a Bland-Altman plot to find the average offset from the discrete bottle samples from the same three tests, with an RMS value of $\pm$0.037.

3.2 Field Data

To visualize the data, I experimented with two different weighted grid mapping techniques in MATLAB and Ocean Data View (ODV) to exhibit the sea surface chemistry within reason. Inverse distance weighting (IDW) and Ordinary Kriging (OK) are commonly used methods for mapping in many geophysical applications (Zarco-Perello & Simões, 2017). IDW assigns weights to each data point as a function of how many neighboring points there are or from a predefined distance, whereas OK uses the data to calculate a function to fit the variogram and employs it to redistribute the data for contour mapping. The resulting maps produced with distance weighting proved to be of higher quality due to its ability to assign a spatial gradient to the distance for each data point (Langella, 2021; Schlitzer, 2015). This was verified by the accepted knowledge that OK typically works best in practice with very high data density which I did not have.

Figure 6 displays the time series along with the ODV generated maps of the various sensor outputs for the deployment of March 18th 2021 where a strong signature of a high salinity, high temperature plume was detected from the outfall of the desalination plant. The length scale limit for the data to be extrapolated of 2.7 was employed per suggestion of best practices for ODV gridding methods (Schlitzer, 2002). The remaining timer series-contour plots can be found in Appendix C**: Supplemental Plots and Figures**.

A comparison of typical sea surface salinity values from the nearby Del Mar buoy to my measured values at the study site is denoted in the example in Figure 7, which helps identify verifiable ambient values for my excursions. These density functions express what we would expect in this scenario, with higher measured values than the nearby salinities of the local coastal region due to the desalination discharge, but lower than buoy data on days where I paddled near the mouth of the lagoon in a near gaussian or bimodal distribution. The remaining empirical and probability density distributions are found in Appendix C**: Supplemental Plots and Figures**.

Figure 6 Time series (left) and surface contours (right) for the March 18th, 2021 survey. The inset plot in the time series denotes the deployment time in reference to the respective daily tidal cycle. The outfall of the desalination plant is located in the top of the contour maps. In this particular survey, a plume appears to be emanating southward.

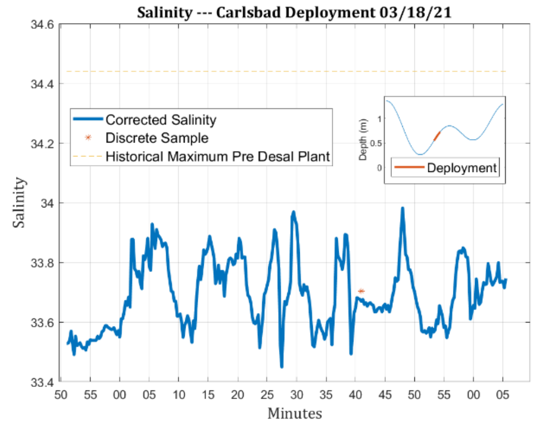
Salinity --- Carlsbad Deployment 03/18/21
Salinity
Minutes
Corrected Salinity
Discrete Sample
Historical Maximum Pre Desal Plant
Depth (m)
Deployment

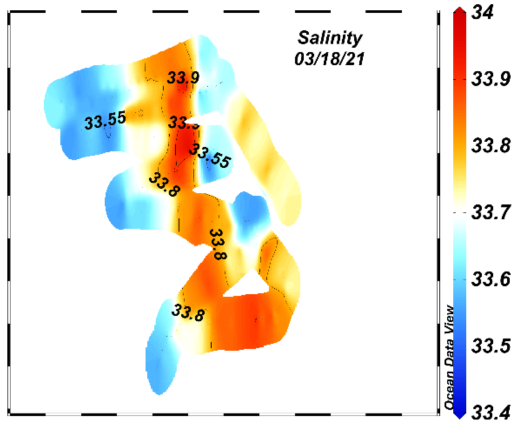
Salinity
03/18/21
33.9
33.55
33.55
33.8
33.8
33.8
Ocean Data View
34
33.9
33.8
33.7
33.6
33.5
33.4

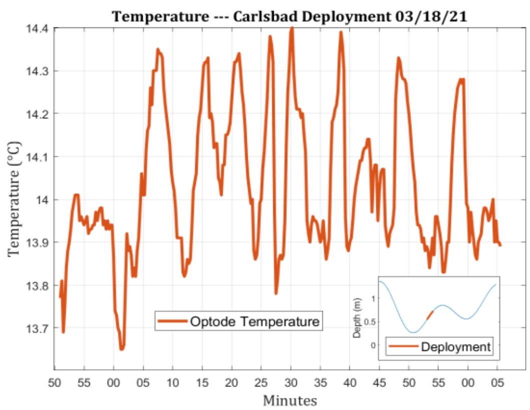
Temperature --- Carlsbad Deployment 03/18/21
Temperature (°C)
Minutes
Optode Temperature
Depth (m)
Deployment

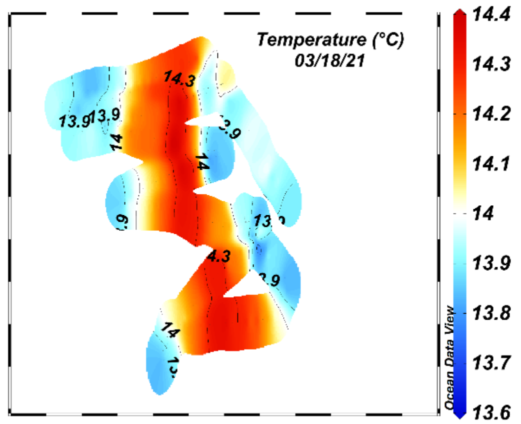
Temperature (°C)
03/18/21
14.3
13.9
13.9
14
14
14
Ocean Data View
14.4
14.3
14.2
14.1
14
13.9
13.8
13.7
13.6

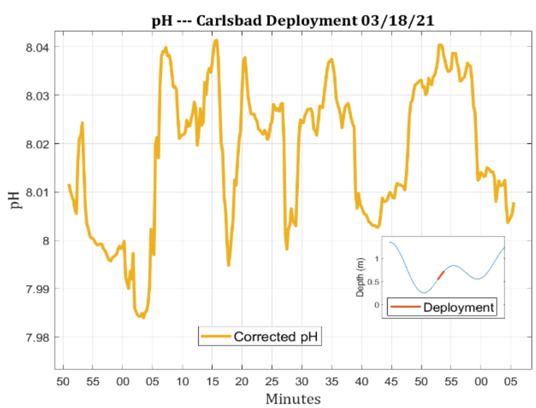
pH --- Carlsbad Deployment 03/18/21
pH
Minutes
Corrected pH
Depth (m)
Deployment

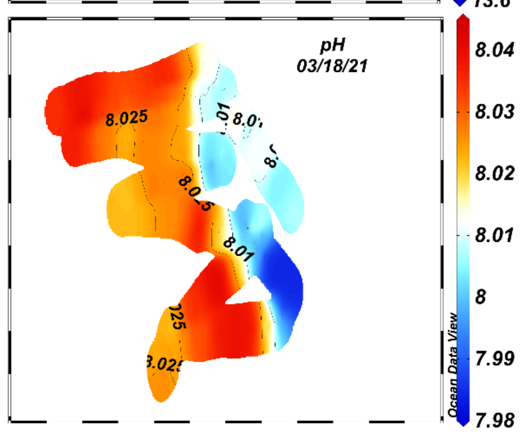
pH
03/18/21
8.025
8.01
Ocean Data View
8.04
8.03
8.02
8.01
8
7.99
7.98

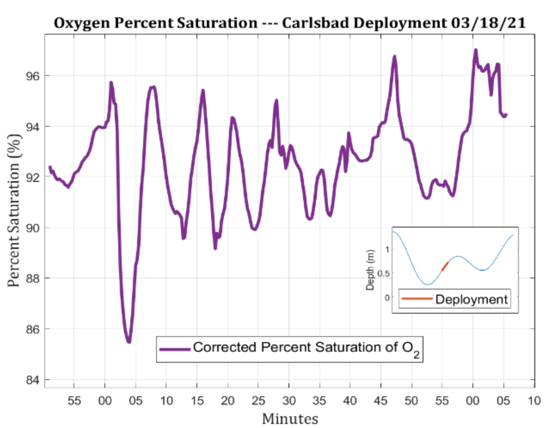
Oxygen Percent Saturation --- Carlsbad Deployment 03/18/21
Percent Saturation (%)
Minutes
Corrected Percent Saturation of O2
Depth (m)
Deployment

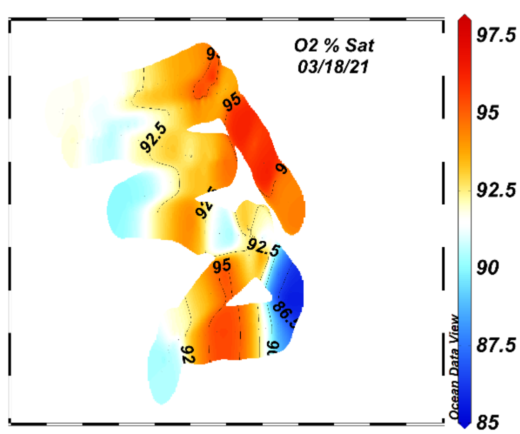
O2 % Sat
03/18/21
95
92.5
92.5
95
92
Ocean Data View
97.5
95
92.5
90
87.5
85

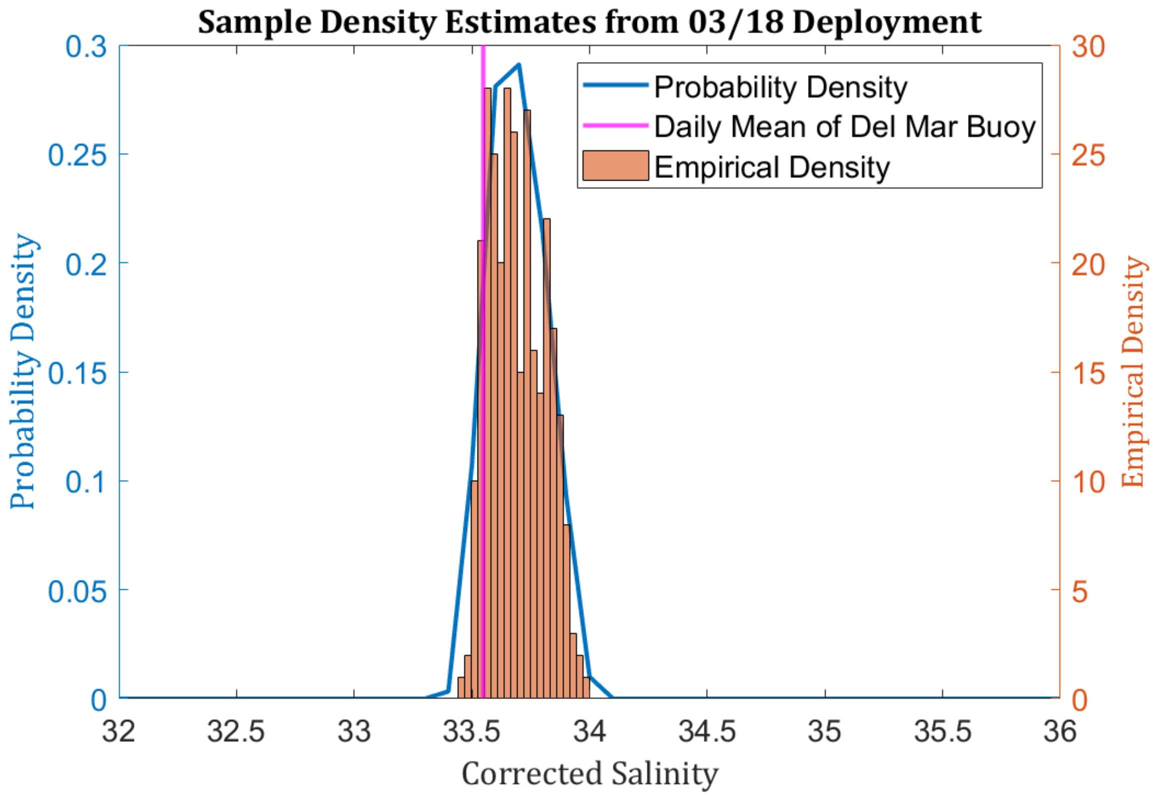

Figure 7 The probability density function overlayed on the empirical density (histogram) for the deployment on March 18th, 2021. The daily mean extracted from the nearby Scripps-operated Del Mar buoy denotes the ambient value for surface salinity as a reference (# of bins = 20). The histograms for other deployment days are found in Appendix C.

DISCUSSION

4.1 Dynamics of Plume

The contour maps in Appendix C display an array of scenarios for the desalination plant's discharge into the nearshore environment. These surveys were performed over an area that was roughly 1 km^2 and the spatial resolution of the WavepHOx allowed for the analysis of the dynamics to discern the plume varies in distinct patterns. Encompassing Carlsbad, the Oceanside Littoral Cell (OLC) is described as a local current that regularly transports sediment from Dana Point down to La Jolla Point, where surface and subsurface waters in this coastal region are subject to southward bound water masses (Young & Ashford, 2006). From our initial deployments where I paddled in an area north of the mouth of the lagoon, I was able to deduce that any plume in this area, fresh or saline, would radiate outwards before begin travelling south. Because of this, a finalized transect was implemented to maximize deployment time in a region with highest salinity gradients. This was verified by the contour maps in later surveys where high saline signatures were visible south of the desalination plant's outfall, and no other sources of high saline water exist in this region. These high values in the southeast corner could indicate entrapment within the rocky reef structure that borders the southern edge of the transect.

Although I observed a strong correlation between areas of higher than ambient salinity with areas of higher than ambient temperature, there were deployments where the suspected plume was not the water mass with the highest temperature. On the March 19th deployment, there is a large region in the northern part of the transect that contains ambient salinity values (~33.55) but is also markedly warmer ($+0.7^{o}C$) than the mean values for that day (mooring.ucsd.edu). Yet, there are noticeable areas in the southern edge of the contour map that correspond with ambient values for that day, giving rise to the possibility of three water masses interacting over the transect. In addition to the SWRO discharge water and the surrounding regular ocean, this high temperature, ambient salinity water could be stemming from the AHL inlet north of this transect, as observed in previous deployments. This propagation of ~600m down the coast line is reasonable since the deployment on March 19th occurred at a tidal stage approaching slack high, giving ample time for the water mass to follow the OLC southward since ebb tide.

Another interesting aspect of the plume was the slight disparity in the distribution of temperature and salinity. Ideally, the contours of these parameters should match up spatiotemporally as the NRG's Carlsbad Energy Center emanates a unique water mass with high temperature and salinity. The deployment of March 18th has a fairly linear and continuous temperature plume southward whereas the saline signature is vaguely more jagged. A likely possibility of this incongruity is due to how each sensor measures its parameters. The Aanderaa optode, used for temperature and oxygen measurements, is essentially a photo diode that analyzes the water inside the WavepHOx end cap; whereas the Aanderaa conductivity probe is picking up a signal that travels through the inductive cell within the WavepHOx end cap, potentially adding an extra amount of residence time, and thus lag, for fluids that pass through the sensor package housing. This factor is dependent on paddle velocity, among other spatial configurations, and has not yet been quantifiable. Despite this, the spatiotemporal differences were still small enough to distinguish a plume propagating into the ambient ocean. A surface temperature signature was prevalent on more days than that of salinity, but there is clear evidence that there are two to three bodies of water that interact in this area from a variety of angles.

For further examination of water differentiation in a more chemical scope, property-property plots of pH vs. percent saturation of oxygen (O_2 % Sat), with the third variables of salinity and temperature for chromatic reference, were created and two examples of such are shown in Figure 8. O_2 % Sat was calculated using Equation 4, and it is also outlined in Garcia and Gordon, 1992.

$$O_2\ \%\ Sat = \frac{O_{2_{meas}}}{O_{2_{Sat}}} \tag{4}$$

Where $O_{2_{meas}}$ is the salinity and temperature-corrected oxygen concentration from the optode output ($\pm 3\ \mu M$), and $O_{2_{Sat}}$ is the oxygen concentration at 100% saturation derived from temperature and salinity (Garcia & Gordon, 1992). Overlaid the property-property plots are slopes that describe the potential effects of a few biogeochemical processes that I would expect in this region (photosynthesis-respiration, salinity change, temperature change). These are quantifiable models because over a range of temperatures and salinities, CO_2 equilibrium chemistry describes how pH will react to these shifts in values (Dickson et al., 2007; Lewis et al., 1998). Similarly, impacts on O_2 solubility from these same environmental changes are well studied (Cumming, 2003; Lange et al., 1972; Limburg et al., 2020). To quantify the effects of photosynthesis and respiration in this scenario, a particular amount of calculable CO_2 in the inorganic form (DIC) is added/removed that corresponds to a specific decrease/increase in pH. The resulting O_2 concentration then must shift to remain Redfieldian (Figure 13). The average induced fluctuations in DIC for my data are $\pm 25\ \frac{\mu mol}{kg}$, which are well within reason for the nearshore environment (Liu et al., 2021; McLaughlin et al., 2018).

There was not a consistent pattern between surveys, but days that indicated a high salinity, high temperature plume also displayed a bimodal distribution of pH vs. percent saturation of oxygen. A common distribution among these figures was along the photosynthesis-respiration line that seemed to follow higher temperatures as pH and percent saturation of oxygen increases. This can be reasoned with the fact that the brine from the SWRO process mixes with the biologically active lagoon water and pools in a reservoir filled with sargassum (*Sargassum horneri*) and feather boa kelp (*Egregia menziesii*) where it can locally increase O_2 and pH, analogous to the common tide pool diurnal photosynthesis-respiration example.

However, because this data comprises of a mixture between two to three water masses in a highly dynamic environment, fine scale models are extremely complex and difficult to predict.

The profiles in Figure 9 denote that there was a definitive subsurface saline signature just offshore of the outfall, but not enough casts were performed to see the subsurface extent of this plume. Interestingly, the WavepHOx measurements for the March 19th survey did not indicate a surface signature of the plume, and a further analysis of the weather conditions for that day denoted a lower-than-normal wind and wave energy, which still raises questions on the feasibility of a decapitation event. The deployment on April 15thcontained eleven casts at varying depths (4.3m – 12.43m) and the subsurface values did not indicate a strong gradient from the surface measurements (Figure 10). However, the overall structure of the profile has higher salinity values than ambient (1.5%) except for the deepest parts of the casts. A likely possibility for this profile stems from the plume’s higher temperature signature inducing a lower density while the less saline, but colder water from depth can wedge itself toward the beach in the nearshore along the seabed.

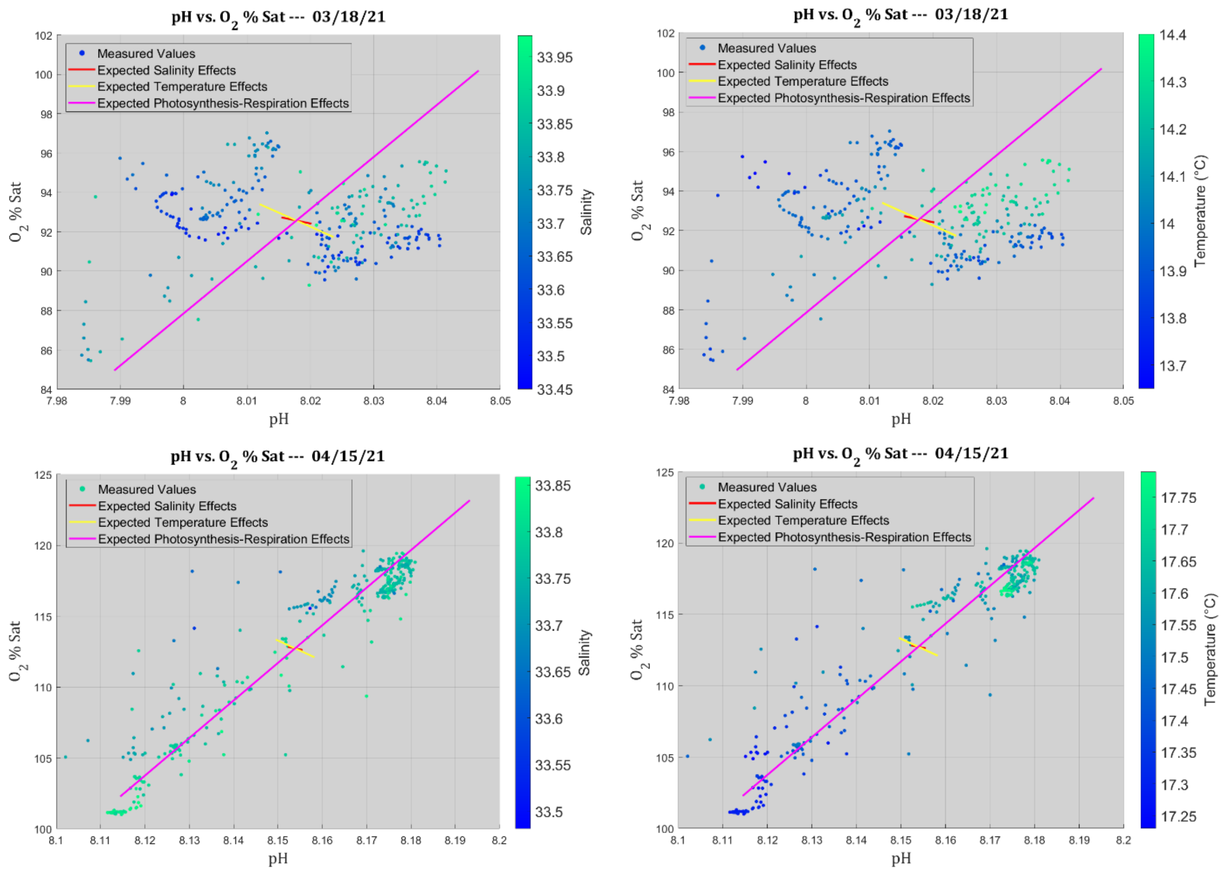

Figure 8 Property-property plots of pH and percent saturation of oxygen for two different deployment days, Marth 18th, 2021 (top) and April 15th, 2021 (bottom), with salinity (left) and temperature (right) as third variables for chromatic reference. The slopes for the expected effects of biogeochemical processes in this region are also plotted and centered on the mean for both axes.

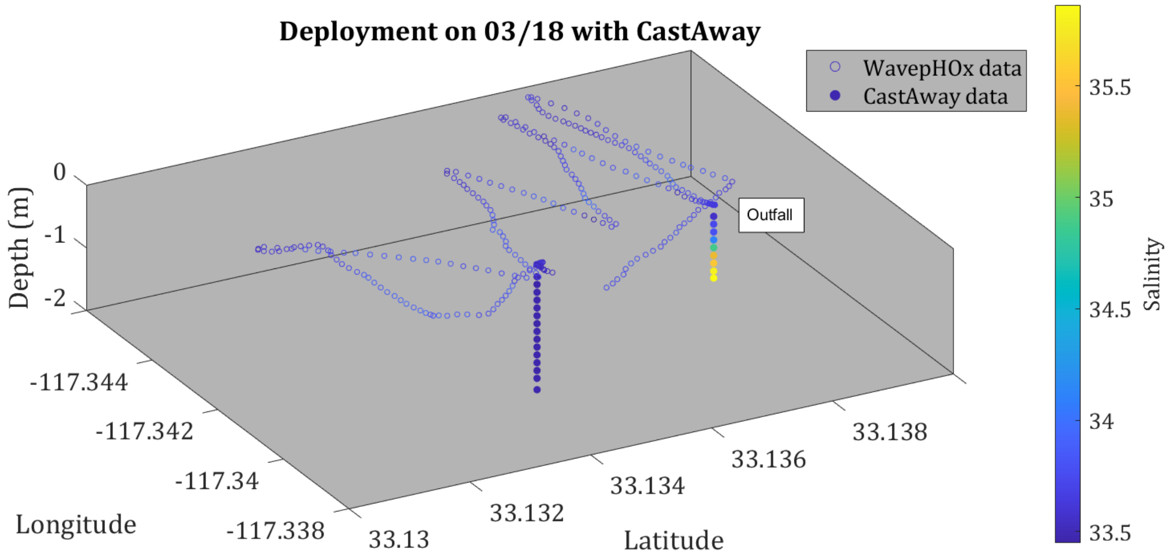

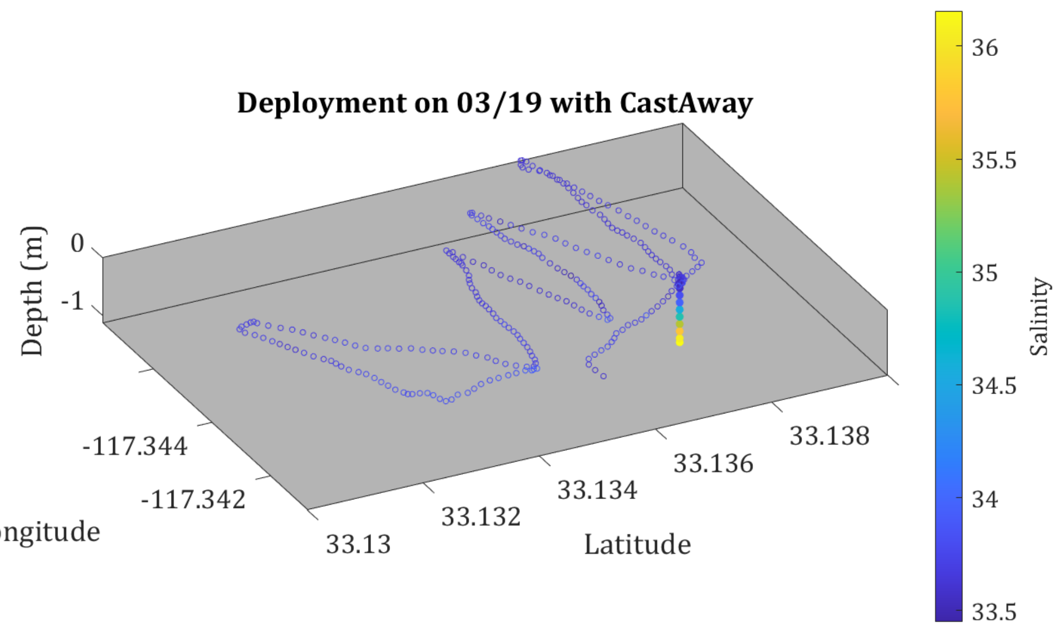

Figure 9 Surface deployments on March 18th and 19th, 2021 with CastAway profiles near the mouth of the outfall. Surface values for the cast salinities were offset to match the average surface values for the WavepHOx. The WavepHOx measurements on March 18th displayed a larger surface plume than the March 19th deployment, but both subsurface profile denoted near maximum values that we would expect from the desalination discharge (36.1). The day of the March 18th survey was characterized with higher wind and wave action. Depths are not to scale and are enlarged for better analysis.

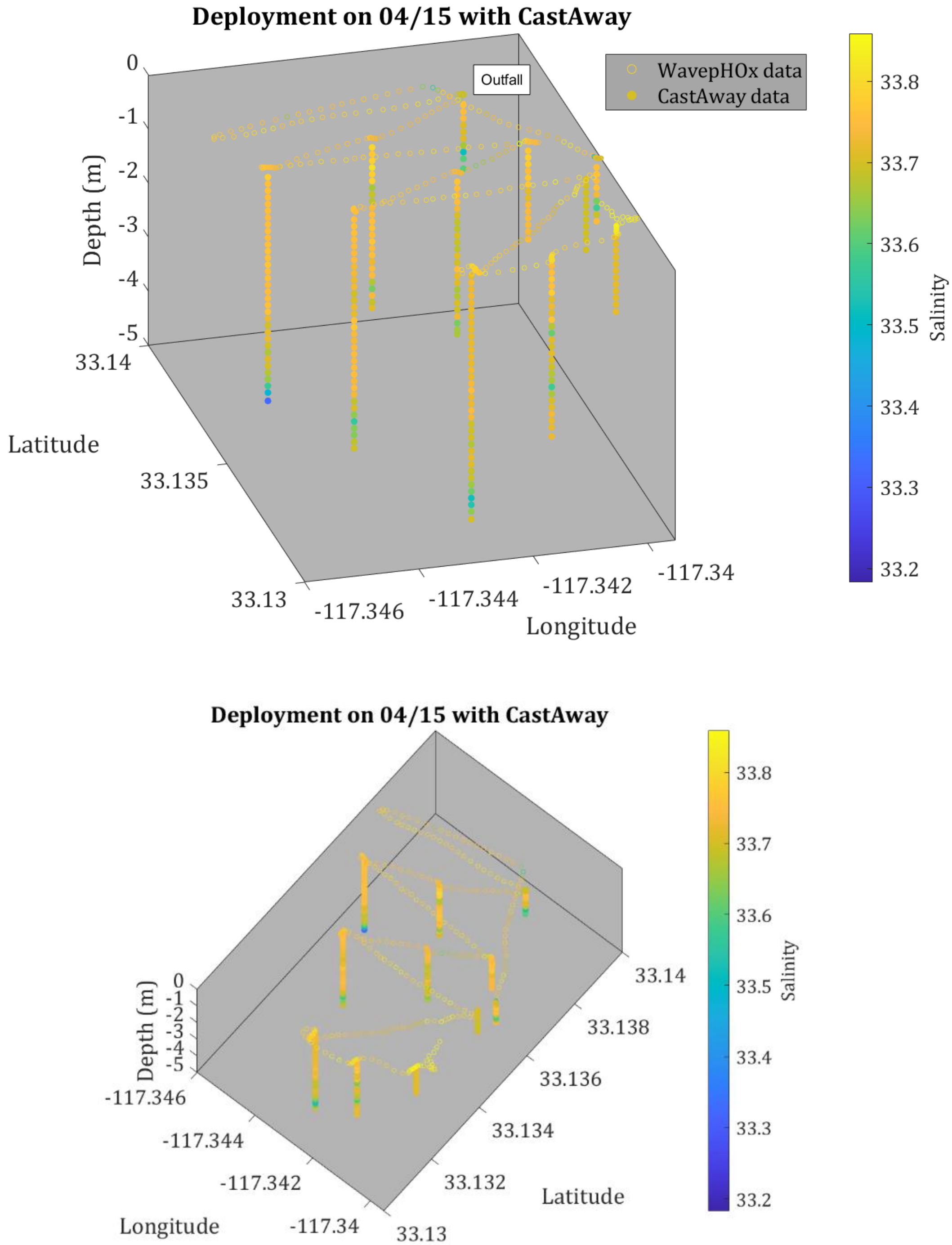

Figure 10 Surface deployment measurements on April 15th, 2021 with eleven CastAway profiles at varying depths. Near uniform water column except for lower values along the seafloor. Two angles are shown for a full perspective view. Depths are not to scale and are enlarged for better analysis.

4.2 Recommendations for Future Work

One of the main challenges in this study was quantifying the temperature influence of the internal controller of the WavepHOx on the sensor outputs. Upon commencing deployment mode for continuous sampling, the internal temperature recorded on the embedded ARM board would begin to ramp upwards before ultimately stabilizing ~6 ºC above the temperature recorded by the sensors (Figure 4). Hence, the conditioning time in the temperature-controlled water bath before each survey was required in order to begin each survey at a stabilized internal temperature. Not only did this ramping impact the sensors' temperature, but calculations of salinity using a stable proxy temperature and the sensor generated conductivity with the GSW Toolbox that resulted in nearly identical values to the original salinity output indicated that electrical signals in the probes were directly affected. This thermal response was not driven by an external gradient but an internal thermal warm-up time. Attempts to define this influence on the salinity output involved decomposing the dependent variables, internal temperature and sensor temperature, outlined by the NIST drift correction procedure, but the characterization proved to be too complex to quantify and the conditioning time in the cooler was acceptable to mitigate this problem altogether (Salit & Turk, 1998). Despite this, travel time between laboratory setup and survey site entry cause a small (~5 minute) temperature ramp before stabilization and the discarding of that data created higher variability in my mapping figures.

For a more comprehensive characterization of the sea surface chemistry, a denser transect would induce a higher spatial resolution, but temporal variability would also need to be further examined because the current method of data collection would allow for external environmental parameters (diurnal temperature change, tidal shifts, etc.) to play a larger role in trends of the data. An enhanced depiction of the salinity distribution in the water surrounding the outfall requires a refined model for the fluid residence time in the Aanderaa 4319 conductivity probe's inductance cell as a function of paddle velocity to quantify the slight variations in sensor response time during deployments, as current flow simulations of the WavepHOx have only accounted for flow in the end cap housing that encases the sensors. Additionally, a more integrated procedure for the CastAway to sample in added locations would render a fuller three-dimensional profile of the salinity plume.

CONCLUSION

This study demonstrated the efficacy of the WavepHOx and a data collection method to map sea surface chemistry in the nearshore environment through the characterization of the CDP discharge plume. The data exhibit that after quality control procedures, the modified sensor package can detect a distinct surface water mass, marked by higher-than-normal coastal salt concentration, emanating from the outfall of the CDP with a salinity uncertainty of $\pm$0.039. Subsurface measurements with a handheld CTD indicated that a water mass with high salinity (36) was detectable at depth even on days without a strong surface signature. The ability to resolve fine-scale surface gradients allowed me to deduce that the discharge plume does not contain the salinity to cause severe osmotic stress, but the concentration of other constituents such as antiscalants and coagulants are still unknown. The ability to capture rapid physical and biogeochemical processes to a high spatiotemporal degree at a relatively low cost and efficient manner paves an innovative way for ocean scientists to accurately map the nearshore environment.

APPENDICES

Appendix A: Density Meter Best Practices

Mettler Toledo DM45 Density Meter

This document outlines measurement procedures for the determination of seawater salinity using the Mettler Toledo DM45 Density Meter. The typical calibration involves a calibration to deionized water (DIW) as outlined in the factory-supplied manual; followed by periodic verification of salinity (or density) from IAPSO salt standards. In general, salinity should be expected to agree to the IAPSO water better than 0.03.

This instrument is capable of measuring samples in a density range of 0 – 3 $\frac{g}{cm^3}$ with a resolution of 0.00001 $\frac{g}{cm^3}$, and in a temperature range of $0 - 91^oC$ with a resolution of 0.02^oC. Using these values and obtaining a pressure measurement to calculate a practical salinity with the Matlab Gibb's Seawater Toolbox that employs TEOS-10, these resolutions correspond to an uncertainty of $\pm$ 0.023 on the PSS-78 scale.

Mettler Toledo designates the different settings on this instrument as "Methods". There are three common Method Types (Measurement (MS), Test (TE), Adjustment (ADJ)); however, only Measurement and Test types are required for each day of use.

<u>Start-up</u>

Upon using the density meter (DM45) for the first time of that day, navigate to the home screen (above) and press Methods/Products and select Methods.

There several different methods stored in the instrument, but only three types. Select the Test method type with ID "TEST1" and Title "DIW TEST". The DM45 should already be in this setting from the previous day of use but it is good practice to select this method type at the beginning of each day.

This method is verifies if the instrument is working properly by returning a good value for DIW (e.g. 0.99820 $\frac{g}{cm^3}$ at 20.00^oC) within the tolerance range that is defined by the instruction manual (0.0003 $\frac{g}{cm^3}$).

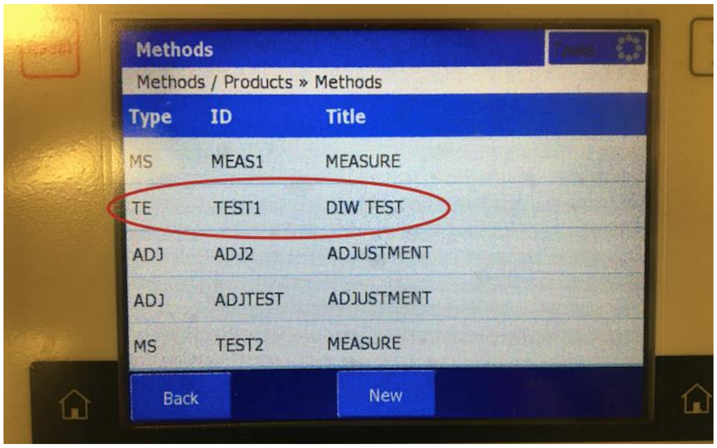

The labeled syringes adjacent to the DM45 are to be used with the corresponding item going into the cell. Use the one labeled "DIW" (deionized water) to extract 10mL of DIW from the Barnstead Nanopure filtration system in the beaker next to the instrument. Flush it through the cell and repeat two more times before you press "START" on the method. Press OK when the "Add Sample" window pops up.

Once the test is done, a deviation number should appear below the measured density of the DIW. Write both of those numbers down for record keeping. Press OK through all the other prompts until you return to the home screen.

Sample Measurements

To measure samples, press Methods/Products and select Methods. Now select Measure method type with ID "MEAS1" and Title "MEASURE", which uses the most recent calibration.

For the first measurement of the day, flush the sample three times through the flow cell before your first measurement to yield best results. Wait a few minutes for the cell to stabilize at 20.00^oC. Press START to begin measurement.

Repeat several times to get a substantial amount of sample values. Convert from $\frac{g}{cm^3}$ to $\frac{kg}{m^3}$ for entry into the GUI. The Matlab GUI (below) performs a calculation derived from the TEOS-10 to arrive at an absolute salinity from a controlled pressure, temperature and density, and converting that to practical salinity from the given parameters.

Only flush cell with DIW if you have different samples you want to compare. DIW flushes between the same samples will give slightly lower values. If you do flush with DIW, make sure you then flush with the next sample several times before taking another measurement.

Once the last sample has been measured, flush the cell with DIW twice and proceed to Test Method.

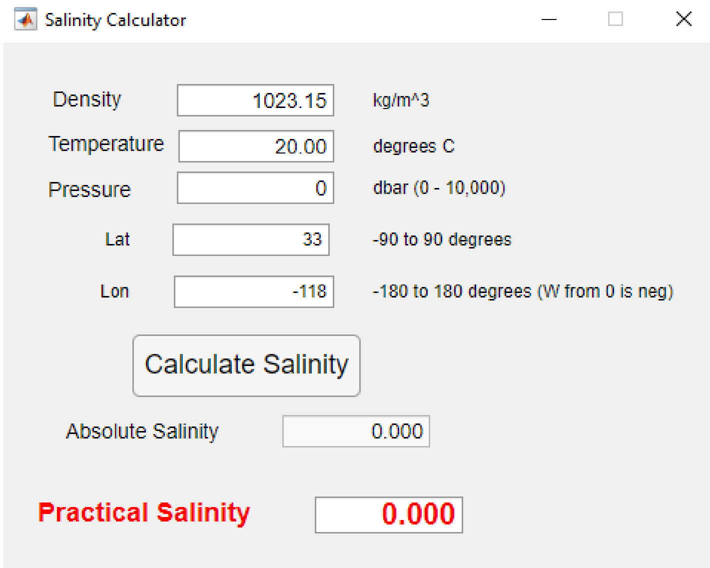

Test Method and Cleaning

From the home menu, select Methods/Products → Methods → DIW Test

Should the test not pass, an error will arise. If it passes, the DM45 will signal to drain the cell. Hit OK.

Flush again. Hit OK.

It will then indicate a rinse with Acetone. Make sure to have a different receptacle to absorb the acetone and place the outlet tube in it. Use the Acetone syringe and inject 10mL into the cell. Clean off the syringe and the area around the inlet opening so no Acetone is visible or left lining the inside cap. Hit OK.

A dry rinse is the final step. An aquarium pump connected to a Drierite tube is located on the same table that can be placed into the DM45 inlet. Insert and leave there for 3-5 minutes. Remove and turn off pump.

Should the test not pass, you will still need to clean, and try the test again. If it does not pass after three cleans, clean the fourth time and you will need to perform an Adjustment Method.

Adjustment Method

This is the “setup calibration” and should not have to be done more than once if the DM45 is regularly cleaned or a new type of sample (not water) is going to be measured.

If the Test Method has failed three times, click the Adjustment Method with ID “ADJTEST” and follow the steps for the first standard (DIW). The next standard entitled “Standard2” is an empty cell after it has been cleaned. Run it and it should reset the values.

If this is an Adjustment Method for a new type of sample, read the instruction manual on what the tolerances should be set to and create a new standard under:
Setup → Adjustments/Tests → Adjustments → New

Create the Adjustment Test for desired standard or substance you will need. Return to the home screen and input the parameters to which the instrument should calibrate the standard by selecting Methods/Products → Methods → [Adjustment Method you just created]. Toggle through the numbered tabs to customize the method.

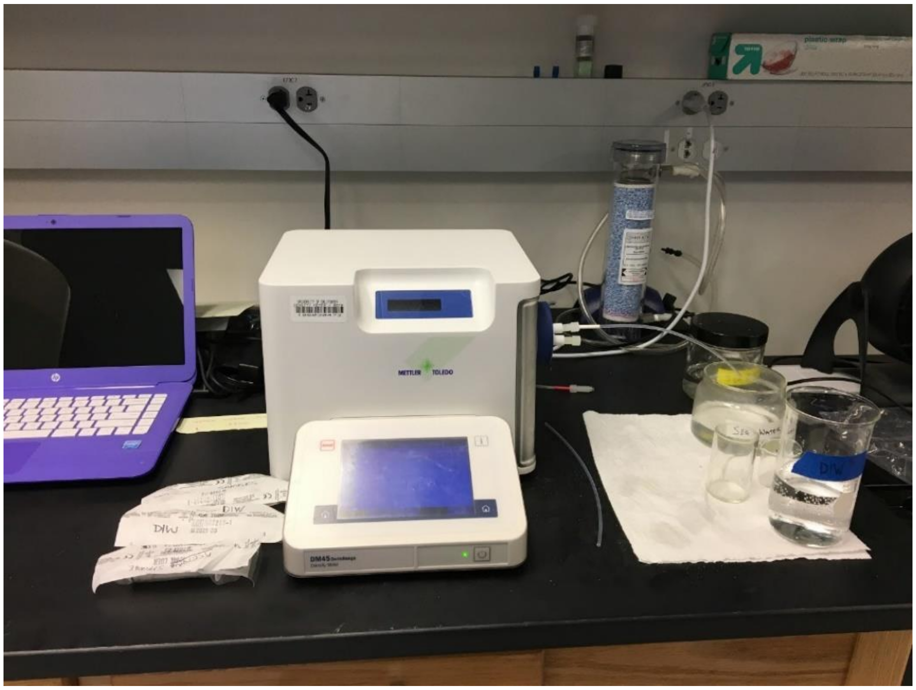

Appendix B: WavepHOx Deployment Protocol

WavepHOx Deployment Protocol

This document serves to provide a guide to deploy the WavepHOx to ensure the most accurate data collection and post-processing techniques, particularly to mitigate the internal temperature influence on the sensors' outputs. These methods are found to be best suited for nearshore environments through previous deployments and were last updated April 13th, 2021.

The Day Prior

Cooler Setup:

- Fill up cooler with sea water from spigot outside of MESOM
- Hook up cooler to water bath and set water bath temperature to 1º C **less** than the predicted value of sea surface temperature of survey site found via windy.com or other reliable SST data repository
- Replace batteries of WavepHOx, remove NPT plugs, set to sleep and place inside of running water bath/cooler setup overnight

The Day of Deployment

WavepHOx Configuration:

- Take WavepHOx out of cooler
- Align time with Garmin Marine Watch
- Set sample interval to 15s
- Set pH sample averaging to 5
- Deploy and place back into cooler

Lab Measurements Pre-Deployment:

- Turn on spectrophotometer system and wait ~30 min for warm up
- Run 3 junk seawater samples to ensure repeatability of measurements
- Extract sample from cooler and record time
- Run 3 tests in the density meter with the sample from cooler and record salinity with Matlab GUI
- Run spectrophotometer system 3 times with sample
- Bilge enough cooler water to a smaller (and more mobile) cooler so that the WavepHOx can be placed there fully submerged. Add small ice pack to smaller cooler to prevent controller temperature ramp while in transit to survey site

Deployment:

- Upon arriving at study site, firmly place WavepHOx on the Velcro-side of the paddleboard until you hear a loud click
- Enter the water in the safest area possible. Once past the break, begin the GPS tracking on the Garmin Marine Watch
- Paddle to a waypoint that is either furthest south or north along the coast. Then paddle directly offshore, perpendicular to the beach for a second waypoint
- Then paddle in a zigzag manner to third waypoint that is located cardinally opposite of the first waypoint (i.e. first waypoint at NE corner, third waypoint will be at SW corner)
- Paddle directly back towards the beach for a fourth waypoint

- Paddle parallel to the shore as close to the break as deemed safe until you reach the approximate spot of entry
- Stop GPS tracking
- Exit water and place WavepHOx into cooler in car

Lab Measurements Post-Deployment:

- Return to the lab and immediately place the WavepHOx back into the original cooler with the water bath connected to it
- Wait about 15 minutes and extract samples for the density meter and spectrophotometer and record the time
- End deployment on WavepHOx

Deployment(Carlsbad specific):

- For the Carlsbad Desalination Plant study site, enter just south of the power station inlet along Hwy 1
- Place paddleboard with WavepHOx strapped underneath in water. Once past the break, begin GPS tracking on Garmin Marine Watch
- Paddle to the farthest SE waypoint and make your way in a direct line to the farthest SW waypoint (refer to Figure 2.1)
- Paddle in a zigzag manner to third waypoint, which is the farthest NW waypoint
- Paddle directly to beach to the fourth waypoint, which is also the farthest NE waypoint and just north of the inlet
- Paddle parallel to the shore as close to the break as deemed safe until you reach the approximate spot of entry
- Stop GPS tracking
- Exit water and place WavepHOx into cooler in car

NOTE: You may take casts and bottle samples at any point along the way during deployment

Appendix C: Supplemental Plots and Figures

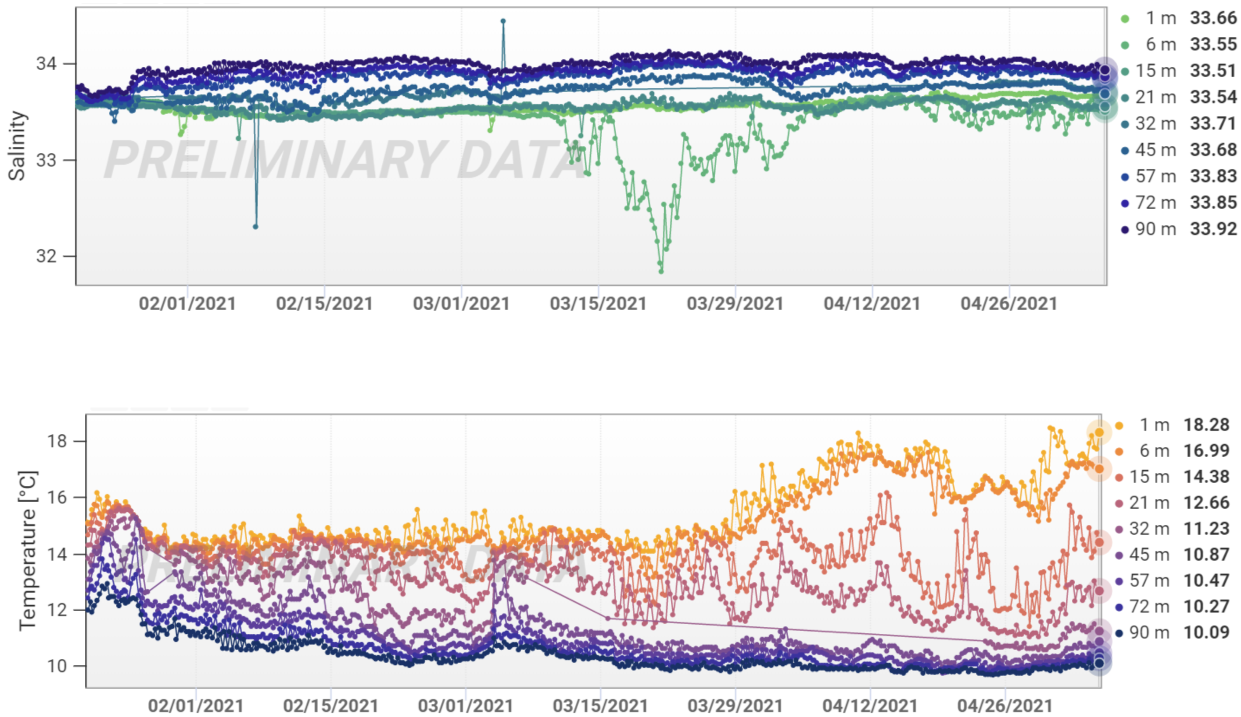

Figure 11 Time series of salinity and temperature from the Scripps Institution of Oceanography's Ocean Time-Series Group for the Del Mar buoy at various depths during the duration of field deployments. Extracted from the publicly available mooring.ucsd.edu website.

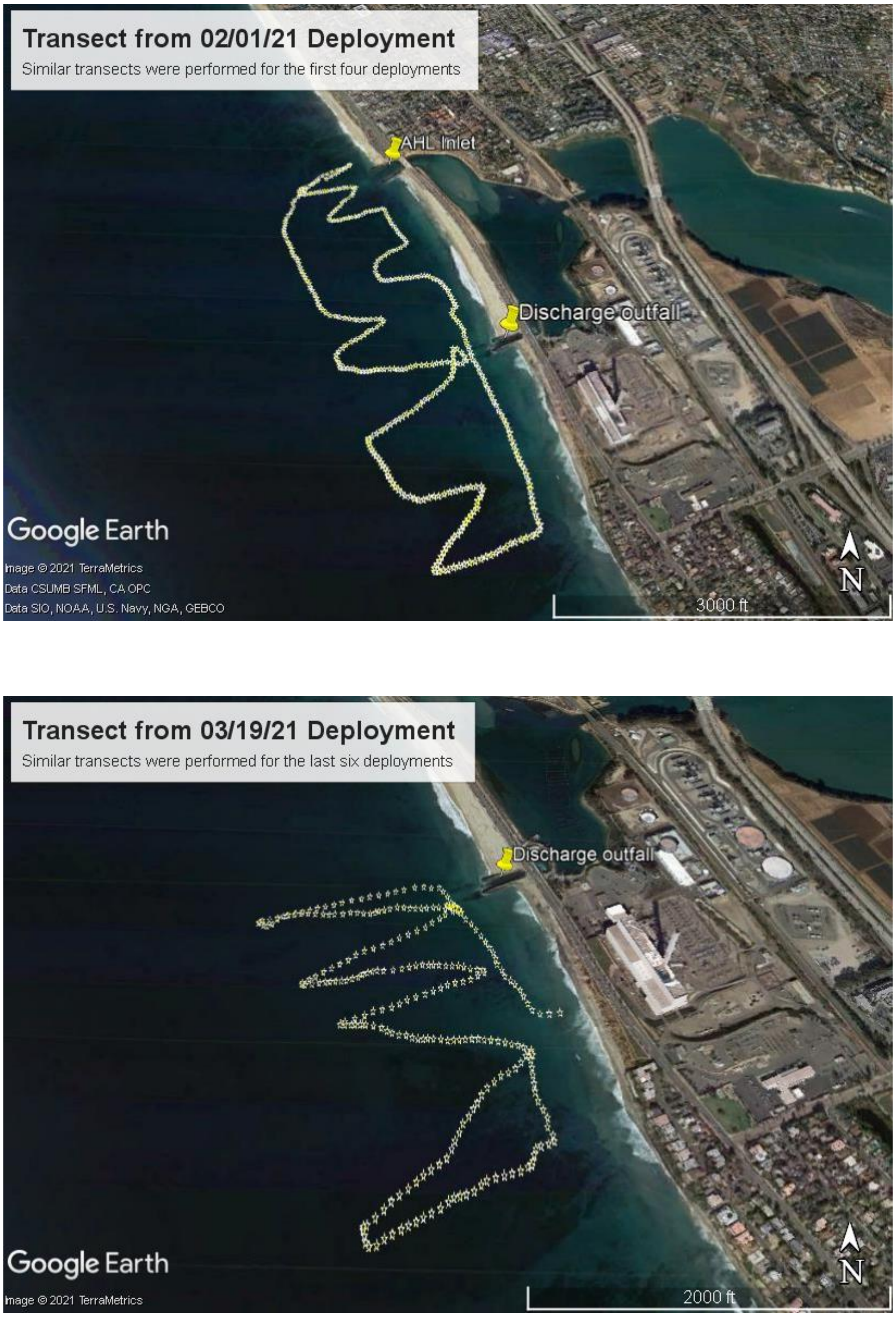

Figure 12 Two types of transects performed at the CDP study site. The first four deployments (top) collected data from north of the AHL inlet to south of the discharge outfall. The last six deployments (bottom) encompassed an area mostly south of the discharge outfall for higher data density (Google, 2021).

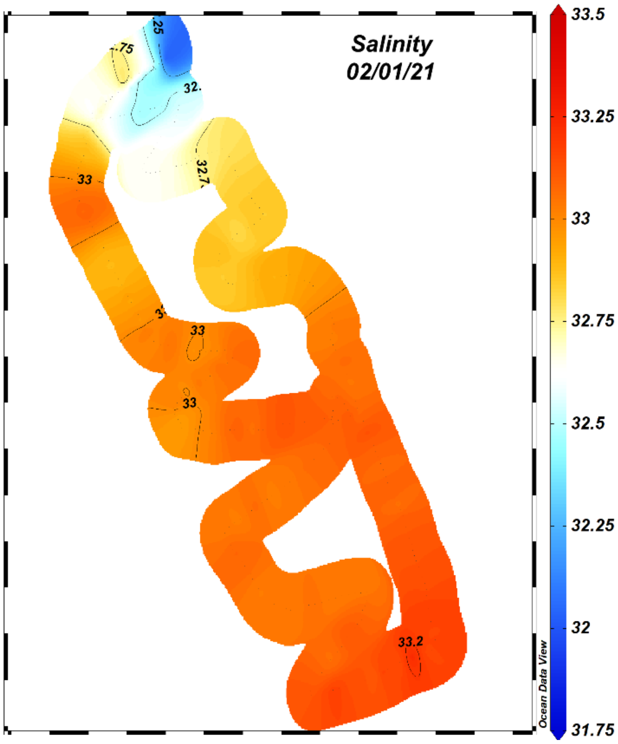
Salinity
02/01/21
33.5
33.25
33
32.75
32.5
32.25
32
31.75
Ocean Data View

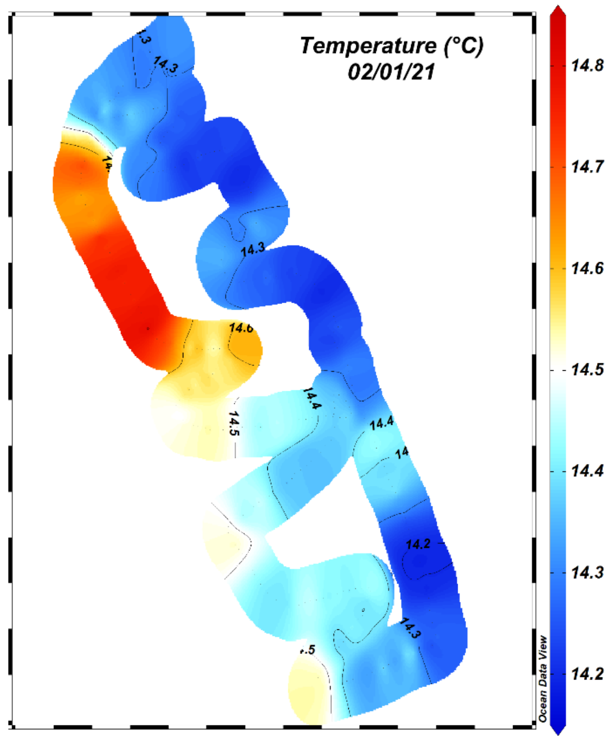
Temperature (°C)
02/01/21
14.8
14.7
14.6
14.5
14.4
14.3
14.2
Ocean Data View

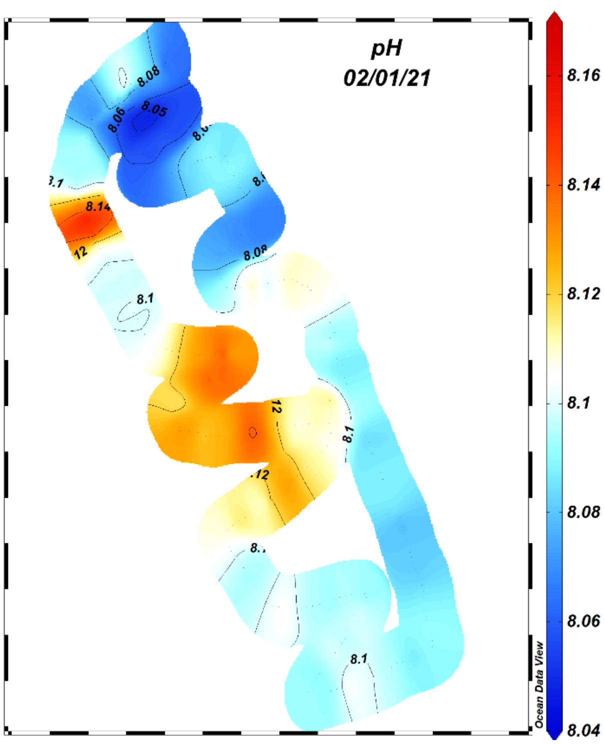
pH
02/01/21
8.16
8.14
8.12
8.1
8.08
8.06
8.04
Ocean Data View

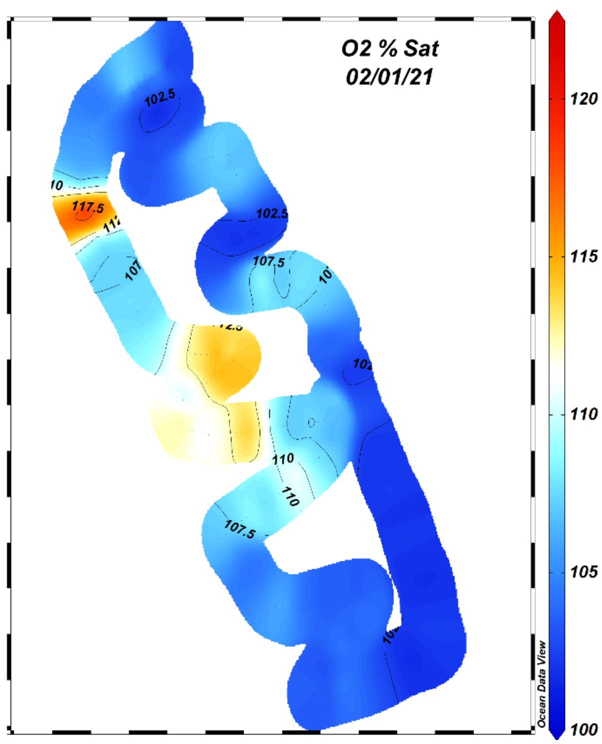
O2 % Sat
02/01/21
120
115
110
105
100
Ocean Data View

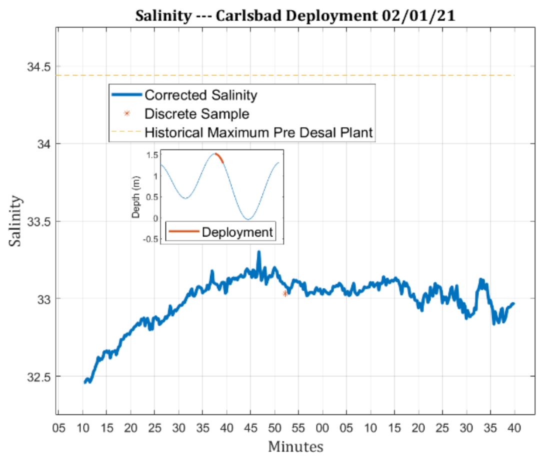

Salinity --- Carlsbad Deployment 02/01/21
Corrected Salinity
Discrete Sample
Historical Maximum Pre Desal Plant
Deployment
Depth (m)
Salinity
Minutes

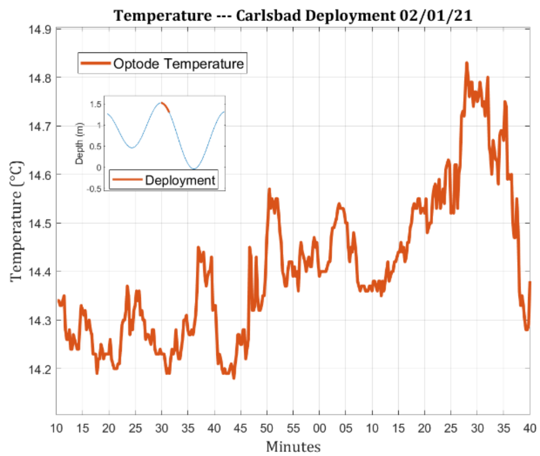

Temperature --- Carlsbad Deployment 02/01/21
Optode Temperature
Deployment
Depth (m)
Temperature (°C)
Minutes

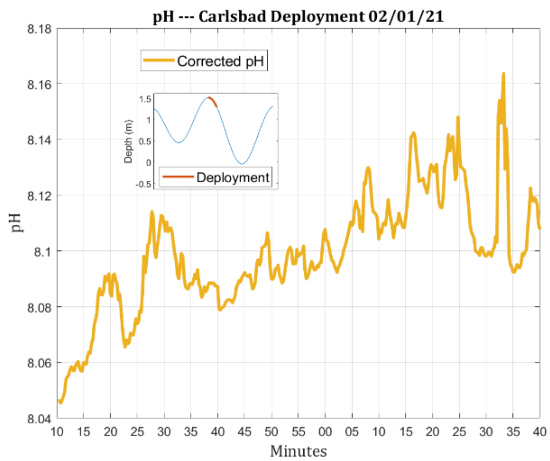

pH --- Carlsbad Deployment 02/01/21
Corrected pH
Deployment
Depth (m)
pH
Minutes

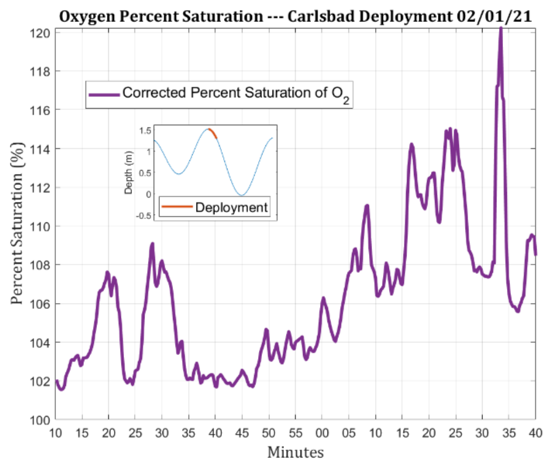

Oxygen Percent Saturation --- Carlsbad Deployment 02/01/21
Corrected Percent Saturation of O2
Deployment
Depth (m)
Percent Saturation (%)
Minutes

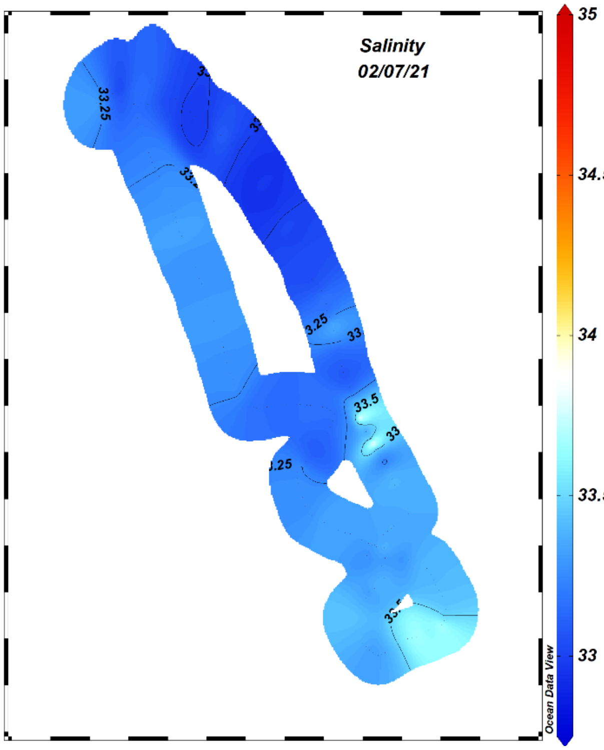
Salinity
02/07/21
35
34.5
34
33.5
33
Ocean Data View

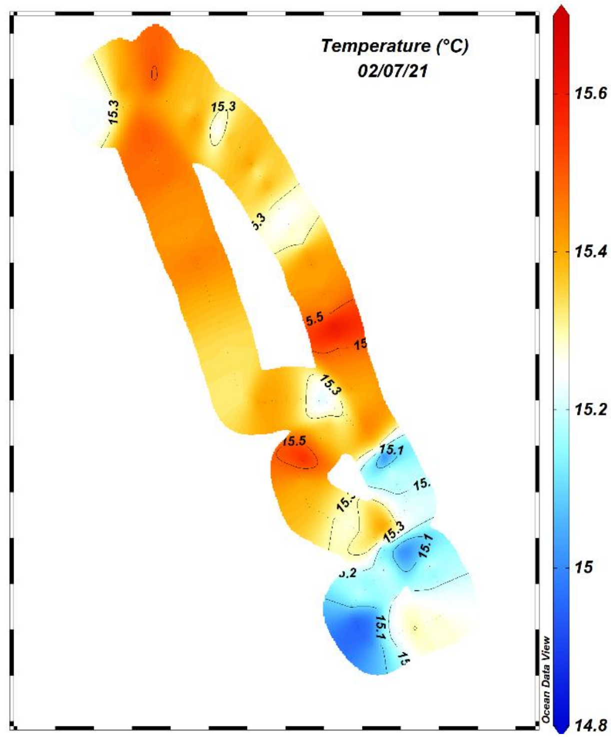
Temperature (°C)
02/07/21
15.6
15.4
15.2
15
14.8
Ocean Data View

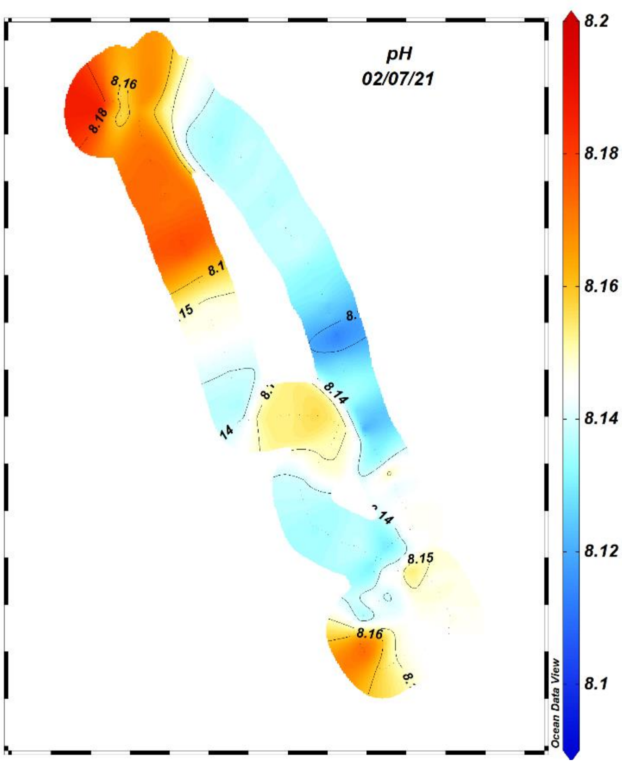
pH
02/07/21
8.2
8.18
8.16
8.14
8.12
8.1
Ocean Data View

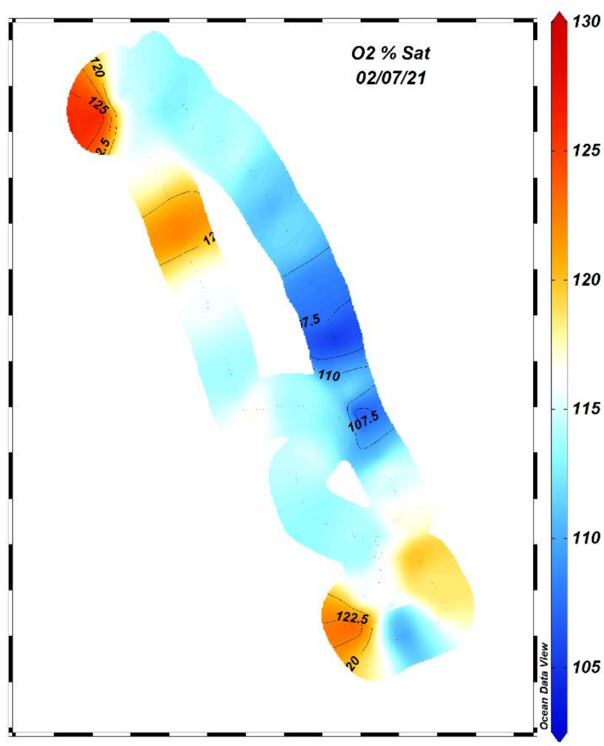
O2 % Sat
02/07/21
130
125
120
115
110
105
Ocean Data View

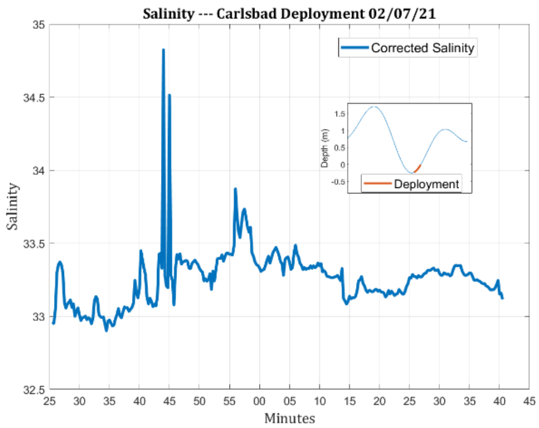
Salinity --- Carlsbad Deployment 02/07/21
Corrected Salinity
Deployment
Depth (m)
Salinity
Minutes

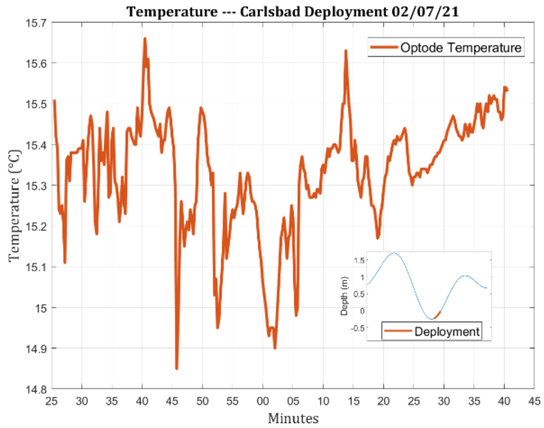
Temperature --- Carlsbad Deployment 02/07/21
Optode Temperature
Deployment
Depth (m)
Temperature (°C)
Minutes

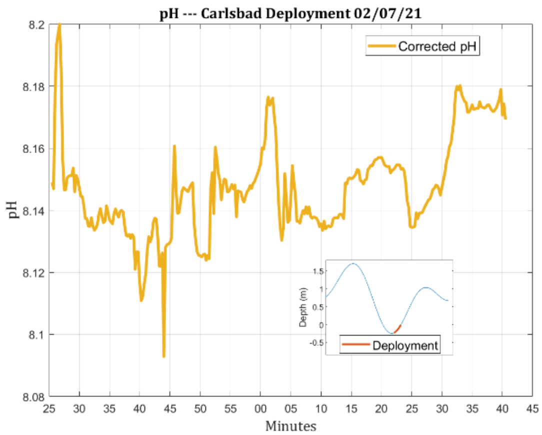
pH --- Carlsbad Deployment 02/07/21
Corrected pH
Deployment
Depth (m)
pH
Minutes

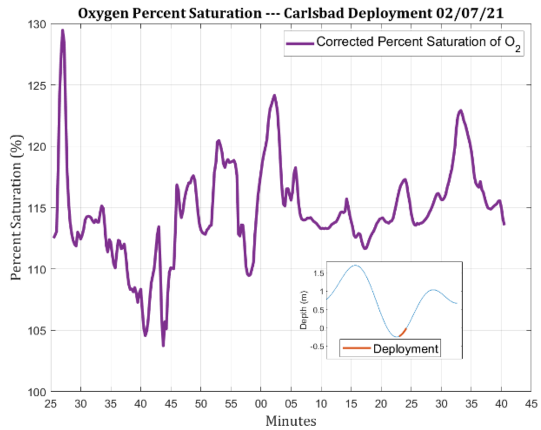
Oxygen Percent Saturation --- Carlsbad Deployment 02/07/21
Corrected Percent Saturation of O_2
Deployment
Depth (m)
Percent Saturation (%)
Minutes

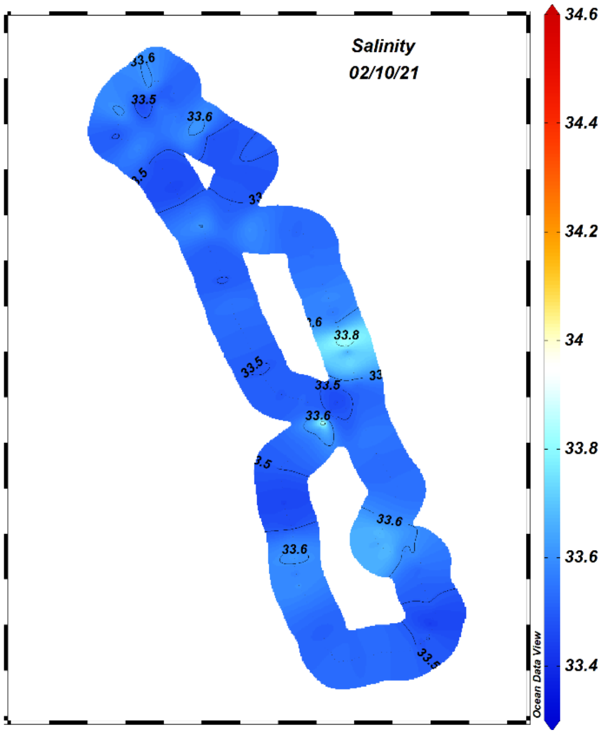
Salinity
02/10/21
34.6
34.4
34.2
34
33.8
33.6
33.4
Ocean Data View

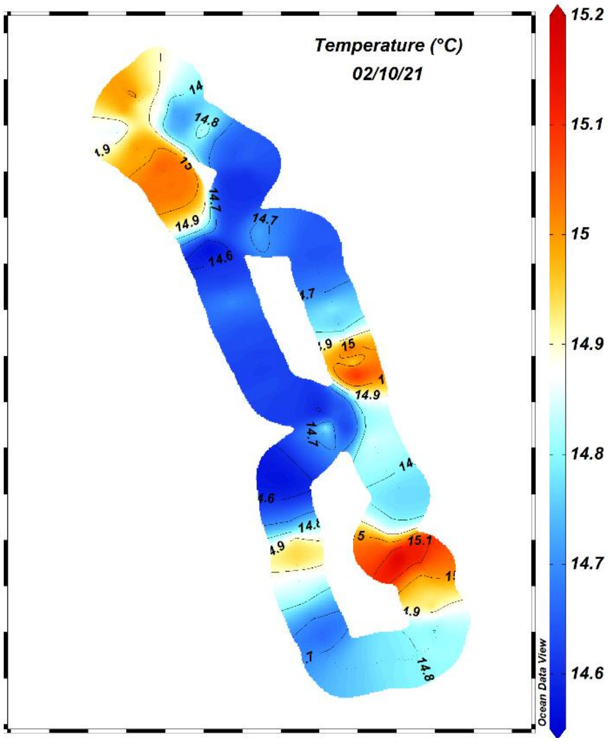
Temperature (°C)
02/10/21
15.2
15.1
15
14.9
14.8
14.7
14.6
Ocean Data View

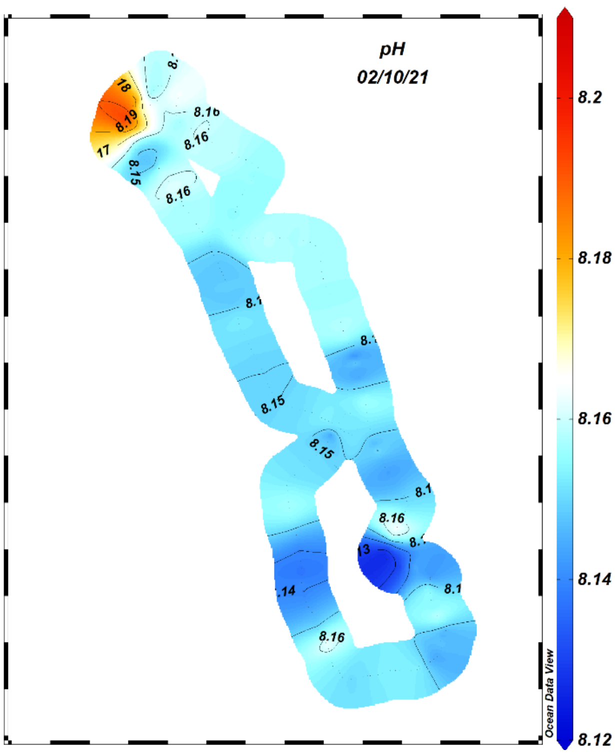
pH
02/10/21
8.2
8.18
8.16
8.14
8.12
Ocean Data View

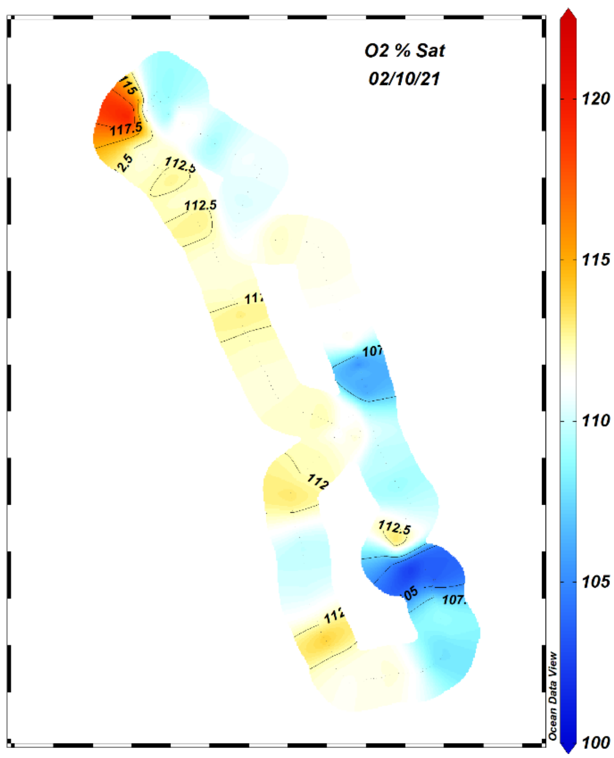
O2 % Sat
02/10/21
120
115
110
105
100
Ocean Data View

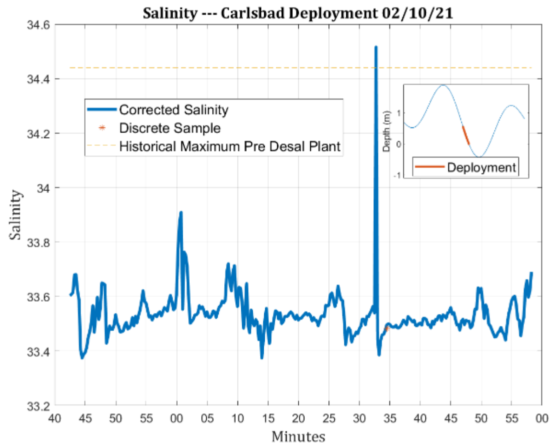

Salinity --- Carlsbad Deployment 02/10/21
Corrected Salinity
Discrete Sample
Historical Maximum Pre Desal Plant
Deployment
Salinity
Minutes

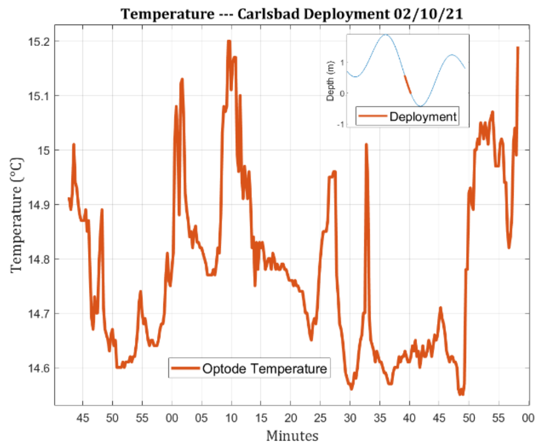

Temperature --- Carlsbad Deployment 02/10/21
Deployment
Optode Temperature
Temperature (°C)
Minutes

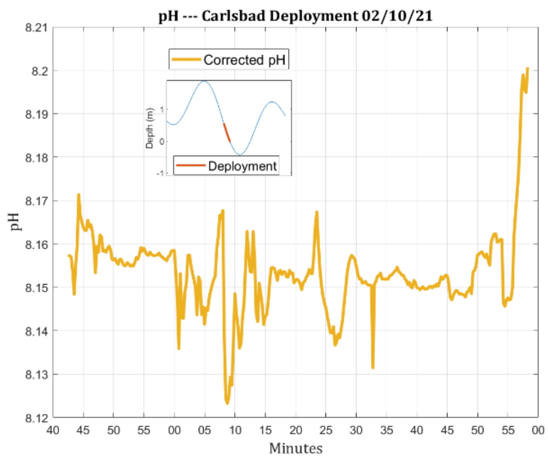

pH --- Carlsbad Deployment 02/10/21
Corrected pH
Deployment
pH
Minutes

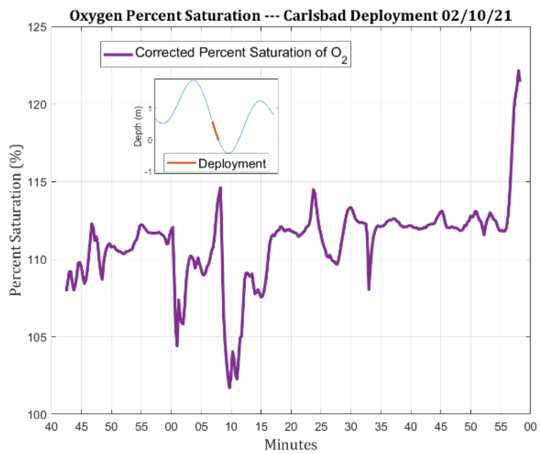

Oxygen Percent Saturation --- Carlsbad Deployment 02/10/21
Corrected Percent Saturation of O2
Deployment
Percent Saturation (%)
Minutes

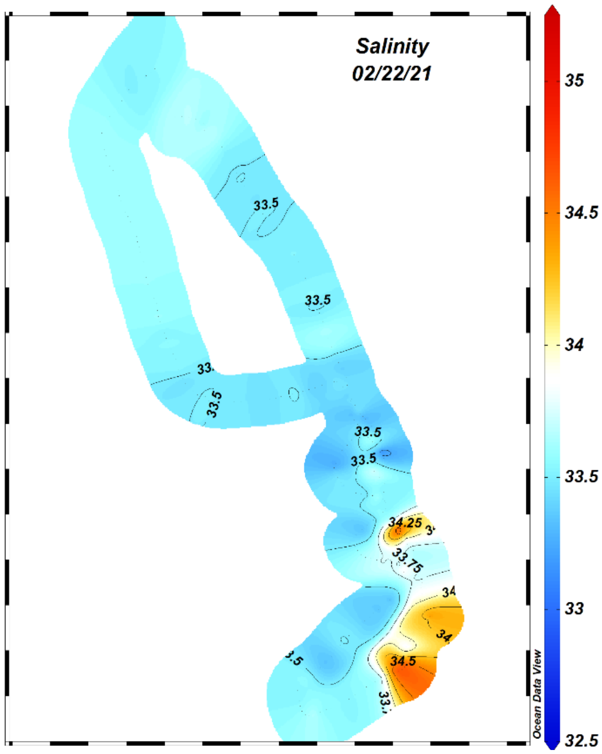
Salinity
02/22/21
35
34.5
34
33.5
33
32.5
Ocean Data View

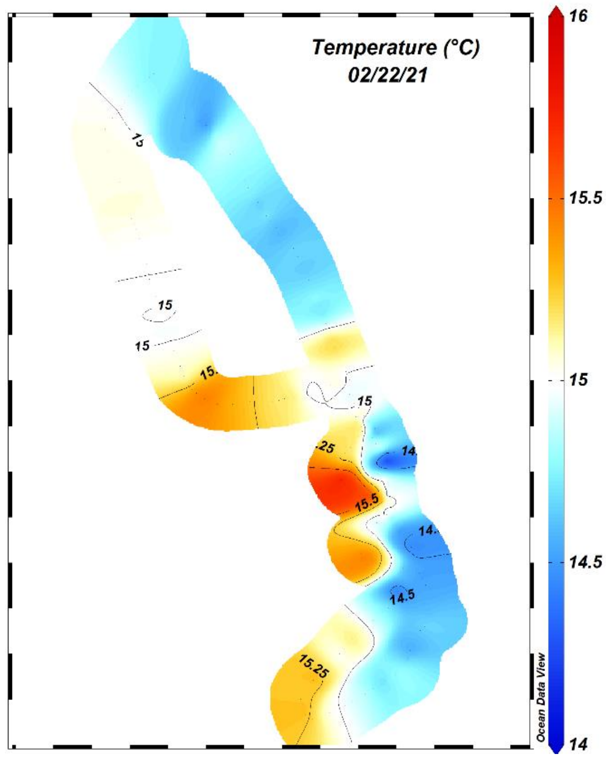
Temperature (°C)
02/22/21
16
15.5
15
14.5
14
Ocean Data View

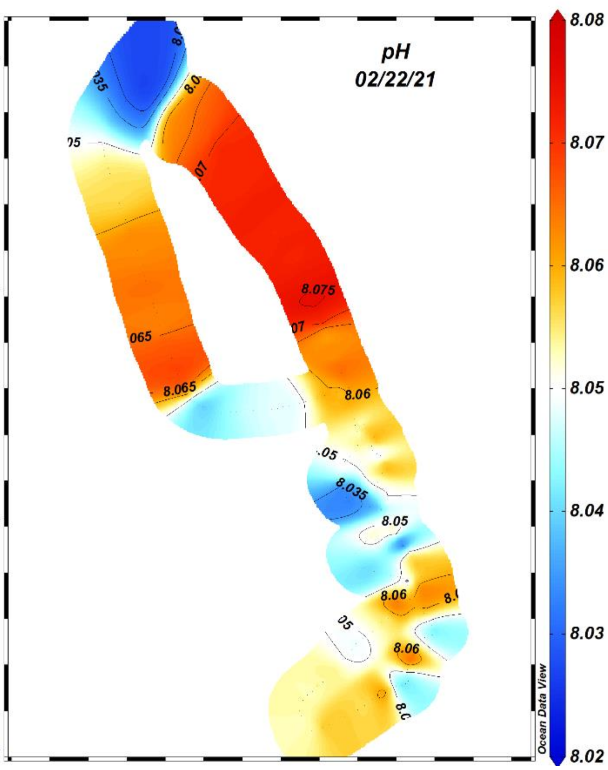
pH
02/22/21
8.08
8.07
8.06
8.05
8.04
8.03
8.02
Ocean Data View

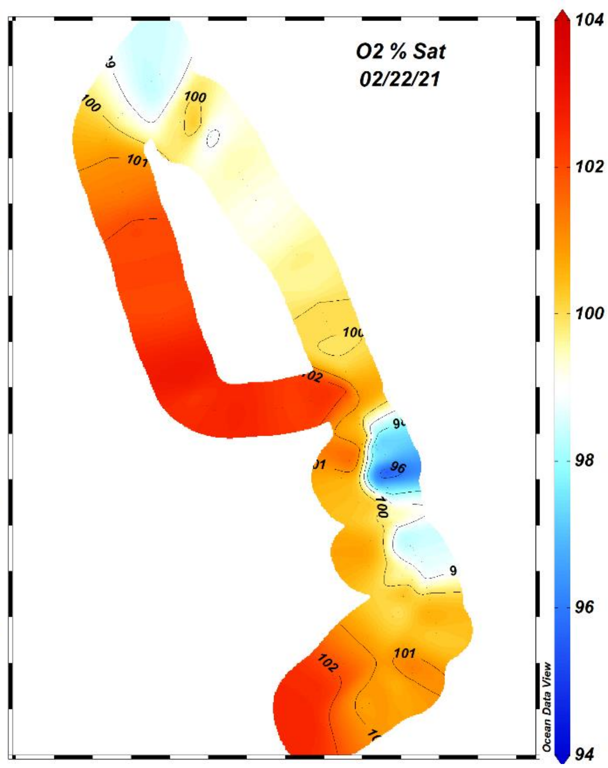
O2 % Sat
02/22/21
104
102
100
98
96
94
Ocean Data View

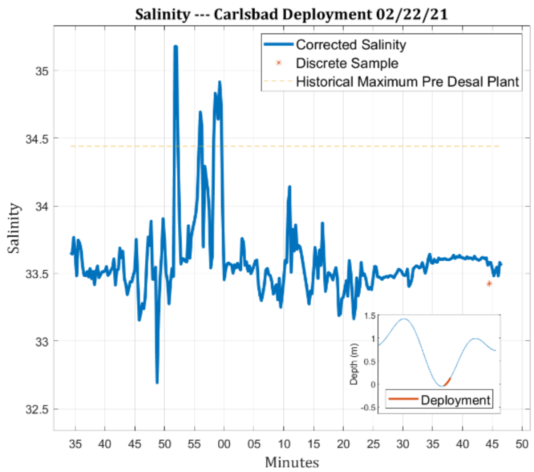
Salinity --- Carlsbad Deployment 02/22/21
Corrected Salinity
Discrete Sample
Historical Maximum Pre Desal Plant
Salinity
Minutes
Depth (m)
Deployment

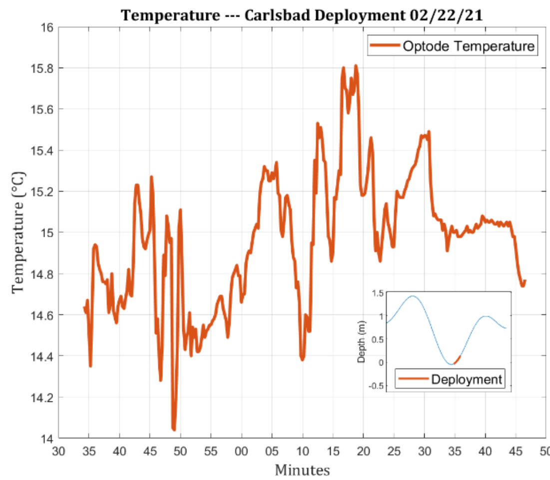
Temperature --- Carlsbad Deployment 02/22/21
Optode Temperature
Temperature (°C)
Minutes
Depth (m)
Deployment

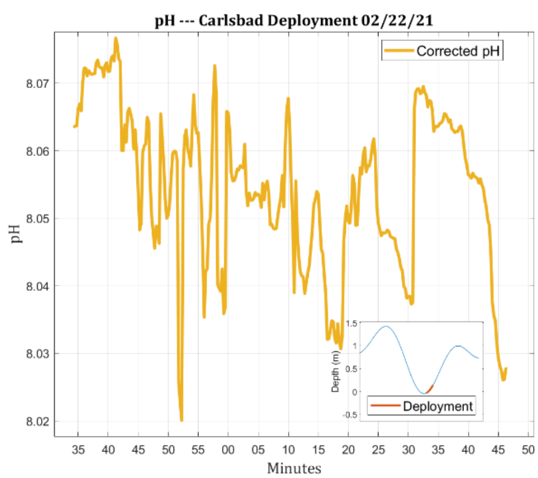
pH --- Carlsbad Deployment 02/22/21
Corrected pH
pH
Minutes
Depth (m)
Deployment

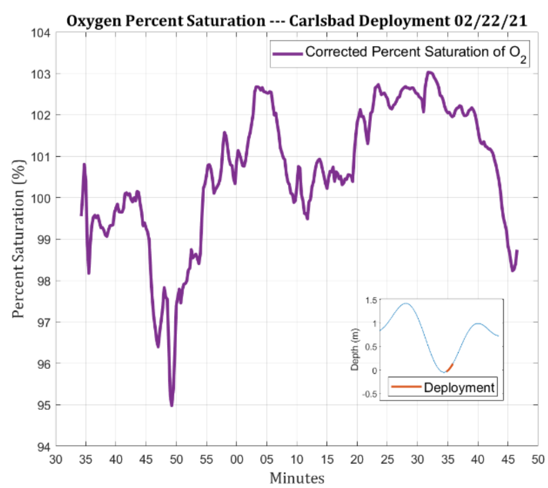
Oxygen Percent Saturation --- Carlsbad Deployment 02/22/21
Corrected Percent Saturation of O_2
Percent Saturation (%)
Minutes
Depth (m)
Deployment

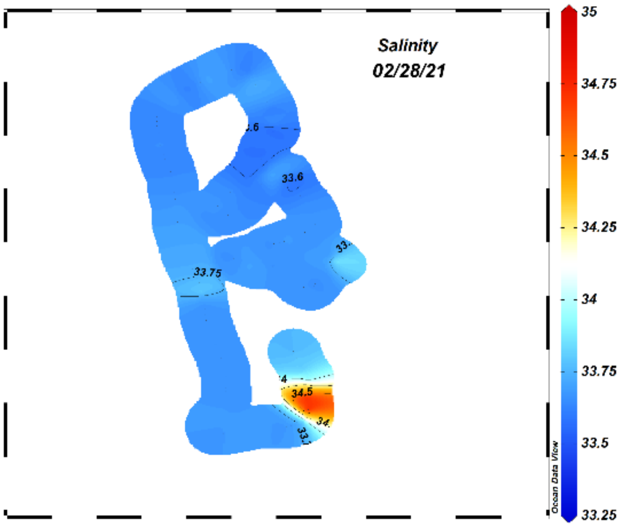
Salinity
02/28/21

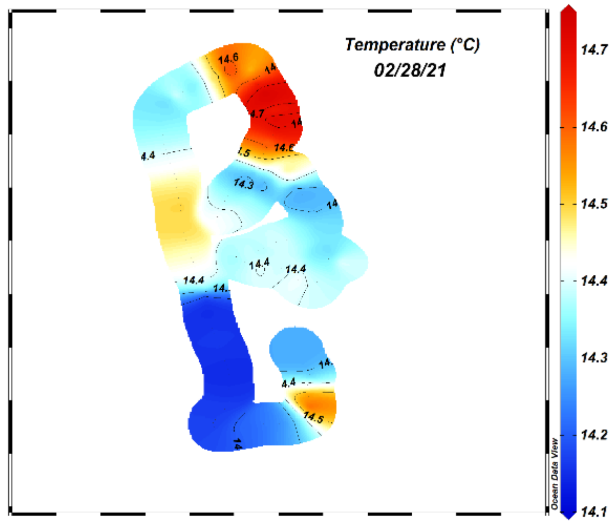
Temperature (°C)
02/28/21

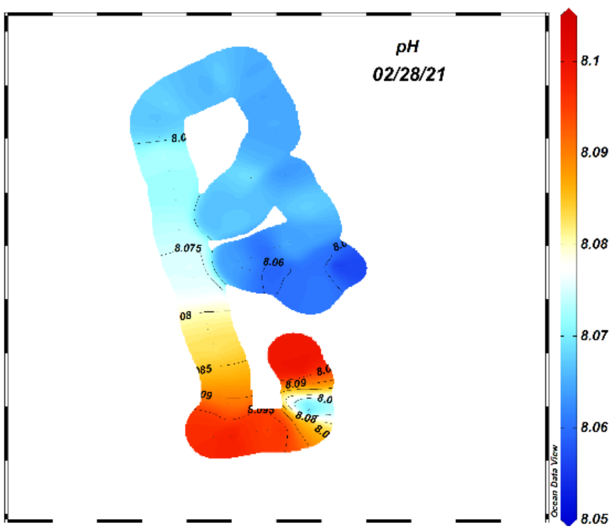
pH
02/28/21

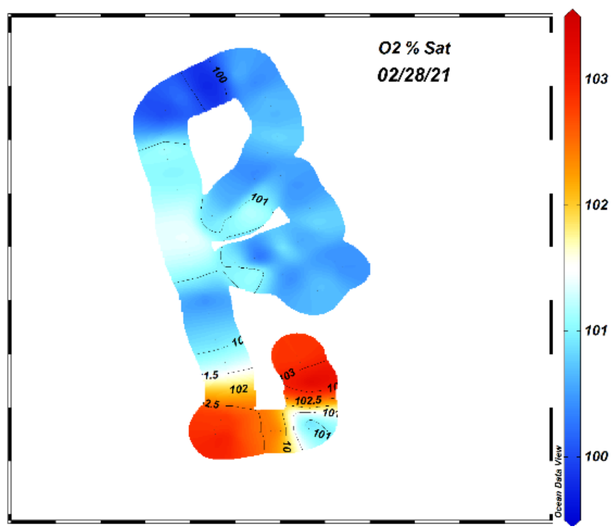
O2 % Sat
02/28/21

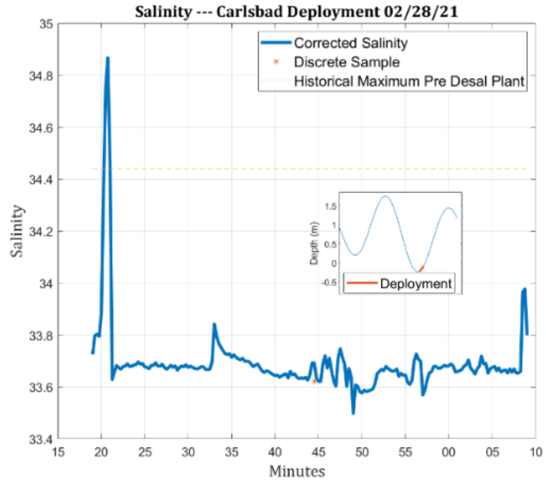
Salinity --- Carlsbad Deployment 02/28/21
Corrected Salinity
Discrete Sample
Historical Maximum Pre Desal Plant
Deployment
Depth (m)
Salinity
Minutes

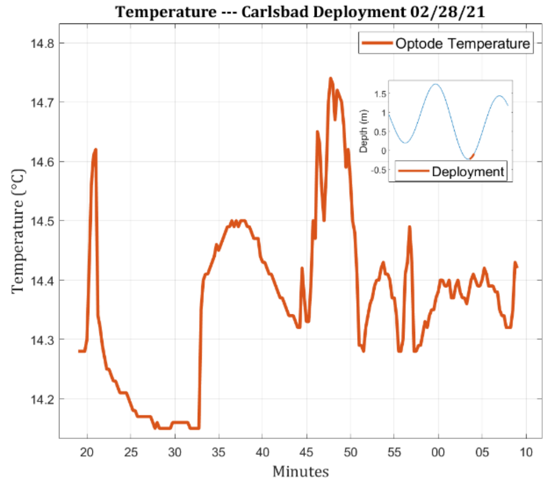
Temperature --- Carlsbad Deployment 02/28/21
Optode Temperature
Deployment
Depth (m)
Temperature (°C)
Minutes

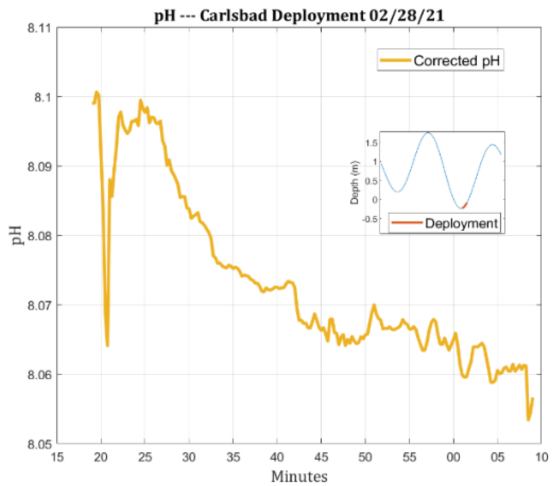
pH --- Carlsbad Deployment 02/28/21
Corrected pH
Deployment
Depth (m)
pH
Minutes

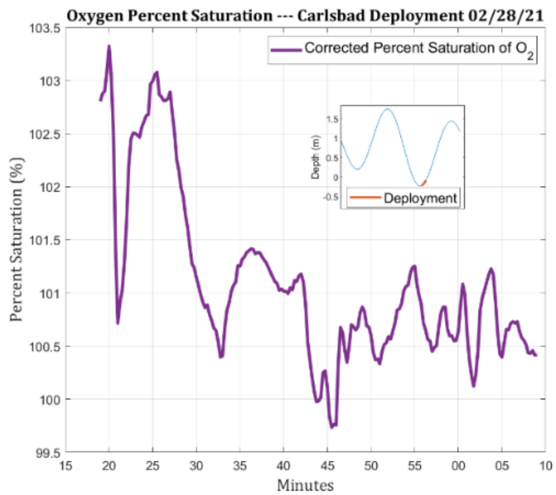
Oxygen Percent Saturation --- Carlsbad Deployment 02/28/21
Corrected Percent Saturation of O2
Deployment
Depth (m)
Percent Saturation (%)
Minutes

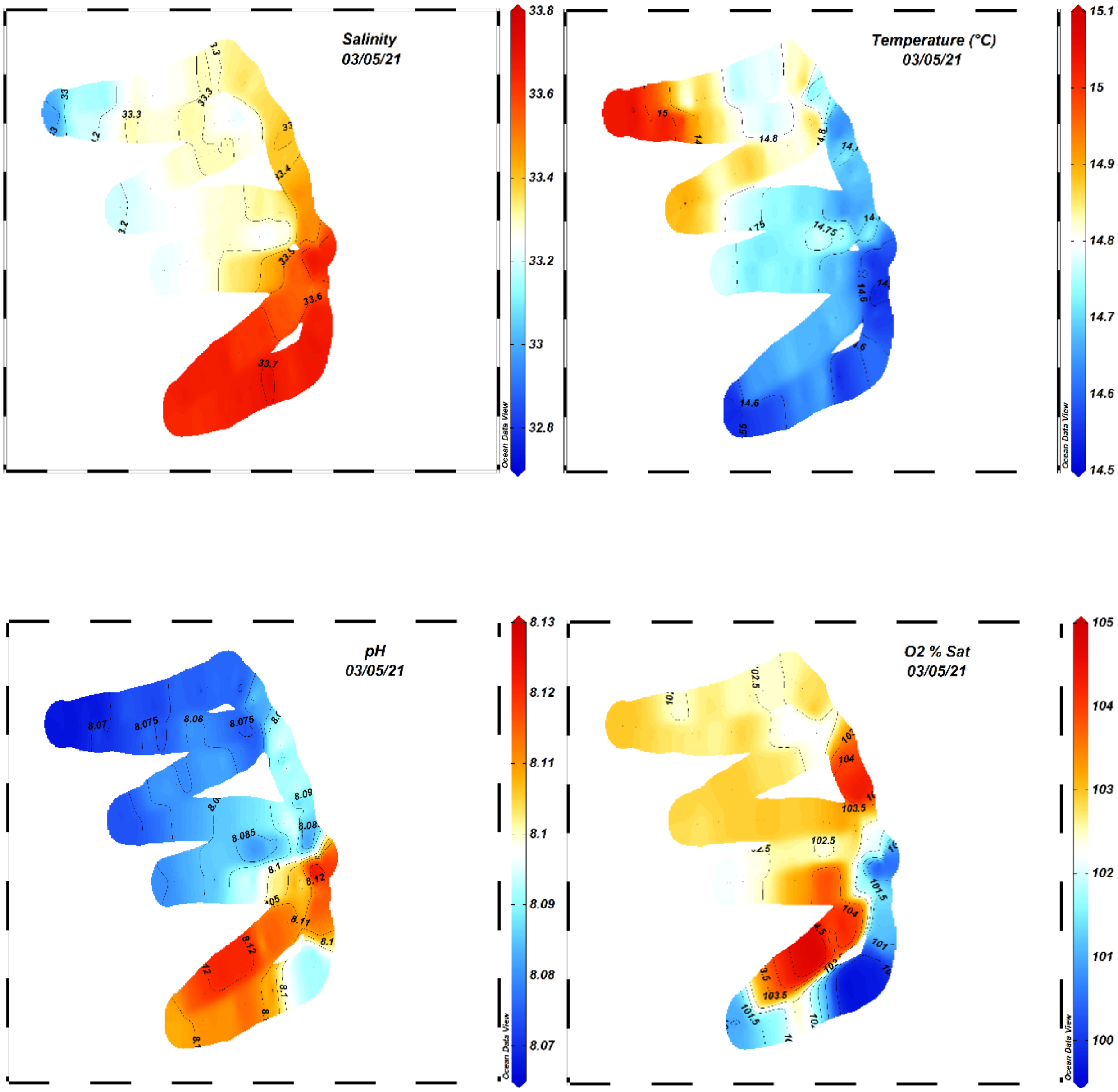
Salinity
03/05/21
33.8
33.6
33.4
33.2
33
32.8
Ocean Data View
Temperature (°C)
03/05/21
15.1
15
14.9
14.8
14.7
14.6
14.5
Ocean Data View
pH
03/05/21
8.13
8.12
8.11
8.1
8.09
8.08
8.07
Ocean Data View
O2 % Sat
03/05/21
105
104
103
102
101
100
Ocean Data View

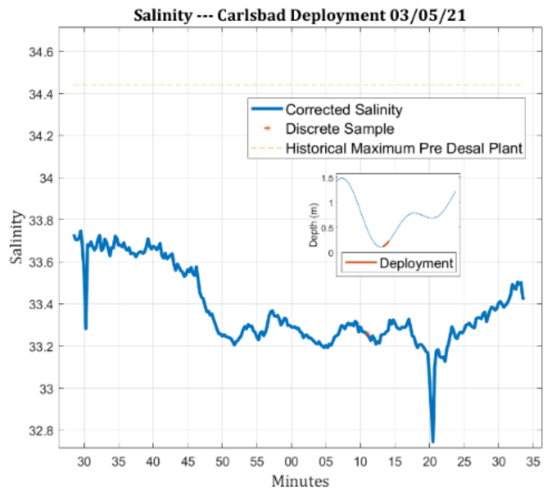
Salinity --- Carlsbad Deployment 03/05/21
Corrected Salinity
Discrete Sample
Historical Maximum Pre Desal Plant
Deployment
Depth (m)
Salinity
Minutes

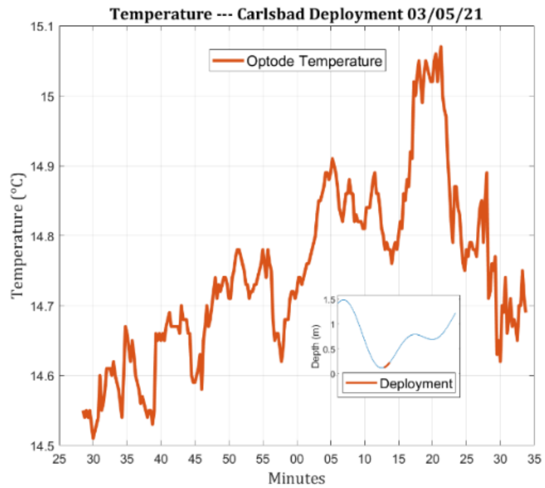
Temperature --- Carlsbad Deployment 03/05/21
Optode Temperature
Deployment
Depth (m)
Temperature (°C)
Minutes

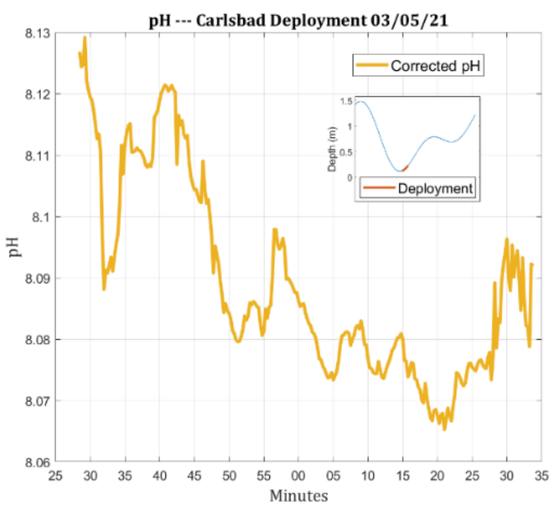
pH --- Carlsbad Deployment 03/05/21
Corrected pH
Deployment
Depth (m)
pH
Minutes

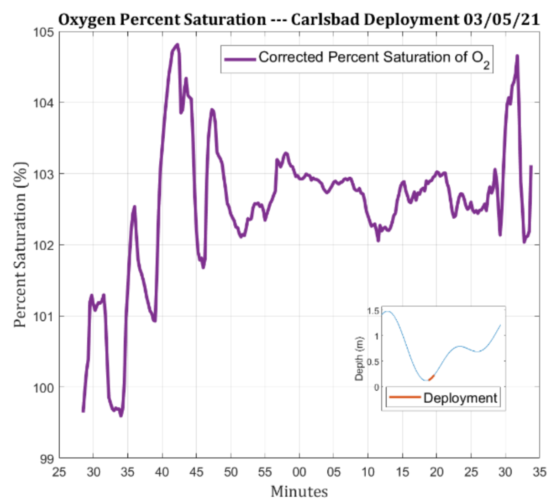
Oxygen Percent Saturation --- Carlsbad Deployment 03/05/21
Corrected Percent Saturation of O2
Deployment
Depth (m)
Percent Saturation (%)
Minutes

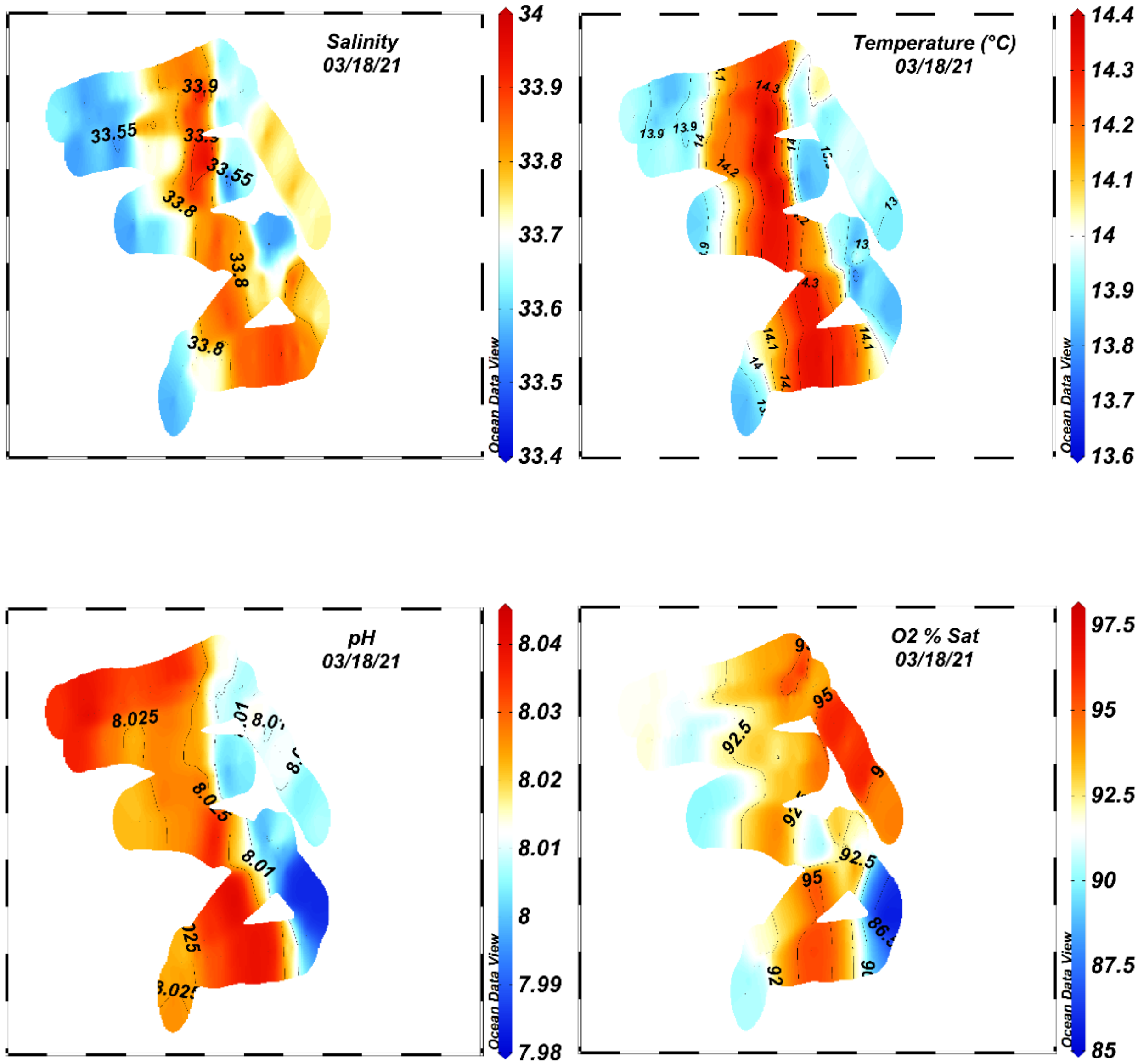
Salinity
03/18/21
34
33.9
33.8
33.7
33.6
33.5
33.4
Ocean Data View
Temperature (°C)
03/18/21
14.4
14.3
14.2
14.1
14
13.9
13.8
13.7
13.6
Ocean Data View
pH
03/18/21
8.04
8.03
8.02
8.01
8
7.99
7.98
Ocean Data View
O2 % Sat
03/18/21
97.5
95
92.5
90
87.5
85
Ocean Data View

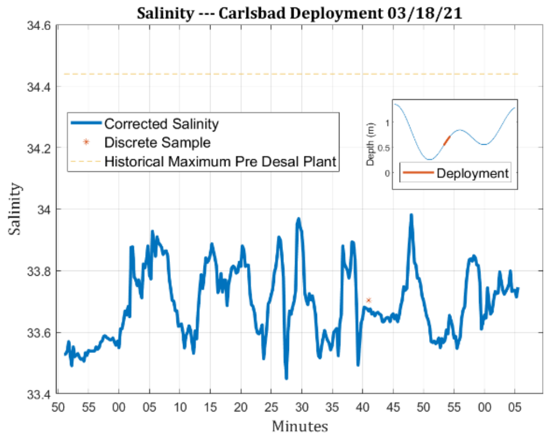
Salinity --- Carlsbad Deployment 03/18/21
Corrected Salinity
Discrete Sample
Historical Maximum Pre Desal Plant
Deployment
Depth (m)
Salinity
Minutes

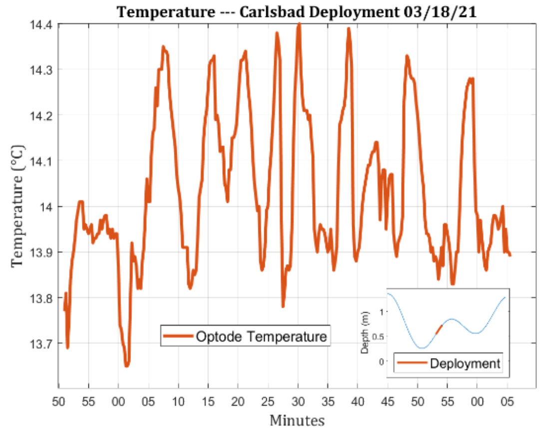
Temperature --- Carlsbad Deployment 03/18/21
Optode Temperature
Deployment
Depth (m)
Temperature (°C)
Minutes

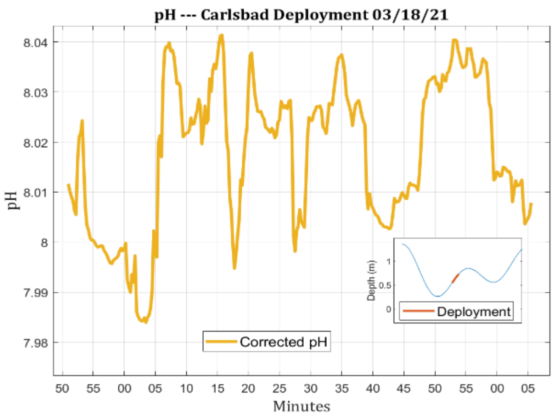
pH --- Carlsbad Deployment 03/18/21
Corrected pH
Deployment
Depth (m)
pH
Minutes

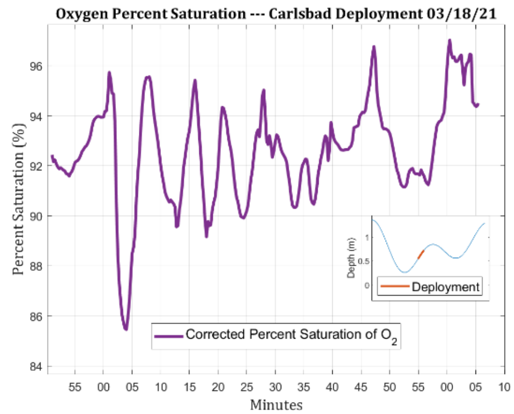
Oxygen Percent Saturation --- Carlsbad Deployment 03/18/21
Corrected Percent Saturation of O2
Deployment
Depth (m)
Percent Saturation (%)
Minutes

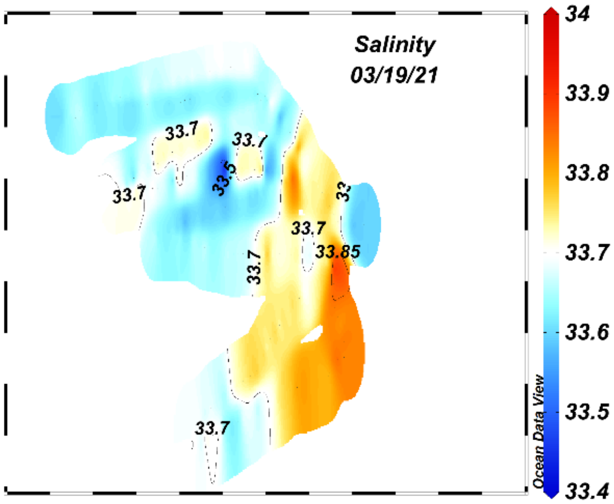
Salinity
03/19/21
34
33.9
33.8
33.7
33.6
33.5
33.4
Ocean Data View

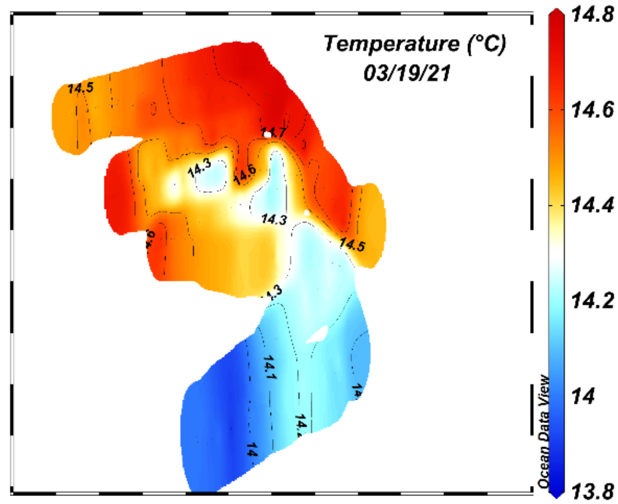
Temperature (°C)
03/19/21
14.8
14.6
14.4
14.2
14
13.8
Ocean Data View

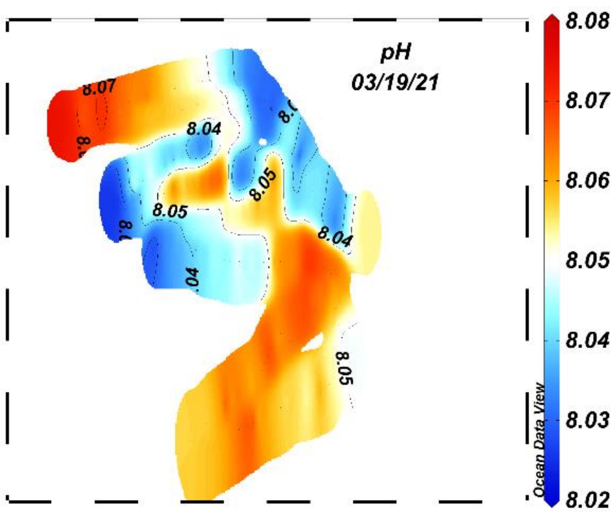
pH
03/19/21
8.08
8.07
8.06
8.05
8.04
8.03
8.02
Ocean Data View

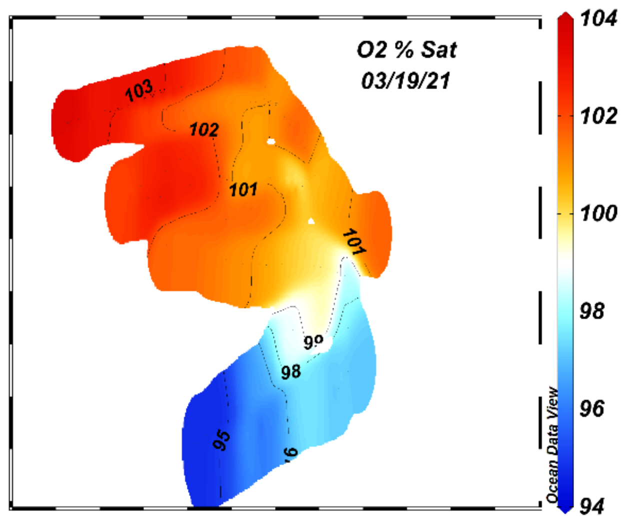
O2 % Sat
03/19/21
104
102
100
98
96
94
Ocean Data View

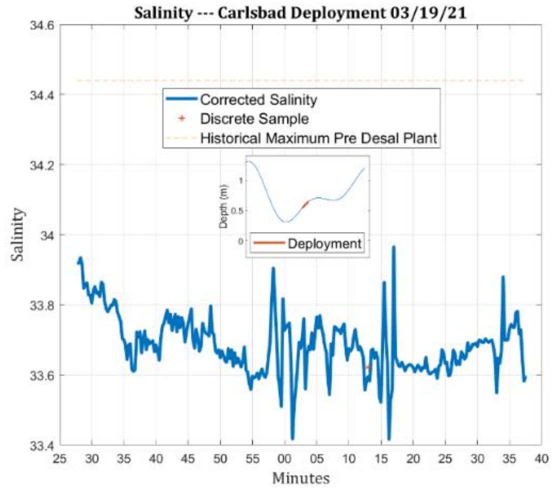
Salinity --- Carlsbad Deployment 03/19/21
Corrected Salinity
Discrete Sample
Historical Maximum Pre Desal Plant
Deployment
Depth (m)
Salinity
Minutes

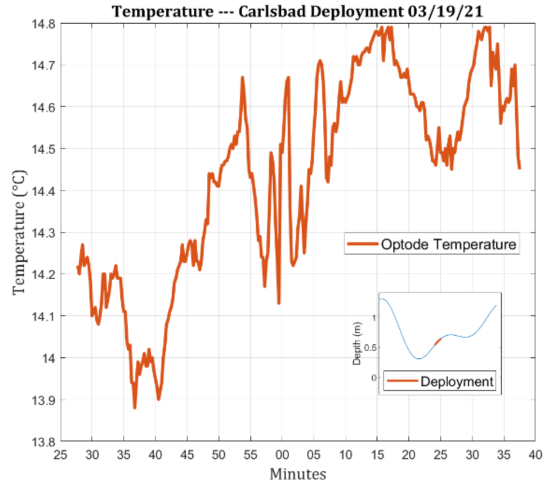
Temperature --- Carlsbad Deployment 03/19/21
Optode Temperature
Deployment
Depth (m)
Temperature (°C)
Minutes

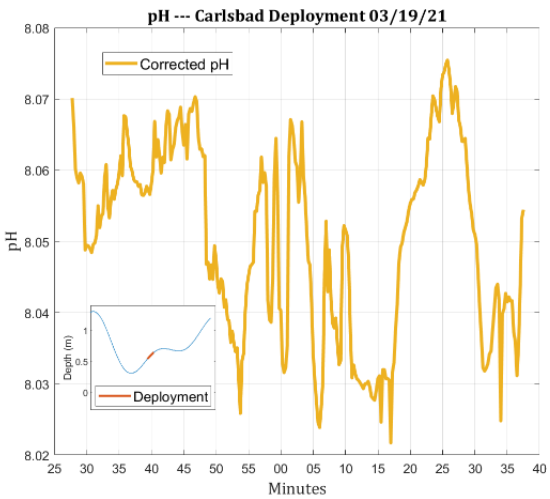
pH --- Carlsbad Deployment 03/19/21
Corrected pH
Deployment
Depth (m)
pH
Minutes

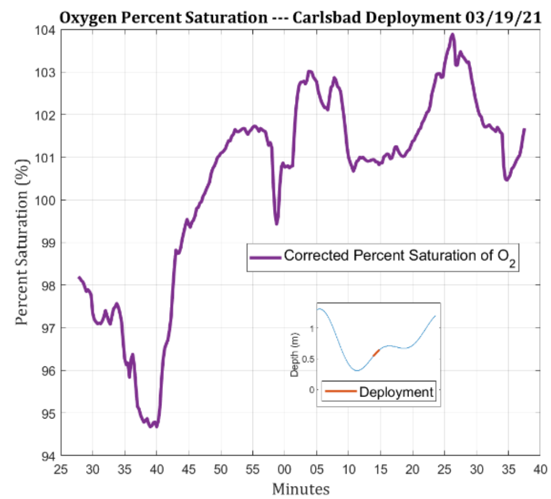
Oxygen Percent Saturation --- Carlsbad Deployment 03/19/21
Corrected Percent Saturation of O2
Deployment
Depth (m)
Percent Saturation (%)
Minutes

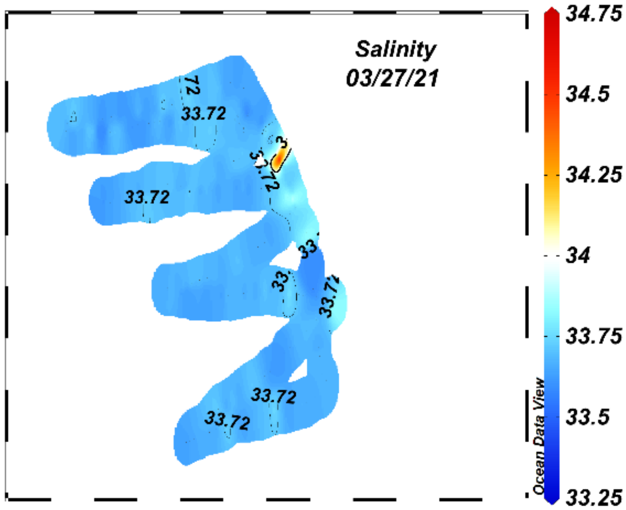
Salinity
03/27/21
34.75
34.5
34.25
34
33.75
33.5
33.25
Ocean Data View

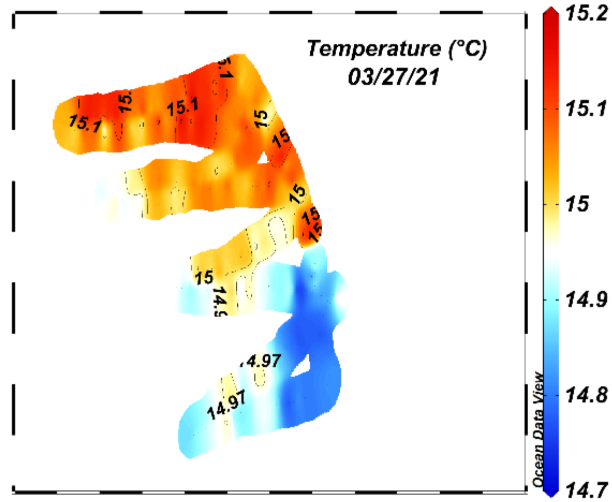
Temperature (°C)
03/27/21
15.2
15.1
15
14.9
14.8
14.7
Ocean Data View

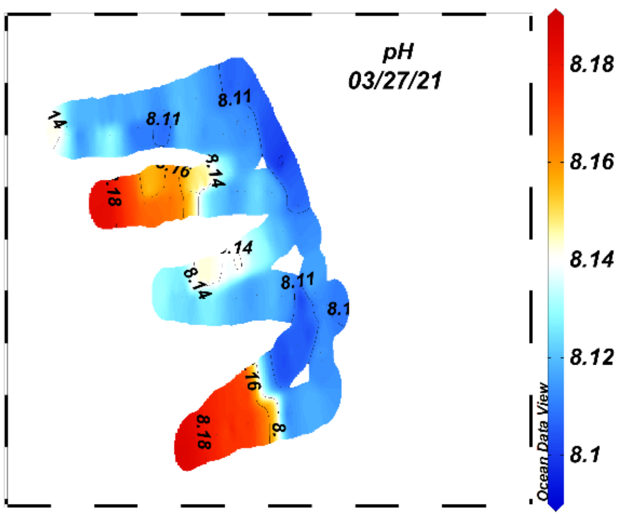
pH
03/27/21
8.18
8.16
8.14
8.12
8.1
Ocean Data View

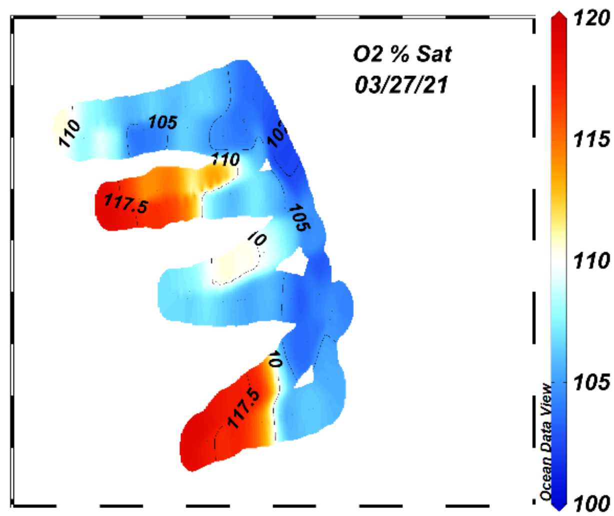
O2 % Sat
03/27/21
120
115
110
105
100
Ocean Data View

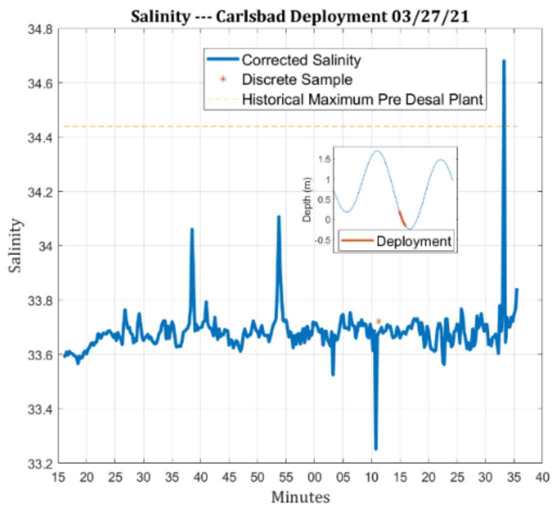
Salinity --- Carlsbad Deployment 03/27/21
Corrected Salinity
Discrete Sample
Historical Maximum Pre Desal Plant
Depth (m)
Deployment
Salinity
Minutes

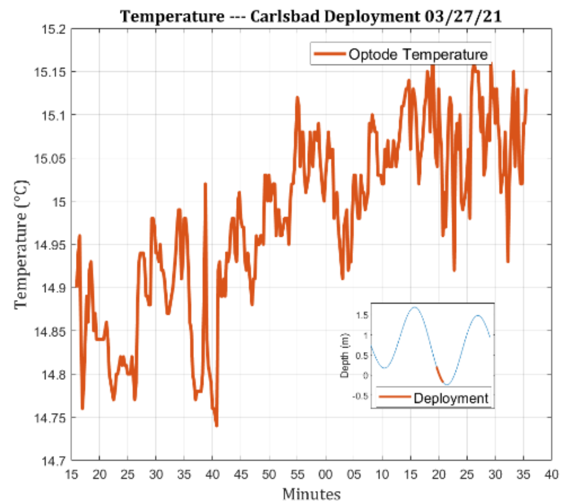
Temperature --- Carlsbad Deployment 03/27/21
Optode Temperature
Depth (m)
Deployment
Temperature (°C)
Minutes

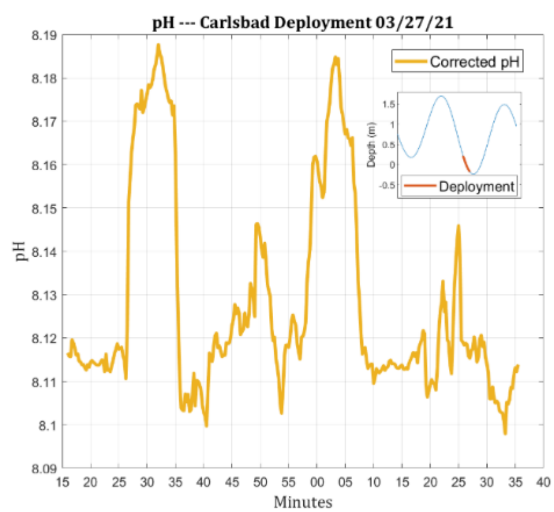
pH --- Carlsbad Deployment 03/27/21
Corrected pH
Depth (m)
Deployment
pH
Minutes

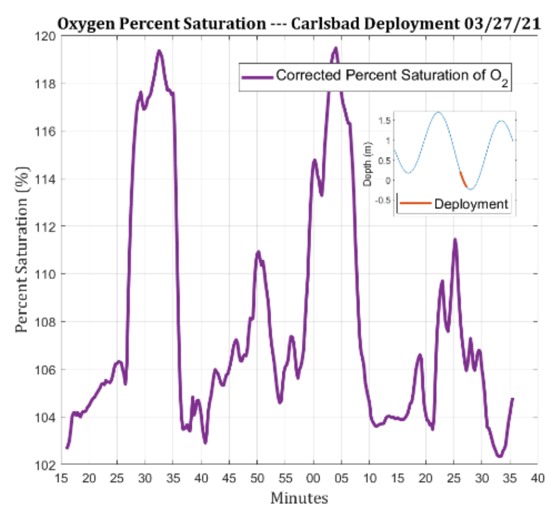
Oxygen Percent Saturation --- Carlsbad Deployment 03/27/21
Corrected Percent Saturation of O2
Depth (m)
Deployment
Percent Saturation (%)
Minutes

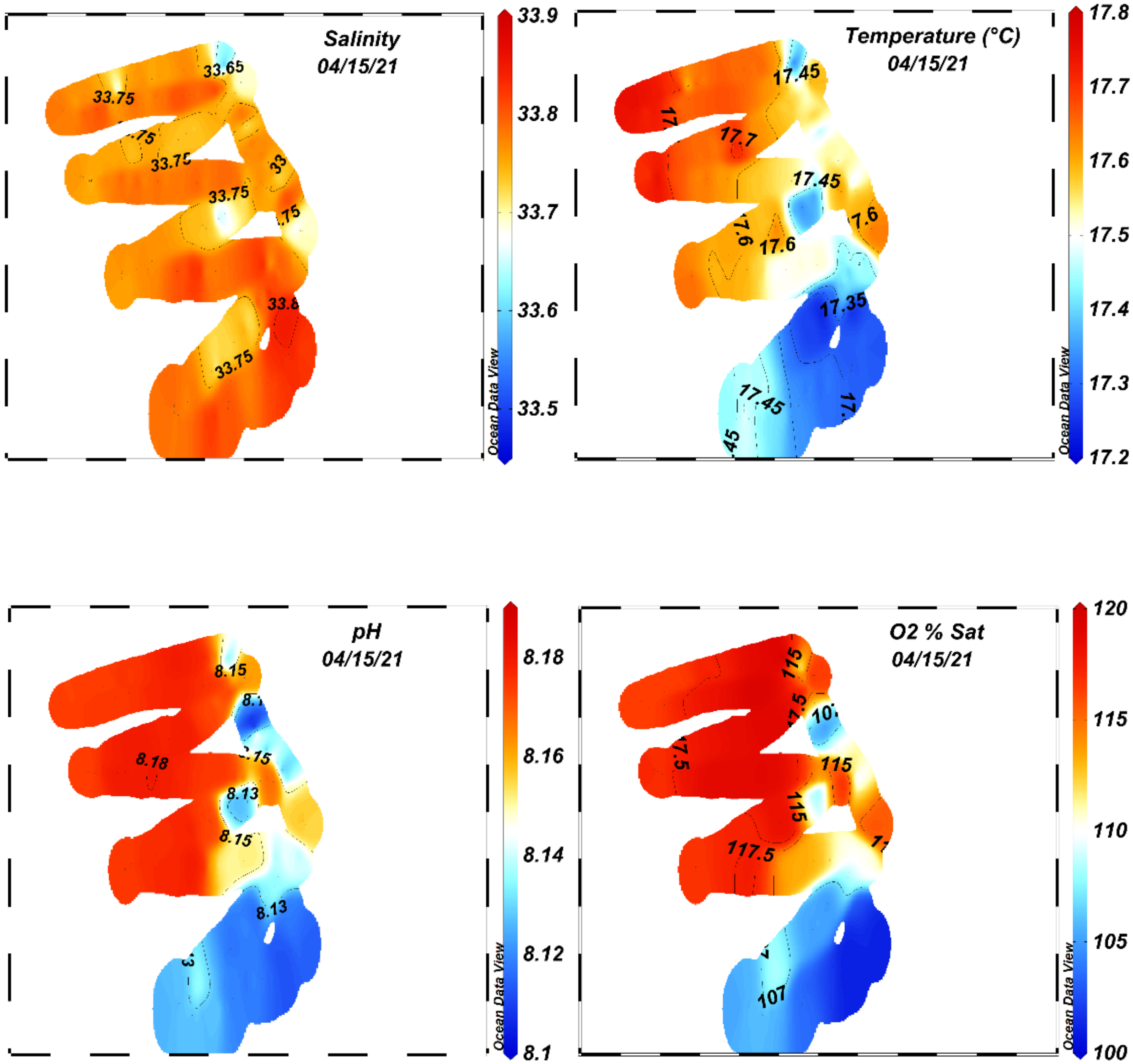
Salinity
04/15/21
33.9
33.8
33.7
33.6
33.5
Ocean Data View
Temperature (°C)
04/15/21
17.8
17.7
17.6
17.5
17.4
17.3
17.2
Ocean Data View
pH
04/15/21
8.18
8.16
8.14
8.12
8.1
Ocean Data View
O2 % Sat
04/15/21
120
115
110
105
100
Ocean Data View

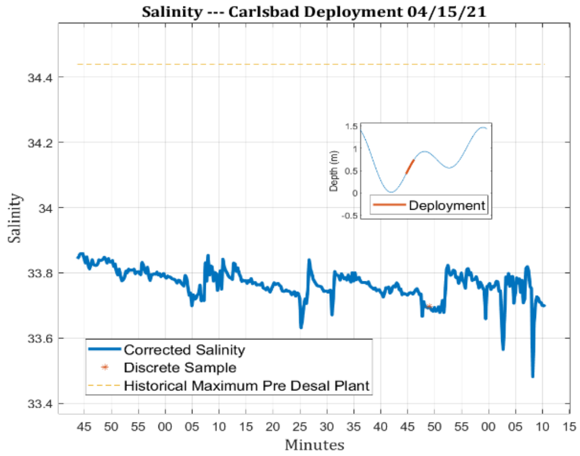
Salinity --- Carlsbad Deployment 04/15/21
Salinity
Minutes
Deployment
Depth (m)
Corrected Salinity
Discrete Sample
Historical Maximum Pre Desal Plant

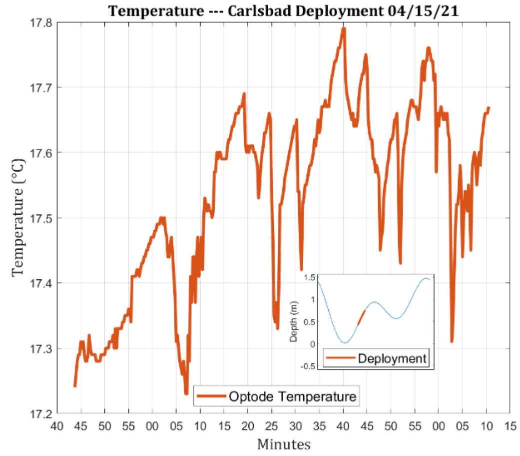
Temperature --- Carlsbad Deployment 04/15/21
Temperature (°C)
Minutes
Deployment
Depth (m)
Optode Temperature

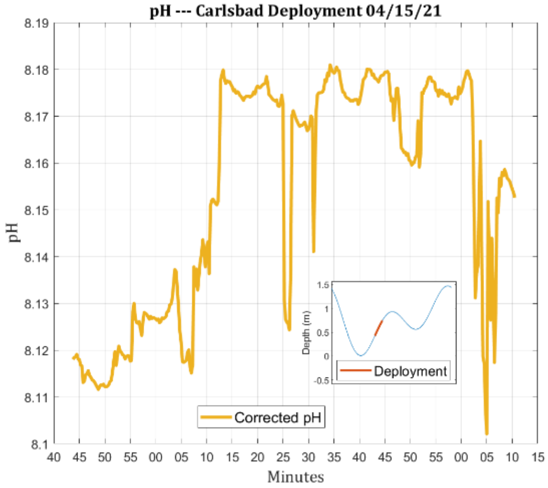
pH --- Carlsbad Deployment 04/15/21
pH
Minutes
Deployment
Depth (m)
Corrected pH

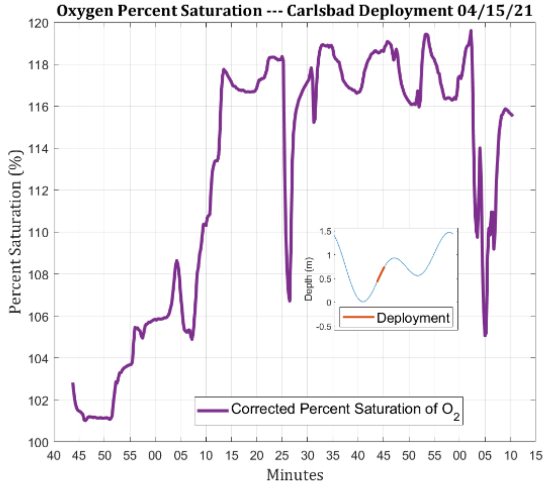
Oxygen Percent Saturation --- Carlsbad Deployment 04/15/21
Percent Saturation (%)
Minutes
Deployment
Depth (m)
Corrected Percent Saturation of O2

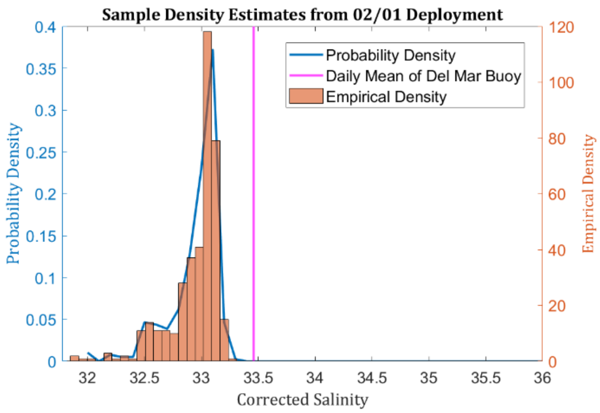
Sample Density Estimates from 02/01 Deployment
Probability Density
Daily Mean of Del Mar Buoy
Empirical Density
Probability Density
Empirical Density
Corrected Salinity

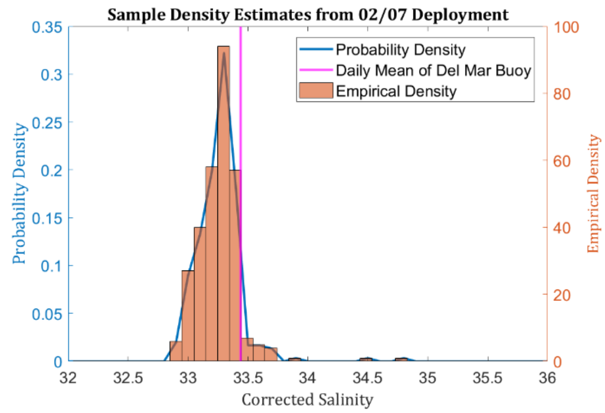
Sample Density Estimates from 02/07 Deployment
Probability Density
Daily Mean of Del Mar Buoy
Empirical Density
Probability Density
Empirical Density
Corrected Salinity

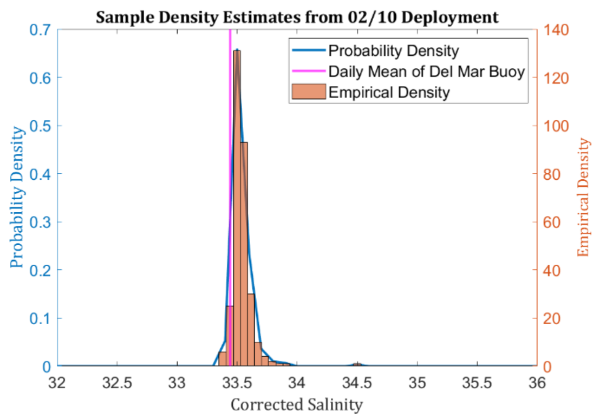
Sample Density Estimates from 02/10 Deployment
Probability Density
Daily Mean of Del Mar Buoy
Empirical Density
Probability Density
Empirical Density
Corrected Salinity

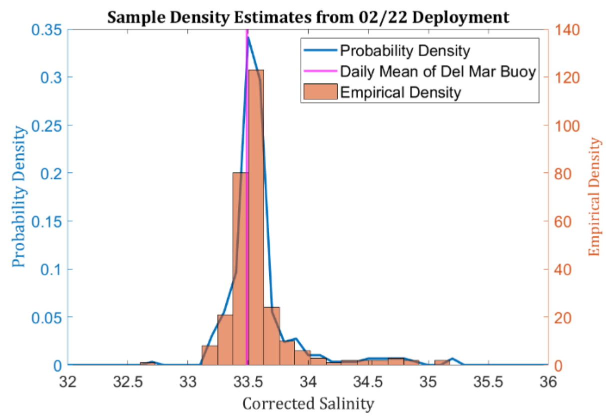
Sample Density Estimates from 02/22 Deployment
Probability Density
Daily Mean of Del Mar Buoy
Empirical Density
Probability Density
Empirical Density
Corrected Salinity

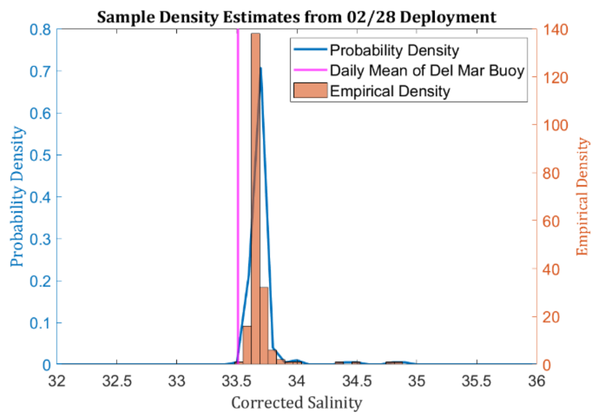
Sample Density Estimates from 02/28 Deployment
Probability Density
Daily Mean of Del Mar Buoy
Empirical Density
Probability Density
Empirical Density
Corrected Salinity

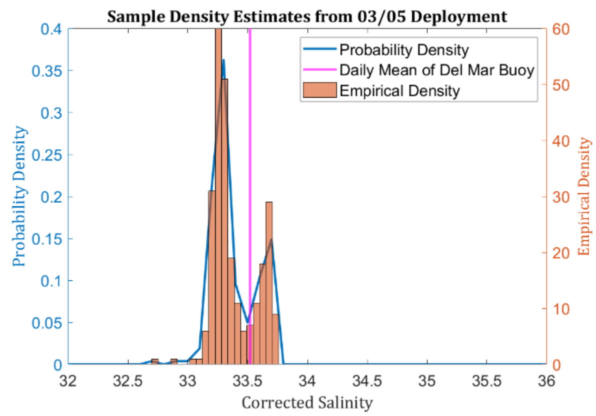
Sample Density Estimates from 03/05 Deployment
Probability Density
Daily Mean of Del Mar Buoy
Empirical Density
Probability Density
Empirical Density
Corrected Salinity

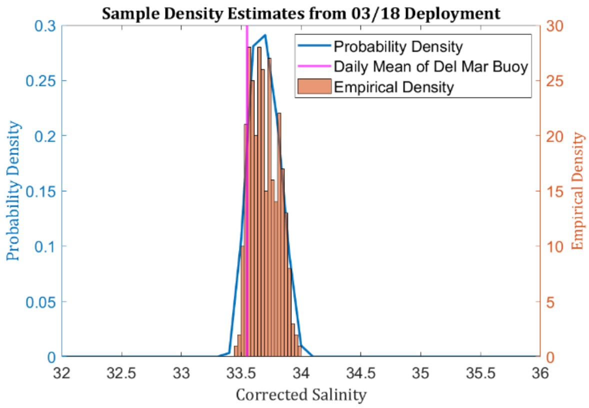
Sample Density Estimates from 03/18 Deployment
Probability Density
Daily Mean of Del Mar Buoy
Empirical Density
Corrected Salinity

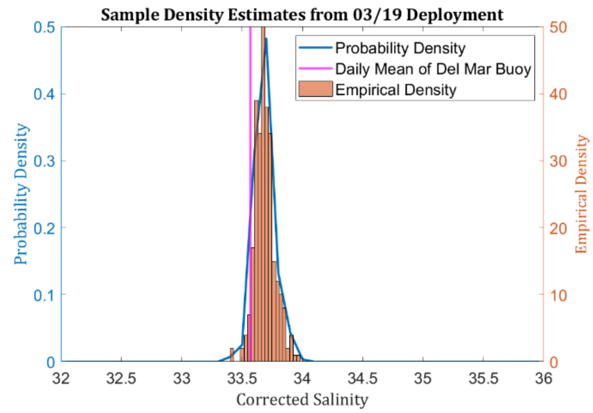
Sample Density Estimates from 03/19 Deployment
Probability Density
Daily Mean of Del Mar Buoy
Empirical Density
Corrected Salinity

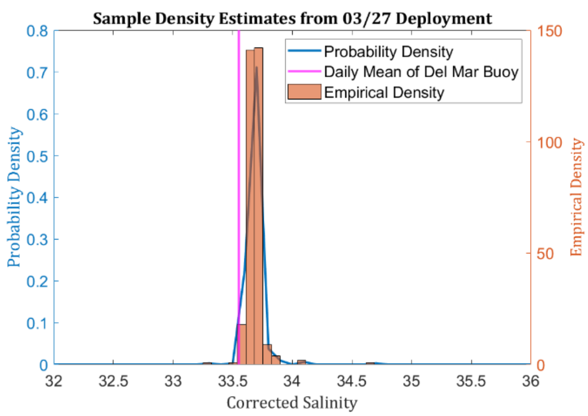
Sample Density Estimates from 03/27 Deployment
Probability Density
Daily Mean of Del Mar Buoy
Empirical Density
Corrected Salinity

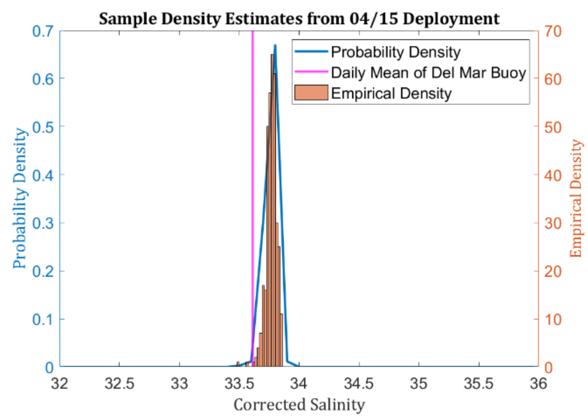
Sample Density Estimates from 04/15 Deployment
Probability Density
Daily Mean of Del Mar Buoy
Empirical Density
Corrected Salinity

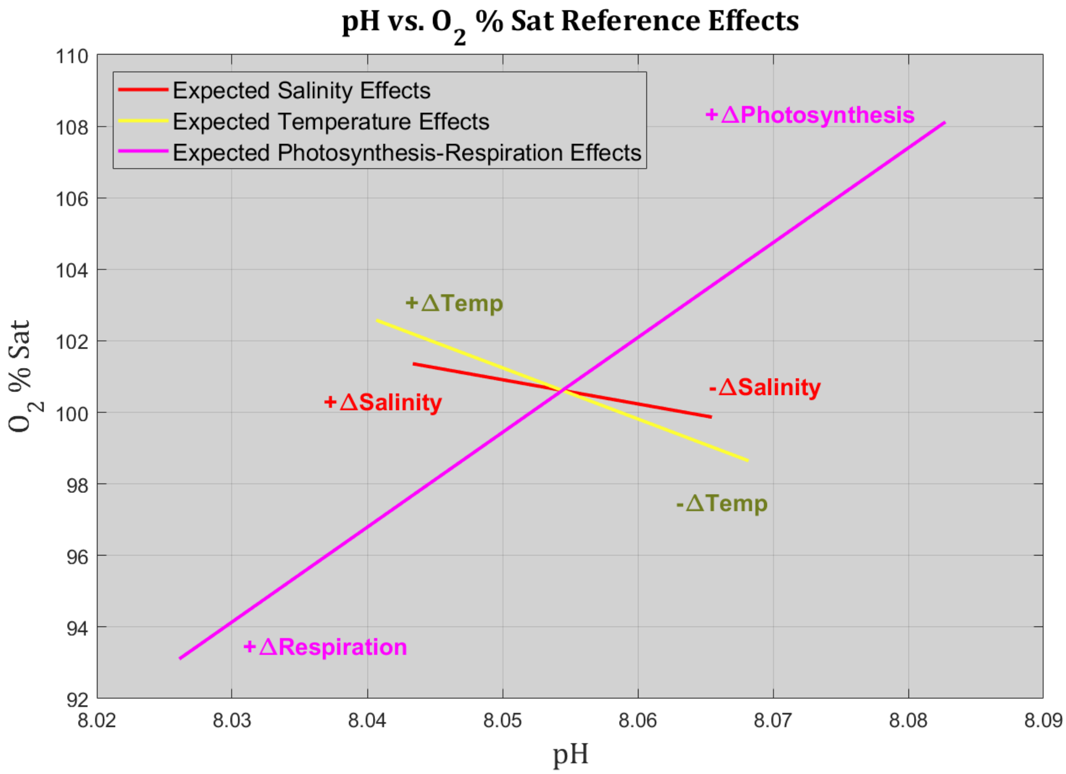

Figure 13 Expected effects on pH and O_2 % Sat from three environmental parameters: temperature, salinity, and photosynthesis-respiration. Slopes derived from a combination of Redfieldian relationships and CO_2 equilibrium chemistry. Data in this figure is centered on averaged values for corrected pH and O_2 % Sat on 03/05/21 deployment. The slopes for temperature and salinity are bounded by maximum and minimum values for measured temperature and salinity for the respective day. The photosynthesis-respiration slope is bounded by pH range.

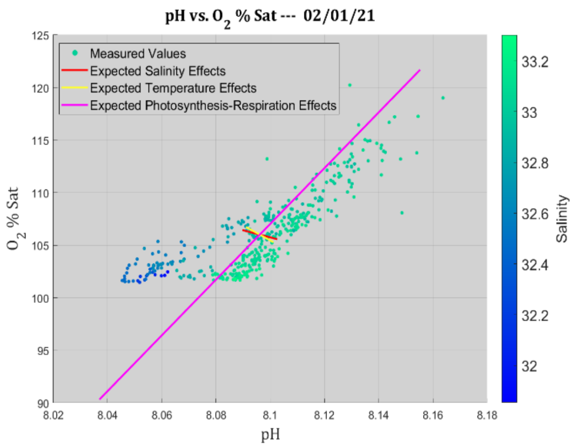
pH vs. O 2 % Sat --- 02/01/21
Measured Values
Expected Salinity Effects
Expected Temperature Effects
Expected Photosynthesis-Respiration Effects
O 2 % Sat
pH
Salinity

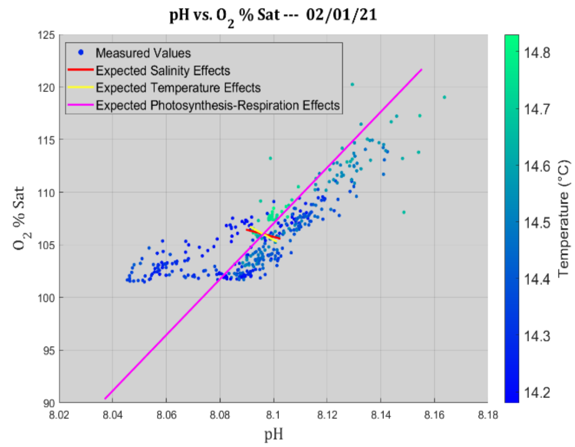
pH vs. O 2 % Sat --- 02/01/21
Measured Values
Expected Salinity Effects
Expected Temperature Effects
Expected Photosynthesis-Respiration Effects
O 2 % Sat
pH
Temperature (°C)

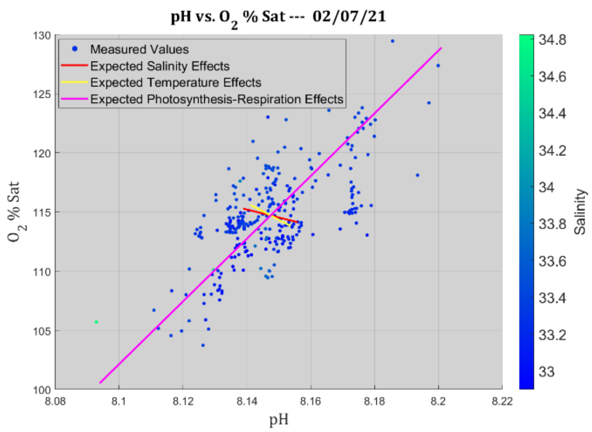
pH vs. O 2 % Sat --- 02/07/21
Measured Values
Expected Salinity Effects
Expected Temperature Effects
Expected Photosynthesis-Respiration Effects
O 2 % Sat
pH
Salinity

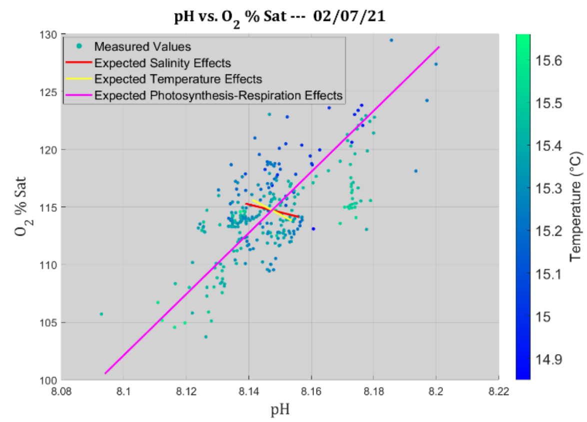
pH vs. O 2 % Sat --- 02/07/21
Measured Values
Expected Salinity Effects
Expected Temperature Effects
Expected Photosynthesis-Respiration Effects
O 2 % Sat
pH
Temperature (°C)

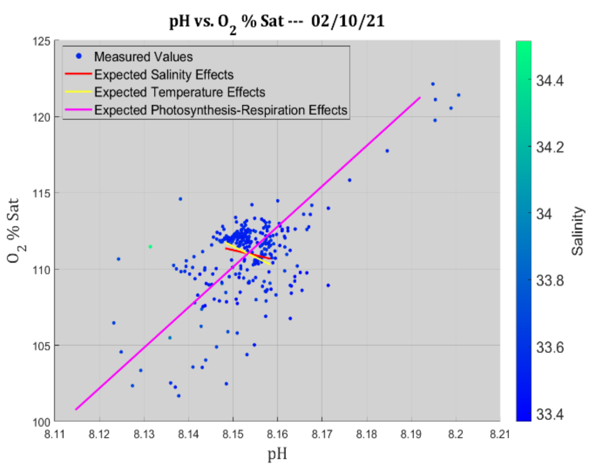
pH vs. O 2 % Sat --- 02/10/21
Measured Values
Expected Salinity Effects
Expected Temperature Effects
Expected Photosynthesis-Respiration Effects
O 2 % Sat
pH
Salinity

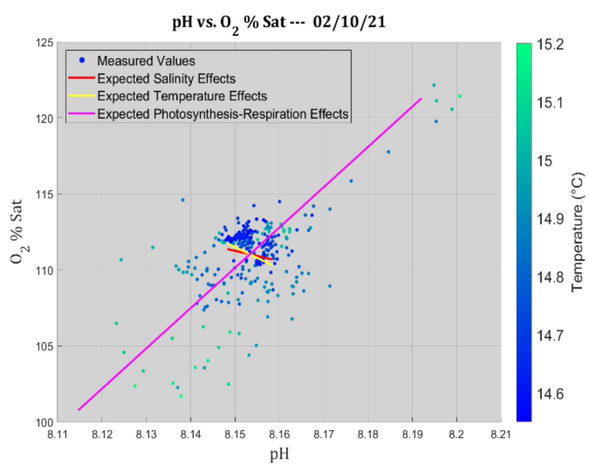
pH vs. O 2 % Sat --- 02/10/21
Measured Values
Expected Salinity Effects
Expected Temperature Effects
Expected Photosynthesis-Respiration Effects
O 2 % Sat
pH
Temperature (°C)

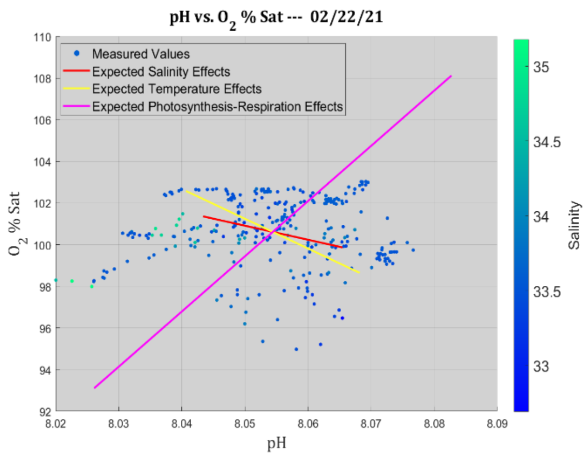
pH vs. O_2 % Sat --- 02/22/21
Measured Values
Expected Salinity Effects
Expected Temperature Effects
Expected Photosynthesis-Respiration Effects
O_2 % Sat
pH
Salinity

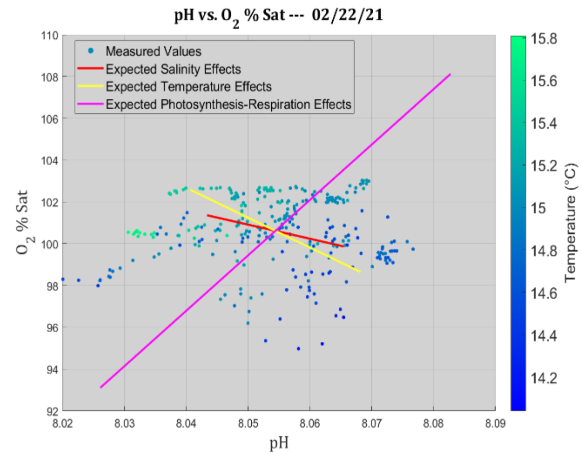
pH vs. O_2 % Sat --- 02/22/21
Measured Values
Expected Salinity Effects
Expected Temperature Effects
Expected Photosynthesis-Respiration Effects
O_2 % Sat
pH
Temperature (°C)

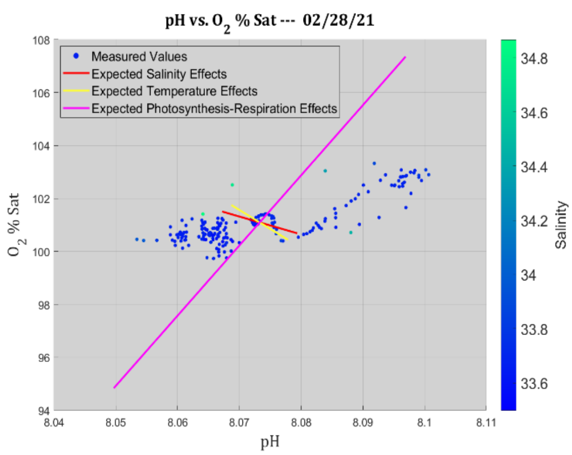
pH vs. O_2 % Sat --- 02/28/21
Measured Values
Expected Salinity Effects
Expected Temperature Effects
Expected Photosynthesis-Respiration Effects
O_2 % Sat
pH
Salinity

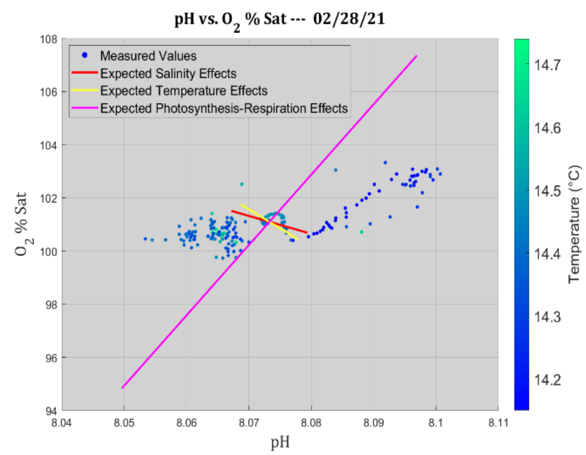
pH vs. O_2 % Sat --- 02/28/21
Measured Values
Expected Salinity Effects
Expected Temperature Effects
Expected Photosynthesis-Respiration Effects
O_2 % Sat
pH
Temperature (°C)

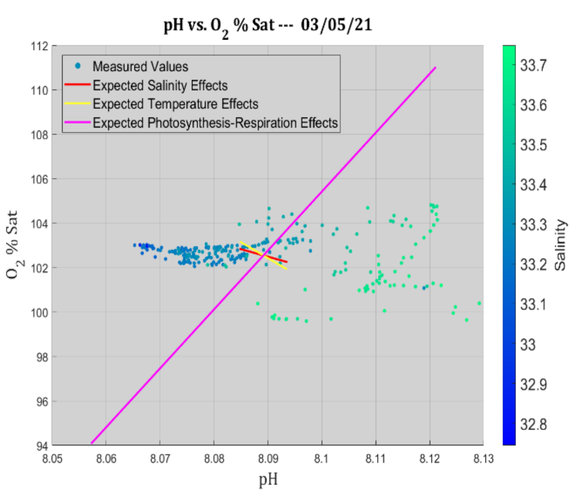
pH vs. O_2 % Sat --- 03/05/21
Measured Values
Expected Salinity Effects
Expected Temperature Effects
Expected Photosynthesis-Respiration Effects
O_2 % Sat
pH
Salinity

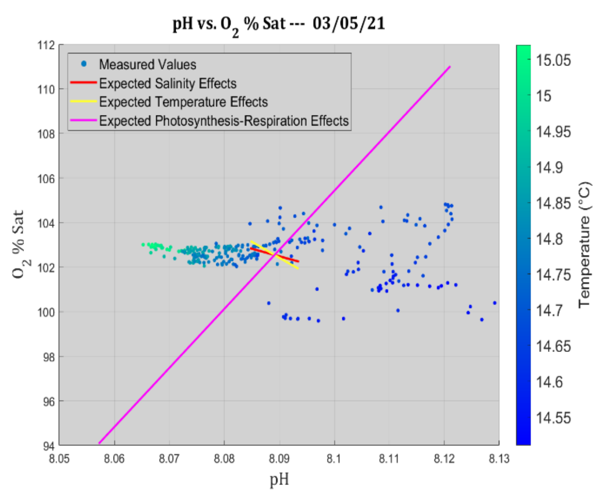
pH vs. O_2 % Sat --- 03/05/21
Measured Values
Expected Salinity Effects
Expected Temperature Effects
Expected Photosynthesis-Respiration Effects
O_2 % Sat
pH
Temperature (°C)

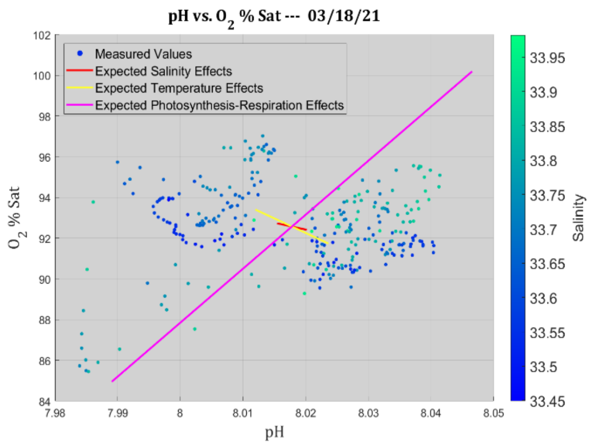

pH vs. O$_2$ % Sat --- 03/18/21
Measured Values
Expected Salinity Effects
Expected Temperature Effects
Expected Photosynthesis-Respiration Effects
O$_2$ % Sat
pH
Salinity

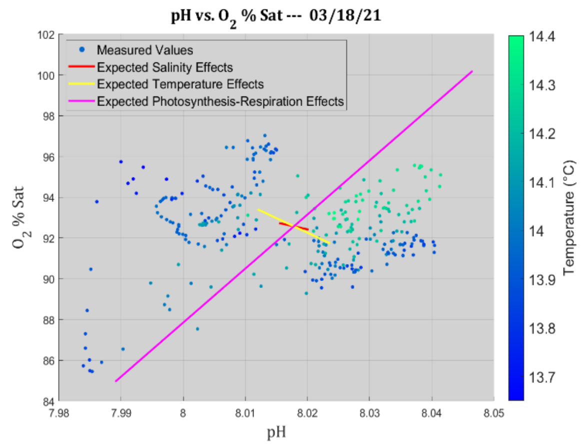

pH vs. O$_2$ % Sat --- 03/18/21
Measured Values
Expected Salinity Effects
Expected Temperature Effects
Expected Photosynthesis-Respiration Effects
O$_2$ % Sat
pH
Temperature (°C)

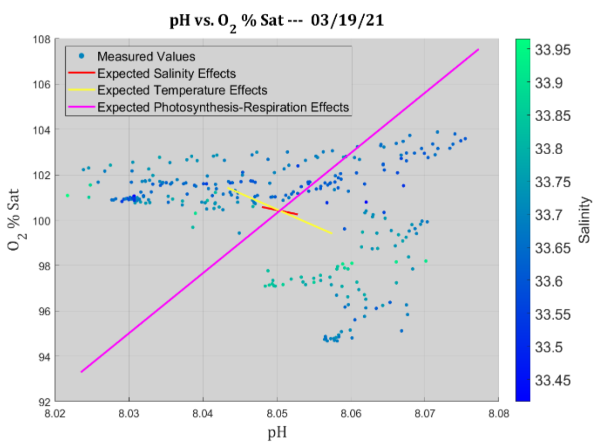

pH vs. O$_2$ % Sat --- 03/19/21
Measured Values
Expected Salinity Effects
Expected Temperature Effects
Expected Photosynthesis-Respiration Effects
O$_2$ % Sat
pH
Salinity

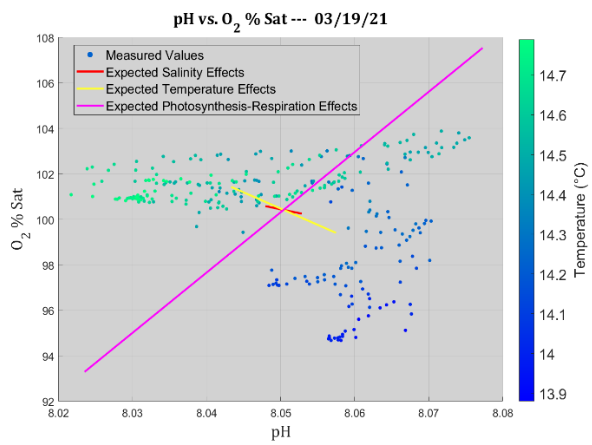

pH vs. O$_2$ % Sat --- 03/19/21
Measured Values
Expected Salinity Effects
Expected Temperature Effects
Expected Photosynthesis-Respiration Effects
O$_2$ % Sat
pH
Temperature (°C)

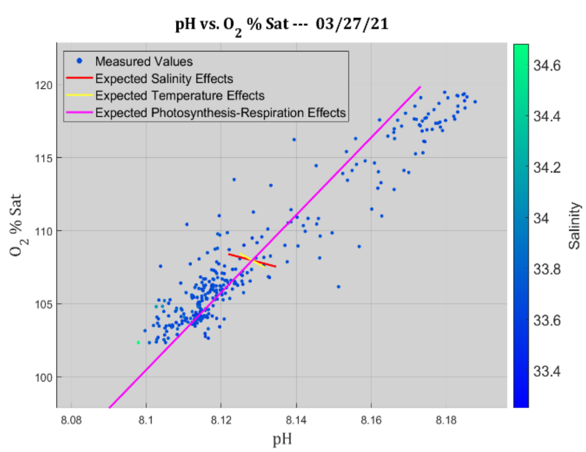

pH vs. O$_2$ % Sat --- 03/27/21
Measured Values
Expected Salinity Effects
Expected Temperature Effects
Expected Photosynthesis-Respiration Effects
O$_2$ % Sat
pH
Salinity

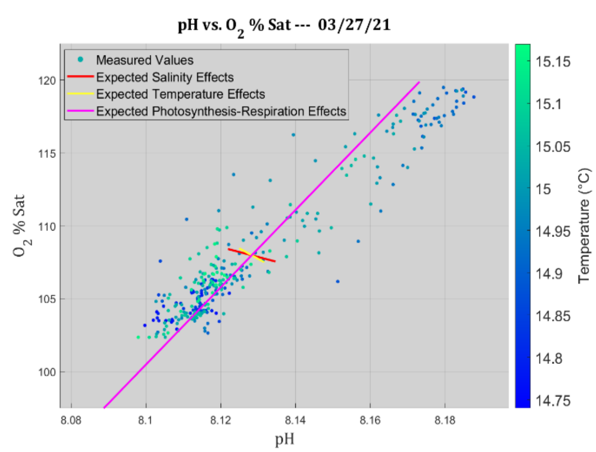

pH vs. O$_2$ % Sat --- 03/27/21
Measured Values
Expected Salinity Effects
Expected Temperature Effects
Expected Photosynthesis-Respiration Effects
O$_2$ % Sat
pH
Temperature (°C)

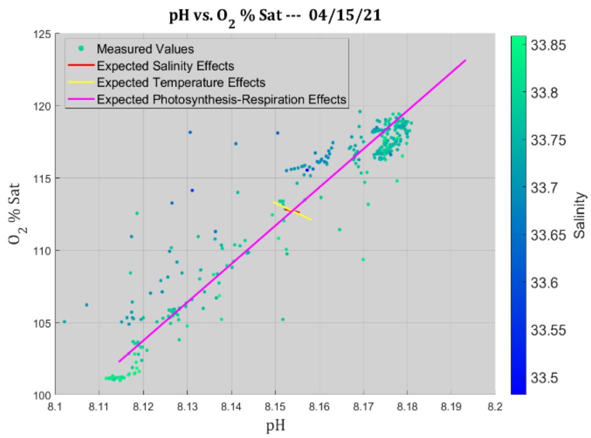

pH vs. O2 % Sat --- 04/15/21
Measured Values
Expected Salinity Effects
Expected Temperature Effects
Expected Photosynthesis-Respiration Effects
O2 % Sat
pH
Salinity

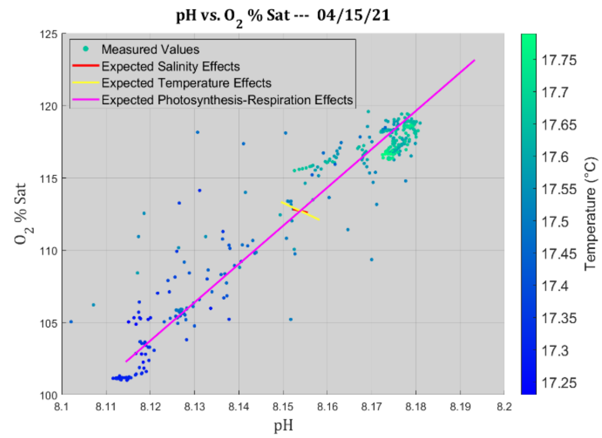

pH vs. O2 % Sat --- 04/15/21
Measured Values
Expected Salinity Effects
Expected Temperature Effects
Expected Photosynthesis-Respiration Effects
O2 % Sat
pH
Temperature (°C)

Appendix D: Atlas Scientific K1.0 Tank Test Results

The Atlas Scientific K1.0 conductivity probe was incorporated into the WavepHOx sensor package and tank tests in a circulating 7000 L seawater test tank were performed at the beginning of this study due to its low cost and relatively simple physical integration. Tests performed alongside a SBE 37 to compare its response rate and stability displayed imprecise measurements even after proper calibration methods were implemented. Time series data for salinity was characterized by a high frequency noise of ± 0.15, a full order of magnitude higher than observed in situ measurements in other highly dynamic environments (Boehme et al., 2008; Wong et al., n.d.). Common practices to mitigate those uncertainties eliminate the possibility to detect fine-scale gradients for water mass differentiation for field deployments. Additionally, the time required for sensor stabilization proved unsuitable for field deployments. Although the same pre-deployment quality control procedure for the WavepHOx was not employed with the Atlas probe, the duration for the conditioning period was ~6 hours upon submersion in the tank. For comparison, the integrated 4319 had a conditioning period of ~100 minutes before the pre-deployment protocol was implemented. The Atlas integrated WavepHOx was immersed in the seawater tank for a full 24 hours before the test on August 21st, 2021 was carried out. This test consisted of a dilution by pouring three 55 L buckets of fresh water into the tank to track its response rate. The results are shown below.

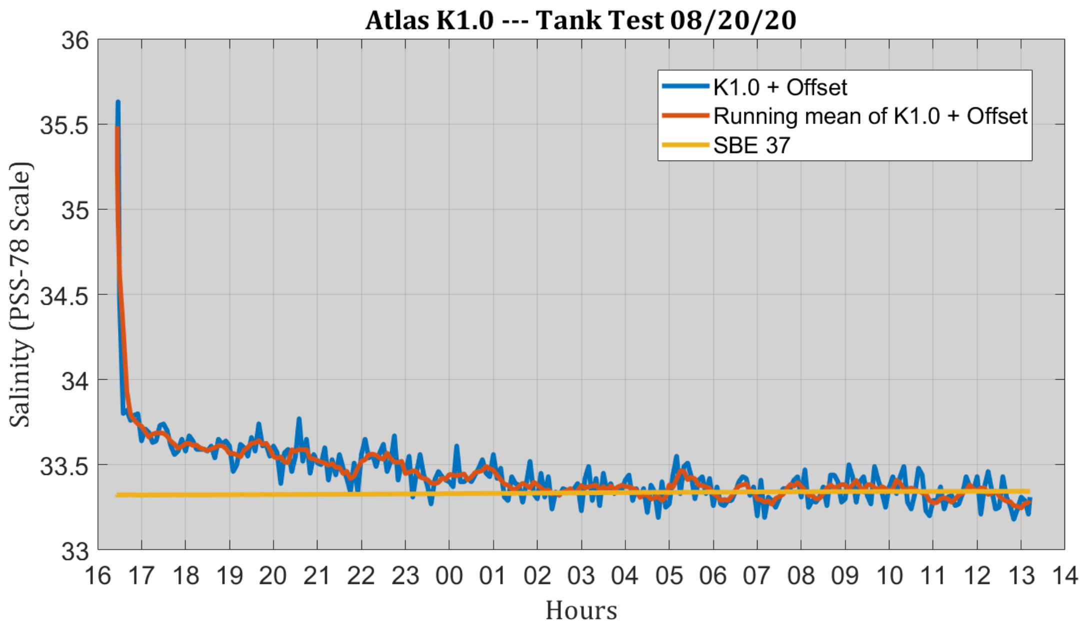
Atlas K1.0 --- Tank Test 08/20/20
36
35.5
35
34.5
34
33.5
33
16 17 18 19 20 21 22 23 00 01 02 03 04 05 06 07 08 09 10 11 12 13 14
Hours
Salinity (PSS-78 Scale)
K1.0 + Offset
Running mean of K1.0 + Offset
SBE 37

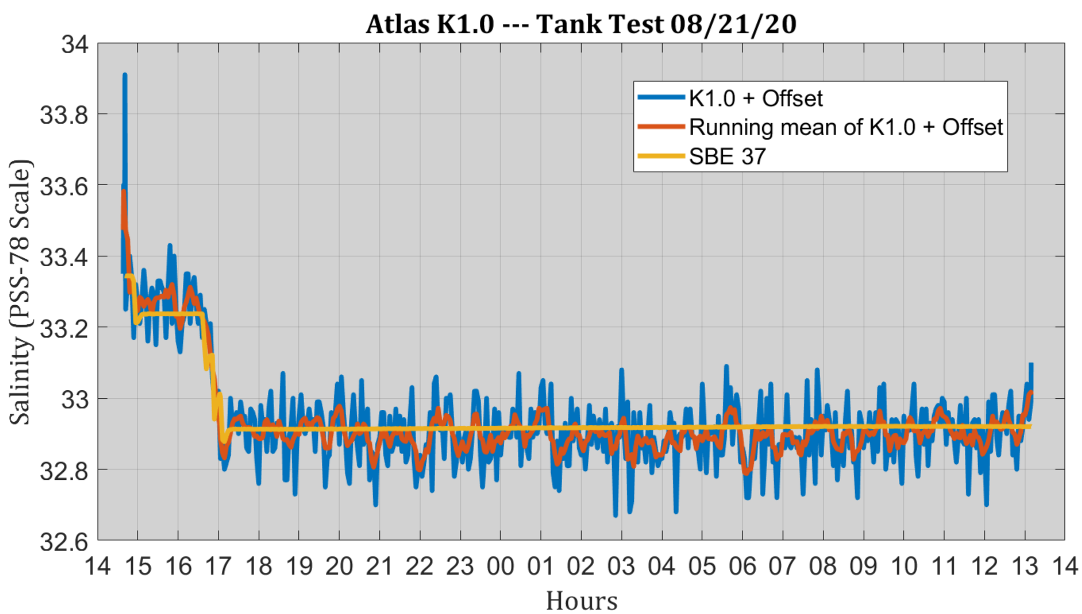
Atlas K1.0 --- Tank Test 08/21/20
34
33.8
33.6
33.4
33.2
33
32.8
32.6
14 15 16 17 18 19 20 21 22 23 00 01 02 03 04 05 06 07 08 09 10 11 12 13 14
Hours
Salinity (PSS-78 Scale)
K1.0 + Offset
Running mean of K1.0 + Offset
SBE 37

REFERENCES

AADI. (2013). *TD 263 OPERATING MANUAL CONDUCTIVITY SENSOR 4319*. Xylem. https://www.aanderaa.com/media/pdfs/TD263-Condcutivity-sensor-4319.pdf

AADI. (2021). *Oxygen Optode 3835*. https://www.aanderaa.com/media/pdfs/d385_aanderaa_oxygen_sensor_4835.pdf

Belkin, N., Rahav, E., Elifantz, H., Kress, N., & Berman-Frank, I. (2017). The effect of coagulants and antiscalants discharged with seawater desalination brines on coastal microbial communities: A laboratory and in situ study from the southeastern Mediterranean. *Water Research*, *110*, 321–331. https://doi.org/10.1016/j.watres.2016.12.013

Bendat, J. S., & Piersol, A. G. (2012). Random Data: Analysis and Measurement Procedures: Fourth Edition. In *Random Data: Analysis and Measurement Procedures: Fourth Edition*. Wiley Blackwell. https://doi.org/10.1002/9781118032428

Boehme, L., Meredith, M. P., Thorpe, S. E., Biuw, M., & Fedak, M. (2008). Antarctic circumpolar current frontal system in the South Atlantic: Monitoring using merged Argo and animal-borne sensor data. *Journal of Geophysical Research: Oceans*, *113*(9). https://doi.org/10.1029/2007JC004647

Bresnahan, P. J., Wirth, T., Martz, T. R., Andersson, A. J., Cyronak, T., D'Angelo, S., Pennise, J., Melville, W. K., Lenain, L., & Statom, N. (2016). A sensor package for mapping pH and oxygen from mobile platforms. *Methods in Oceanography*, *17*, 1–13. https://doi.org/10.1016/j.mio.2016.04.004

Cao, F., & Tzortziou, M. (2021). Capturing dissolved organic carbon dynamics with Landsat-8 and Sentinel-2 in tidally influenced wetland–estuarine systems. *Science of the Total Environment*, *777*, 145910. https://doi.org/10.1016/j.scitotenv.2021.145910

City of Carlsbad. (2005). *Precise Development Plan and Desalination Plant Project*.

Cumming, B. (2003). Limnology: Lake and River Ecosystems . Third Edition. By Robert G Wetzel. San Diego (California): Academic Press . $74.95. xvi + 1006 p; ill.; index. ISBN: 0-12-744760-1. 2001. . *The Quarterly Review of Biology*, *78*(3), 368–369. https://doi.org/10.1086/380040

Dickson, A. G., Sabine, C. L., & Christian, J. R. (2007). *Guide to Best Practices for Ocean CO2 Measurements* . North Pacific Marine Science Organization. www.pices.int

EPA. (1998, July). Nearshore Waters and Your Coastal Watershed | NEPIS | US EPA. *National Service Center for Environmental Publications (NSCEP)*, 1–1. https://nepis.epa.gov/Exe/ZyNET.exe/200050HE.TXT?ZyActionD=ZyDocument&Client=EPA&Index=1995+Thru+1999&Docs=&Query=&Time=&EndTime=&SearchMethod=1&TocRestrict=n&Toc=&TocEntry=&QField=&QFieldYear=&QFieldMonth=&QFieldDay=&IntQFieldOp=0&ExtQFieldOp=0&XmlQuery=

Garcia, H. E., & Gordon, L. I. (1992). Oxygen solubility in seawater: Better fitting equations. In *Limnology and Oceanography* (Vol. 37, Issue 6, pp. 1307–1312). John Wiley & Sons, Ltd. https://doi.org/10.4319/lo.1992.37.6.1307

Goodridge, B. M. (2018). The influence of submarine groundwater discharge on nearshore marine dissolved organic carbon reactivity, concentration dynamics, and offshore export.

Geochimica et Cosmochimica Acta, *241*, 108–119. https://doi.org/10.1016/j.gca.2018.08.040

Google. (2021). *Google Earth*. https://earth.google.com/web/@0,0,0a,22251752.77375655d,35y,0h,0t,0r

Hofmann, G., Kelley, A. L., Shaw, E. C., Martz, T. R., & Hofmann, G. E. (2015). Near-shore Antarctic pH variability has implications for the design of ocean acidification experiments. *Scientific Reports*, *5*(1), 1–10. https://doi.org/10.1038/srep09638

IOC, SCOR, & IAPSO. (2010). *The International Thermodynamic Equation of Seawater 2010 (TEOS-10): Calculation and Use of Thermodynamic Properties* (UNESCO (ed.); Manuals an). Intergovernmental Oceanographic Commission. https://www.researchgate.net/publication/216028042_The_International_Thermodynamic_Equation_of_Seawater_2010_TEOS-10_Calculation_and_Use_of_Thermodynamic_Properties

Janfelt, C., Lauritsen, F. R., Toler, S. K., Bell, R. J., & Short, R. T. (2007). Method for quantification of chemicals in a pollution plume using a moving membrane-based sensor exemplified by mass spectrometry. *Analytical Chemistry*, *79*(14), 5336–5342. https://doi.org/10.1021/ac070408f

Jenkins, S. A., & Wasyl, J. (2005). *Hydrodynamic modeling of dispersion and dilution of concentrated seawater produced by the ocean desalination project at the Encina Power Plant*.

Kang Hui, S., Jang, H., Kim Gum, C., Yu Song, C., & Kim Yong, H. (2020). A new design of inductive conductivity sensor for measuring electrolyte concentration in industrial field. *Sensors and Actuators, A: Physical*, *301*, 111761. https://doi.org/10.1016/j.sna.2019.111761

Kekuewa, S. A. (2020). Seawater CO2-Chemistry Variability in the Near-Shore Environment of the Southern California Bight [University of California, San Diego]. In *UC San Diego*. https://escholarship.org/uc/item/5ng2r1p5#author

Kononets, M., Atamanchuk, D., & Tengberg, A. (2012). *Koljoe Fjord observatory YSI EXO2 and AADI Seaguard*.

Lange, R., Staaland, H., & Mostad, A. (1972). THE EFFECT OF SALINITY AND TEMPERATURE ON SOLUBILITY OF OXYGEN AND RESPIRATORY RATE IN OXYGEN-DEPENDENT MARINE INVERTEBRATES. In *mar. Biol. Ecol* (Vol. 9). ~) North,Holland Publishing Company.

Langella, G. (2021). *Inverse Distance Weighted (IDW) or Simple Moving Average (SMA) INTERPOLATION - File Exchange - MATLAB Central* (1.00.00). Mathworks. https://www.mathworks.com/matlabcentral/fileexchange/27562-inverse-distance-weighted-idw-or-simple-moving-average-sma-interpolation

Le, C., Gao, Y., Cai, W. J., Lehrter, J. C., Bai, Y., & Jiang, Z. P. (2019). Estimating summer sea surface pCO 2 on a river-dominated continental shelf using a satellite-based semi-mechanistic model. *Remote Sensing of Environment*, *225*, 115–126. https://doi.org/10.1016/j.rse.2019.02.023

Lewis, E., Wallace, D., & Allison, L. J. (1998). *Program developed for CO{sub 2} system calculations*. https://doi.org/10.2172/639712

Liévana MacTavish, A., Ladah, L. B., Lavín, M. F., Filonov, A., Tapia, F. J., & Leichter, J. (2016). High frequency (hourly) variation in vertical distribution and abundance of meroplanktonic larvae in nearshore waters during strong internal tidal forcing. *Continental Shelf Research*, *117*, 92–99. https://doi.org/10.1016/j.csr.2016.02.004

Limburg, K. E., Breitburg, D., Swaney, D. P., & Jacinto, G. (2020). Ocean Deoxygenation: A Primer. *One Earth*, *2*(1), 24–29. https://doi.org/10.1016/j.oneear.2020.01.001

Liu, Y., Jiao, J. J., Liang, W., Santos, I. R., Kuang, X., & Robinson, C. E. (2021). Inorganic carbon and alkalinity biogeochemistry and fluxes in an intertidal beach aquifer: Implications for ocean acidification. *Journal of Hydrology*, *595*, 126036. https://doi.org/10.1016/j.jhydrol.2021.126036

Martz, T. R., Connery, J. G., & Johnson, K. S. (2010). Testing the Honeywell Durafet® for seawater pH applications. *Limnology and Oceanography: Methods*, *8*(MAY), 172–184. https://doi.org/10.4319/lom.2010.8.172

Martz, T., Send, U., Ohman, M. D., Takeshita, Y., Bresnahan, P., Kim, H.-J., & Nam, S. (2014). Dynamic variability of biogeochemical ratios in the Southern California Current System. *Wiley Online Library*, *41*(7), 2496–2501. https://doi.org/10.1002/2014GL059332

McDougall, T., & Barker, P. (2015). *Practical Salinity from conductivity, C*. The Gibbs SeaWater (GSW) Oceanographic Toolbox of TEOS-10. http://www.teos-10.org/pubs/gsw/html/gsw_SP_from_C.html

McLaughlin, K., Nezlin, N. P., Weisberg, S. B., Dickson, A. G., Booth, J. A. T., Cash, C. L., Feit, A., Gully, J. R., Howard, M. D. A., Johnson, S., Latker, A., Mengel, M. J., Robertson, G. L., Steele, A., & Terriquez, L. (2018). Seasonal patterns in aragonite saturation state on the southern California continental shelf. *Continental Shelf Research*, *167*, 77–86. https://doi.org/10.1016/j.csr.2018.07.009

Mettler Toledo. (2010). *Density Meters DM40/45/50*. https://www.mt.com/us/en/home/phased_out_products/Laboratory_Analytics_Browse/Density_Family_Browse_main/DE_Benchtop/DM45.html

Omand, M. M., Leichter, J. J., Franks, P. J. S., Guza, R. T., Lucas, A. J., & Feddersen, F. (2011). Physical and biological processes underlying the sudden surface appearance of a red tide in the nearshore. *Limnology and Oceanography*, *56*(3), 787–801. https://doi.org/10.4319/lo.2011.56.3.0787

Ouillon, R., Meiburg, E., Meiburg, E., Ouellette, N. T., & Koseff, J. R. (2019). Interaction of a downslope gravity current with an internal wave. *Journal of Fluid Mechanics*, *873*, 889–913. https://doi.org/10.1017/jfm.2019.414

Petersen, K. L., Frank, H., Paytan, A., & Bar-Zeev, E. (2018). Impacts of Seawater Desalination on Coastal Environments. In *Sustainable Desalination Handbook: Plant Selection, Design and Implementation* (pp. 437–463). Elsevier. https://doi.org/10.1016/B978-0-12-809240-8.00011-3

Roberts, D. A., Johnston, E. L., & Knott, N. A. (2010). Impacts of desalination plant discharges on the marine environment: A critical review of published studies. In *Water Research* (Vol. 44, Issue 18, pp. 5117–5128). Elsevier Ltd. https://doi.org/10.1016/j.watres.2010.04.036

Roquet, F., Charrassin, J. B., Marchand, S., Boehme, L., Fedak, M., Reverdin, G., & Guinet, C. (2011). Delayed-mode calibration of hydrographic data obtained from animal-borne satellite relay data loggers. *Journal of Atmospheric and Oceanic Technology*, *28*(6), 787–801. https://doi.org/10.1175/2010JTECHO801.1

Salit, M. L., & Turk, G. C. (1998). A Drift Correction Procedure. *Analytical Chemistry*, *70*(15), 3184–3190. https://doi.org/10.1021/ac980095b

Schlitzer, R. (2002). Interactive analysis and visualization of geoscience data with Ocean Data View $. In *Computers & Geosciences* (Vol. 28). http://whpo.ucsd.edu/

Schlitzer, R. (2015). Data Analysis and Visualization with Ocean Data View. *EPIC3CMOS Bulletin SCMO, Canadian Meteorological and Oceanographic Society, 43(1), Pp. 9-13, ISSN: 1195-8898*. http://www.cmos.ca/site/cmos_bulletin

Sea-Bird Scientific. (2018, July). *SBE 37-SI and SIP MicroCAT*. https://www.seabird.com/moored/sbe-37-si-and-sip-microcat/family?productCategoryId=54627473785

Shanafield, M., Banks, E. W., Arkwright, J. W., & Hausner, M. B. (2018). Fiber-Optic Sensing for Environmental Applications: Where We Have Come From and What Is Possible. In *Water Resources Research* (Vol. 54, Issue 11, pp. 8552–8557). Blackwell Publishing Ltd. https://doi.org/10.1029/2018WR022768

Short, R. T., Toler, S. K., Kibelka, G. P. G., Rueda Roa, D. T., Bell, R. J., & Byrne, R. H. (2006). Detection and quantification of chemical plumes using a portable underwater membrane introduction mass spectrometer. *TrAC - Trends in Analytical Chemistry*, *25*(7), 637–646. https://doi.org/10.1016/j.trac.2006.05.002

Sinnett, G., Davis, K. A., Lucas, A. J., Giddings, S. N., Reid, E., Harvey, M. E., & Stokes, I. (2020). Distributed temperature sensing for oceanographic applications. *Journal of Atmospheric and Oceanic Technology*, *37*(11), 1987–1997. https://doi.org/10.1175/JTECH-D-20-0066.1

Volpe, A. M., & Esser, B. K. (2002). Real-time ocean chemistry for improved biogeochemical observation in dynamic coastal environments. *Journal of Marine Systems*, *36*(1–2), 51–74. https://doi.org/10.1016/S0924-7963(02)00125-2

Water Resources Control Board, S. (2019). *Water Quality Control Plan Ocean Waters of California State Water Resources Control Board California Environmental Protection Agency*. http://www.waterboards.ca.gov

Wong, A., … G. J.-J. of A., & 2003, undefined. (n.d.). Delayed-Mode Calibration of Autonomous CTD Profiling Float Salinity Data by θ–S Climatology. *Journals.Ametsoc.Org*. Retrieved May 28, 2021, from https://journals.ametsoc.org/view/journals/atot/20/2/1520-0426_2003_020_0308_dmcoac_2_0_co_2.xml

Young, A. P., & Ashford, S. A. (2006). Application of airborne LIDAR for seacliff volumetric change and beach-sediment budget contributions. *Journal of Coastal Research*, *22*(2), 307–318. https://doi.org/10.2112/05-0548.1

Zarco-Perello, S., & Simões, N. (2017). Ordinary kriging vs inverse distance weighting: Spatial interpolation of the sessile community of Madagascar reef, Gulf of Mexico. *PeerJ*, *2017*(11), e4078. https://doi.org/10.7717/peerj.4078